AALTO UNIVERSITY
School of Engineering
Department of Civil and Structural Engineering

Eero Virtanen

ASSESSMENT OF VIBRATION COMFORT CRITERIA FOR TALL BUILDINGS

Thesis submitted in partial fulfilment of the requirements for the degree of Master of Science in Technology

Espoo 19.05.2015

Supervisor: Professor Risto Kiviluoma, Aalto University
Instructor: M.Sc. (Tech) Arto Sivill, Sweco Rakennetekniikka Oy
M.Sc. (Tech) Hannu Nissinen, Sweco Rakennetekniikka Oy

Aalto-yliopisto
Insinööritieteiden
korkeakoulu

Aalto-yliopisto, PL 12100, 00076 AALTO
www.aalto.fi
Diplomityön tiivistelmä

Tekijä Eero Virtanen		
Työn nimi Korkeiden rakennusten värähtelykriteerien tarkastelu		
Laitos Rakennetekniikka		
Professuuri Sillanrakennustekniikka		**Professuurikoodi** Rak-43
Työn valvoja Prof. Risto Kiviluoma		
Työn ohjaaja(t) DI Arto Sivill ja DI Hannu Nissinen		
Päivämäärä 19.05.2015	**Sivumäärä** 71+20	**Kieli** Englanti

Tiivistelmä

Tässä diplomityössä on tutkittu tuulen korkeisiin rakennuksiin aiheuttaman värähtelyn arviointimenetelmiä sekä hyväksymiskriteereitä. Aiheesta on tehty kirjallisuustutkimus eri maiden rakennusmääräyksiin ja –ohjeisiin. Fysikaaliset periaatteet ja ilmiöt sekä useita erilaisia laskentamenetelmiä dynaamisesti herkkien rakenteiden käyttäytymisestä tuulikuormituksessa on myös esitetty.

Haasteet rakennuksen tuulikuormituksen värähtelyvasteen tarkassa ennustamisessa on eritelty. Suurimmat ongelmat ja virhelähteet liittyvät tuulen ominaisuuksiin sekä rakennuksen dynaamisten ominaisuuksien tarkkaan määrittämiseen suunnitteluvaiheessa. Työssä on esitetty useita lähestymistapoja, sekä perinteisiä että uudempia kehitysaskelia, näiden haasteiden ratkaisemiseen. Eri menetelmien käyttökelpoisuutta sekä käytön rajoitteita on myös arvioitu.

Työssä on tehty esimerkkilaskenta Suomen mittakaavassa korkealle, Helsinkiin sijoitettavalle tornitalolle. Värähtelyvasteen kiihtyvyyden huippuarvot on laskettu Eurokoodin, japanilaisen AIJ ohjeistuksen, Australian/Uuden-Seelannin rakennusmääräysten sekä amerikkalaista ASCE-normia täydentävän kirjallisuuslähteen mukaan. Vaikka tuloksena saaduissa arvoissa on merkittävää hajontaa, verrattaessa kunkin normin antamia kiihtyvyysarvoja vastaaviin hyväksymiskriteereihin, osoittavat kaikki normien mukaiset laskentamenetelmät värähtelytasojen olevan hyväksyttäviä toimistorakennukselle. Työssä on tehty myös kokeellinen tarkempi analyysi aikatasossa dynaamisella elementtimenetelmälaskennalla, jolla on yritetty simuloida rakenteen todellista käyttäytymistä tuulessa. Analyysin pohjana on käytetty japanilaisesta tuulitunnelikoetietokannasta saatuja tuulen painekertoimien arvoja. Tuloksena saadut kiihtyvyysarvot ovat merkittävästi suurempia kuin normien ennusteet ja mahdollisia syitä tähän on pohdittu. Kyseinen menetelmä on myös todettu merkittävästi työläämmäksi kuin normien laskentamenetelmät, eikä sen käyttöä käytännön suunnittelutyössä voi siksi pitää mielekkäänä.

Työssä on myös esitetty kaksi vaihtoehtoista tapaa rakenteen vasteen rajoittamiseksi: rakenteen jäykkyyden lisääminen sekä vaimennuksen lisääminen. Kummatkin menetelmät toimivat ylimpien kerrosten vaakakiihtyvyyksien rajoittamisessa, mutta alustavan analyysin perusteella vaimennuksen lisääminen rajoittaa värähtelyä tehokkaammin, joskaan se ei muista, esimerkiksi taloudellisista, syistä olekaan tämän korkeusluokan rakennuksissa järkevää.

Avainsanat Tuulikuorma, värähtely, korkea rakentaminen

Aalto-yliopisto
Insinööritieteiden
korkeakoulu

Aalto-yliopisto, PL 12100, 00076 AALTO
www.aalto.fi

Diplomityön tiivistelmä

Author	Eero Virtanen
Title of thesis	Assessment of vibration control criteria for tall buildings
Department	Department of structural engineering
Professorship	Bridge engineering
Code of professorship	Rak-43
Thesis supervisor	Prof. Risto Kiviluoma
Thesis advisor(s)	M.Sc (Tech) Arto Sivill and M.Sc (Tech) Hannu Nissinen
Date	19.05.2015
Number of pages	71+20
Language	English

Abstract

The estimation methods and acceptance criteria of wind-induced vibrations of tall buildings have been studied in this master's thesis. A literature survey on different building codes and guidelines has been made on this subject. The physical phenomena and principles behind the behaviour of dynamically sensitive structures as well as vibration response estimation methods under wind loading have been presented.

The difficulties included in precisely estimating building dynamic response under wind loading have been identified. The characteristics of wind itself as well as the prediction of dynamic properties of the building itself are the main sources of difficulty and error in the estimates. Different approaches, both traditional and newer advancements, have been studied to counter these problems and the usefulness and limitations of these methods has been evaluated.

As a case study a mid-rise office building to be built in Helsinki has been studied. Vibration acceleration values have been calculated using the Eurocode, Architectural Institute of Japan guidelines, Australian/New-Zealand standard and a literature reference supplementary to the ASCE standard. A large variation in the results is observed, but reflecting the results from different design guidelines to respective acceptance criteria, the results are unambiguous: vibration levels as given by the guidelines are acceptable for an office building. As a possible method for more accurate analysis dynamic finite element calculations in the time domain have also been made based on wind pressure measurements acquired from a Japanese wind tunnel experiment database. The analysis showed noticeably larger acceleration values than predicted by the guideline methods and the possible reasons behind this result are discussed. The analysis method has also been found out as too cumbersome for use in design practice.

Two different modifications to the original structural design aimed at further reducing vibration acceleration are also presented: adding stiffness to the structure and adding extra damping. Both work at reducing peak acceleration values, but an additional damper system is more efficient at reducing vibration levels. However, such systems are for other, e.g. economical, reasons usually not feasible in mid-rise buildings.

Keywords Wind load, vibration, tall building

Table of contents

Notation

a	acceleration
b	breadth
c_{prob}	probability coefficient
d	damping ratio
e	internal energy
f_L	non-dimensional frequency
g	gravitational acceleration
g_R	peak factor
h	height
k	stiffness
k_p	peak factor
m	mass
n	natural frequency
n_s	number of shielding buildings
n_{st}	vortex shedding frequency
p	pressure
r_m	radius of gyration
s	shielding parameter
t	time
v_m	mean velocity
y_{pk}	across-wind deflection
z	reference height
z_0	roughness length
A	area
B	background response factor
C	wind force coefficient
C_l	leeward side wind force coefficient
C_w	windward side wind force coefficient
D	dimensionless damping ratio
E_t	turbulence spectrum
F	force

I	turbulence intensity
I_s	average spacing of shielding buildings
K	stiffness matrix
K_x	coefficient
L	length
L_s	turbulence length scale
M	mass matrix
M_D	generalized mass of building
N_1	dimensionless frequency
R	resonant response factor
R_e	Reynolds number
R_h, R_b	aerodynamic admittance function
S_L	wind power spectral density
T	wind averaging time
T_{rms}	rms base torsional moment
V	velocity
V_1	dynamic amplification factor
W	work
α	constant
β	constant
λ	mode correction factor
ρ	density
ρ_b	building density
τ	shear stress
μ	fluid viscosity
ν	kinematic viscosity
ω	angular frequency
Φ	natural mode shape
σ	standard deviation
ζ	damping ratio
δ	logarithmic damping decrement

1 Introduction

Buildings taller than 100 m are a rarity in Finland. The few structures over that height that exist are mostly radio masts or other non-building structures. A new interest in constructing taller buildings than before has however risen lately, especially in the capital region of Helsinki and the surrounding municipalities of Espoo and Vantaa. Several projects which aim at the construction of multiple office and apartment buildings of approximately 100…150 m height are in the planning or pre-planning stage. The successful design of these buildings requires more knowledge of wind and related phenomena than has previously been necessary, and there are only a few people in Finland who have international experience of such projects.

If the effects of wind are not taken into account with the required level of accuracy in the design process, one possible result is unwanted vibration phenomena. The dynamic properties of wind may cause horizontal vibrations to occur, which are at their strongest at the top floors of the building. With inadequate structural design the vibrations at top floors may become not only noticeable but also disturbingly strong. This may lead to decrease in the property value. Gaining insight into these phenomena and their prevention by structural means has been the motivation of this thesis. Evaluating different assessment methods and related acceptance criteria have been the goals in this work. This has been accomplished by studying literature and building codes and guidelines related to the topic as well as by carrying out example calculations with different methods and comparing the results.

Especially the planned use of these buildings as apartments makes the assessment of vibration phenomena of crucial importance in the design. Helsinki is also a coastal city and many of the planned projects are located almost exactly at the seaside; therefore wind speeds similar to open sea with city-like turbulence conditions are to be expected. This makes the study of building vibrations to be of even bigger importance. Because most of these projects include not only one tall building but rather a group of several closely spaced buildings, wind-related interference effects have been chosen as one of the focal points of this study. Vibrations in the across-wind direction and torsional vibrations, which are often related to interference effects, are also studied in more detail.

Early high-rise construction in industrialized countries, most notably in North America, was often characterized by heavy structures, including large amounts of masonry. The true development of structural wind engineering, which studies wind and its effects on buildings and people, began with the adaption of new and lighter building materials, such as steel, and the demand to build ever taller and more slender structures. One of the most notably Figures in the field was the Canadian professor Alan Davenport, who developed many of the theories and techniques still in use today [1].

Even though advancements in computing have provided great advancements in many fields of civil and structural engineering, their effect in wind engineering is still limited. Noticeable advancements obviously exist, but a major breakthrough and a transition to adequately accurate entirely computational design has not yet been achieved [1]. At the source of the difficulty of computational wind engineering lays the complicatedness of wind itself. Current numerical calculation techniques are not yet sufficient to analyze the real behavior of a wind flow with the required level of accuracy. Therefore, wind

engineering still largely relies on statistical methods, simplifications and experimental methods, most notably on wind tunnel measurements.

The current state-of-the art research and practice in wind engineering focuses largely on the development of computational methods and the design of a new generation of super tall and super slender structures. Especially the aerodynamic design of buildings has advanced lately, as new skyscrapers are exceeding the old record heights of approximately 500 m with the 1 km barrier likely to be reached in the near future and new techniques have to be adapted to realize such projects within reasonable economical limits.

Because such structures and such heights are far beyond what is expected to be built in Finland in the coming years, issues related with them are addressed only briefly within this study. The emphasis is more on the basic principles of wind engineering and building vibrations and the current design methods and practices involved. A case study with the preliminary plans of one mid-rise building to be built in Helsinki is also presented. The main goals of this study are to find suitable estimation methods for the vibration analysis of mid-rise buildings from existing design guidelines and to assess their reliability. Comparing different vibration acceptance criteria found in literature has also been an important goal. Experimenting with a more advanced calculation method using dynamic finite element analysis and the creation of Mathcad-based calculation sheets for preliminary vibration analysis of mid-rise buildings using the guideline calculation methods are also objectives of this thesis.

2 Basics of wind engineering

Wind is a complex natural phenomenon and solid understanding of its nature and behavior is crucial for assessing its effects on structures. Wind engineering as a subject studies the properties and behavior of wind and its effects on structures and people. Properties of wind being studied in wind engineering include not only the general characteristics of wind but also e.g. local wind environments. The effects of wind on structures is studied not only from the mechanical point of view, but wind effects on e.g. building heat and ventilation systems as well as pollutant diffusion within the atmosphere are also studied.

Rigid low-rise buildings, which are typical of the Finnish building habit, are not sensitive to wind induced motions and their design can easily be carried out by the standard procedures given in building norms (the eurocode) or other design guides. However, special structures such as long span bridges or tall and slender buildings require a more thorough analysis. The aim of this Chapter is to provide a basic understanding of wind and its effect on structures, with the emphasis on tall buildings. This includes dealing with fluid mechanics (especially fluid dynamics), the atmosphere, structural dynamics and the interaction of all three.

2.1 Fluid mechanics

Fluid mechanics is a vast topic that deals with the behavior of fluids under many different circumstances, both static and dynamic. These include e.g. problems related to surface tension, fluid statics, flow in enclosed bodies, flow stability etc. The area of fluid mechanics that is of interest here is fluid flow around bodies. The subject has been researched in detail and many textbooks have been written of it. The following presentation is based on [2] and [4].

The behavior of a fluid flow depends on fluid properties and flow conditions. The most important fluid properties are its density and viscosity, which are also dependent on the fluid temperature. The nature of the flow is then greatly dependent on the geometry of the situation and flow velocity. Many dimensionless numbers based on these values have also been developed to describe different properties of the flow.

To analyze a simple flow, few basic concepts and Equations are needed. First, ignoring the fluid viscosity, the Bernoulli Equation relates flow velocity and pressure along a streamline:

$$p + \frac{1}{2}\rho V^2 = constant \tag{1}$$

where p = static pressure, ρ = fluid density and V = flow velocity.

Real flows also experience shear stresses. A shear stress occurs e.g. when a difference in velocity is present between two streamlines in direction perpendicular to the flow. The shear stress in such situation is

$$\tau = \mu \frac{dV}{dz} \tag{2}$$

where μ = fluid viscosity.

These viscous forces mean friction is present in the flow. Relating the inertial forces caused by flow velocity to these viscous forces yields the Reynolds number, which is an important parameter in defining the characteristics of the flow

$$Re = \frac{VL}{\nu} \tag{3}$$

where L = flow dimension, e.g. distance from the edge of a plate as shown by coordinate x in Figure 1 and ν = kinematic viscosity [2]

$$\nu = \frac{\mu}{\rho} \tag{4}$$

One important division in types of fluid flow is the difference between laminar and turbulent flow: In a laminar flow the fluid flows in parallel layers without mixing of the layers, whereas in a turbulent flow the motion of the fluid is more complex, being characterized by time-varying eddies and seemingly random motion. Whether the flow is laminar or turbulent is usually characterized based on the Reynolds number. Large values of the Reynolds number indicate turbulent flow and low laminar flow. The limit values for assuming turbulent flow depend on the geometry of the situation. For a fluid flow over a flat plate (which is assumed to depict air flow over earth surface), as shown in Figure 1, the flow is usually assumed turbulent if Re>500 000. The air flow encountered when investigating wind is almost always turbulent.

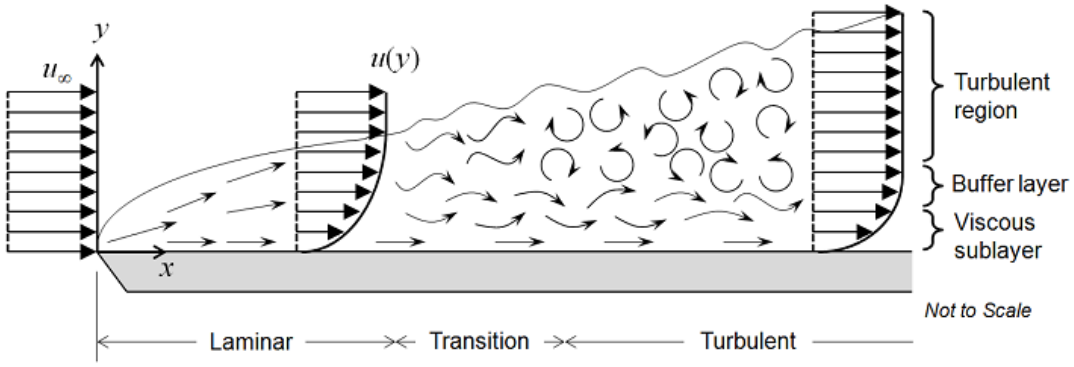

Figure 1. Transition from laminar to turbulent flow over a flat plate [3]

In a turbulent flow a large array of different sized eddies are present. Large eddies are on the size range of buildings and other flow affecting obstacles, while small ones can be measured in millimeters. In a turbulent flow, kinetic energy is dissipated downwards on the turbulence size scale. Large eddies extract energy from the main flow while small ones extract it from larger ones. Therefore, larger amounts of turbulence (higher Reynolds number) mean more energy dissipation from the flow and thus lower flow velocities.

Another important concept in analyzing flow around bodies and over surfaces is called the no-slip condition. Because of the viscous friction forces, the flow velocity at a fluid-solid boundary is zero and increases as the distance from the surface increases until we

reach the undisturbed free flow region. The height of this disturbed flow region, the boundary layer, depends on the properties of the flow and the surface material and roughness. This condition creates a velocity gradient above surfaces, which is important in defining e.g. wind velocities in the atmosphere. [4]

Flow behavior around a body is also affected by the body shape. If the area through which flow occurs decreases, the flow velocity needs to be amplified since the amount of fluid flowing through the two sections has to be equal. Similarly, if the area increases, the flow velocity decreases, which is the case for example at the leeward side of a body. This steep velocity gradient may then cause flow reversal or flow separation to occur, often accompanied by a turbulent shear layer. These phenomena are illustrated in Figures 2 and 3.[2]

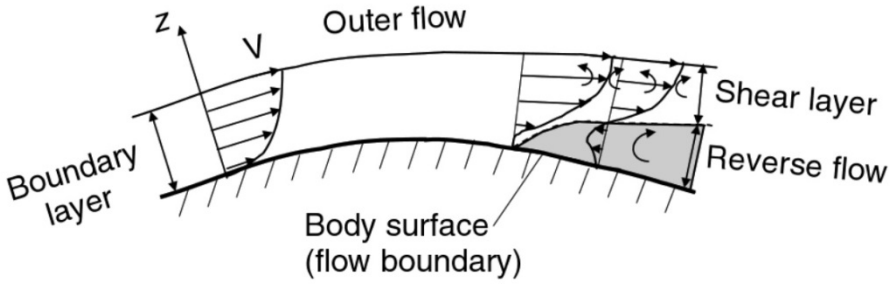

Figure 2. Flow separation [2]

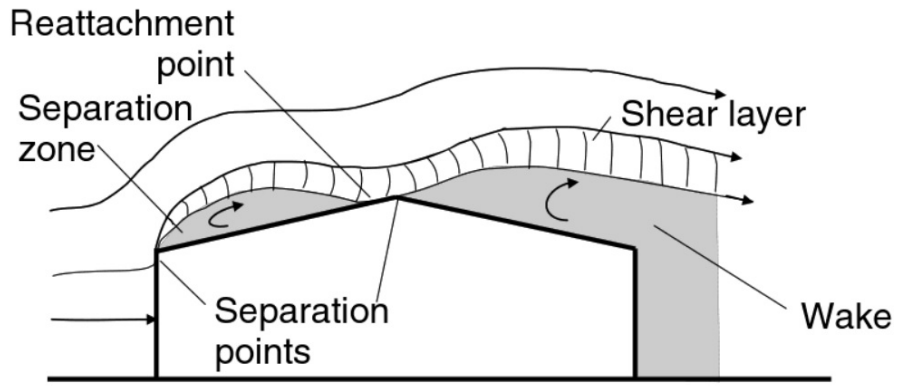

Figure 3. Flow separation and reattachment around a building with sharp edges [2]

The exact behavior of a flow (laminar or turbulent) is described by a set of Equations called the Navier-Stokes equations, presented in Equations 5-7. These Equations depict the conservation of mass, momentum and energy for an arbitrary portion of the fluid, called the control volume. Solving this system of equations yields knowledge of e.g. the velocity (direction and magnitude) of a wind flow at any point at any time in the flow field, which is important for the design of structures with complex geometry or a group of wind-sensitive structures. Due to their complicity, an analytical solution for these equations exists in only very few and limited situations, so in most real-life problems the equations have to be solved numerically. The different techniques applied and problems affiliated with them are described in later Chapters. [4]

$$\frac{\partial \rho}{\partial t} + \nabla \rho V = 0 \tag{5}$$

$$\frac{\partial \rho V}{\partial t} + \nabla \rho VV + \nabla \mathrm{p} = \nabla \tau_{ij} + \rho g \tag{6}$$

$$\frac{\partial \rho (e + \frac{V^2}{2})}{\partial t} + \nabla \rho V \left(e + \frac{V^2}{2} + \frac{p}{\rho} \right) = \nabla \mathrm{k} \nabla \mathrm{T} + \nabla (\mathrm{V} \tau_{ij}) \tag{7}$$

where e = internal energy and k = heat conductivity [5].

2.2 Wind and the atmosphere

Earth's atmosphere consists of hydrogen (78%), oxygen (21%) and other gases (1%). This fluid, air, is set to motion by pressure differences which in turn are mainly caused by temperature differences. Differences in air temperature, caused by e.g. differing amounts of solar radiation or local geographies, induce buoyancy effects that cause warmer (and thus lighter) air to rise, thus causing pressure differences. The result is a horizontal air flow over earth's surface.

The direction of this flow is affected by Earth's rotation. As the planet rotates around its axis, it deflects air currents directed towards low-pressure areas clockwise in the northern hemisphere and counterclockwise in the southern hemisphere. This phenomenon is known as the Coriolis effect and the apparent force affiliated with it as the Coriolis force. The Coriolis force is directed perpendicular to the fluid motion. The effect of the Coriolis force is depicted in Figure 4.

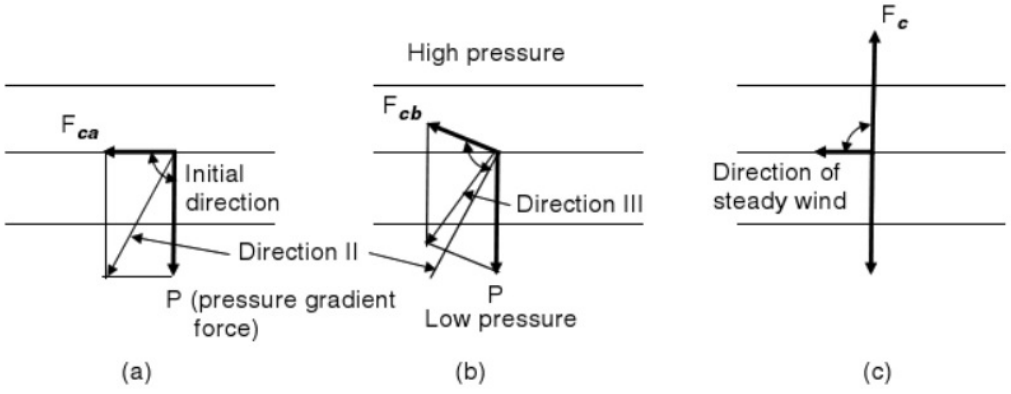

Figure 4. The effect of Coriolis force on wind direction. [2]

The third major phenomenon affecting wind flow is the friction caused by earth's surface. As stated in the previous Chapter, a flow over a surface is affected by the no-slip condition and further disturbed by surface roughness. The rougher the surface, the higher the disrupted region. Friction force will always act in the opposite direction to the wind flow. In the atmosphere this friction-effected zone is called the atmospheric boundary layer. Within this layer, wind speeds increase with height as the effect of friction diminishes. At smoother surfaces, such as over oceans, wind speed will increase more steeply with altitude while at rougher surfaces, such as over cities, the flow is more disrupted and more turbulent, and the velocity will increase slower with altitude but the flow is less stable. The effect of terrain roughness on wind speed profile is

shown in Figure 5. The height of the boundary layer is usually assumed as few hundred meters. The effect of surface roughness on wind profile within the boundary layer is usually accounted for in the norms by dividing different terrain types into a few terrain categories and using respective roughness length coefficients for these categories.

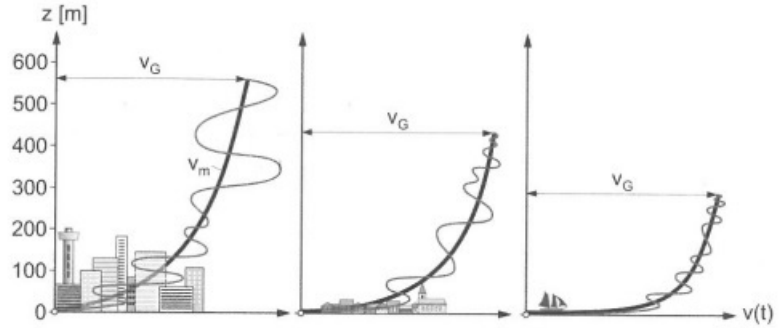

Figure 5. Wind speed profiles at different terrain types. [6]

A combined effect of these three forces is that winds originally headed directly towards low pressure centers will instead start circulating them. Since the Coriolis force is dependent on the flow velocity, which in turn is due to friction dependent on the height above ground, wind direction will be different at higher altitudes than at ground level. In wind engineering this phenomenon is called veering. The magnitude of the veering angle depends on the terrain roughness. Over open terrain the veering angle will be approximately 3° at 100 m height and 7° at 300 m height, while over suburban terrain the respective angles will be 5° and 10°. The dependency of wind velocity and direction on the height above ground can be depicted by the Ekman spiral shown in Figure 6. The effect of veering on structural design and building vibrations has not been studied in detail and it is not incorporated in most design codes.[2]

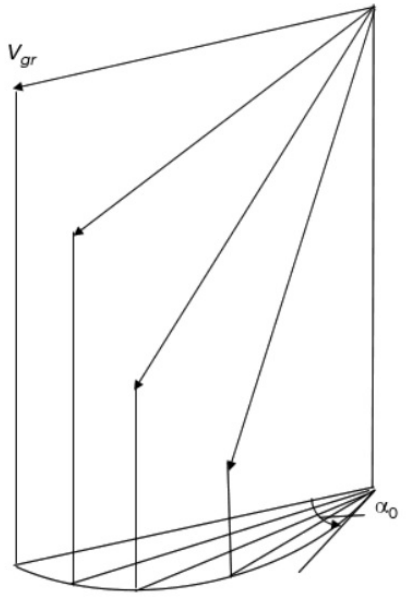

Figure 6. The Ekman spiral [2]

Because natural wind flow is practically always turbulent and the flow-governing Navier-Stokes Equations are so complex, it is not possible to describe the time-dependent nature of wind with simple functions of time and location. Therefore statistical methods are usually applied. Measurements of wind speeds at weather stations have been gathered as a basis, an example of which is given in Figure 7. In

analyzing wind effects on buildings the wind is generally assumed to consist of a stationary and time-dependent part, the mean wind speed and turbulent gusts. [6]

$$v(t) = v_m + v_t(t) \tag{8}$$

where v_m = mean wind speed and v_t = time-dependent component

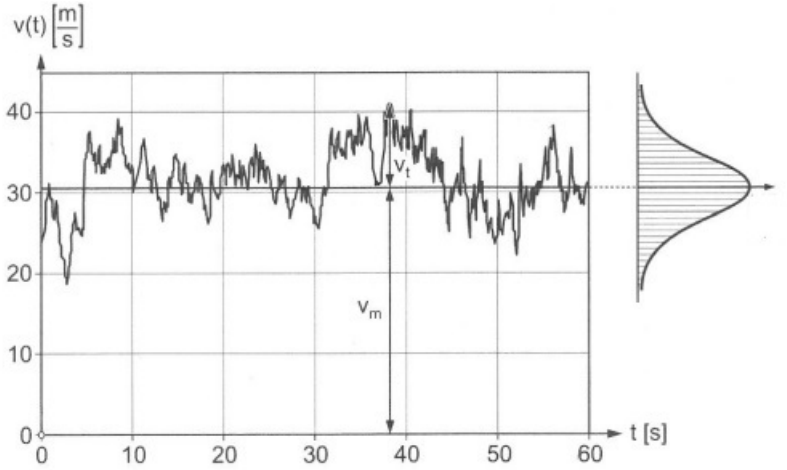

Figure 7. Measurement of wind speed time history [6]

The mean wind speed is simply a time-averaged mean wind velocity over a specified time. The magnitude of gust effects is dependent on amount of deviation from the mean wind speed. The variable commonly used to describe gustiness is the turbulence intensity, which is defined as the ratio of standard deviation of velocity fluctuation σ_u to the mean velocity over a specified averaging time [1]:

$$I = \frac{\sigma_u}{v_m} \tag{9}$$

Another important parameter of turbulence is the length scale, which relates the size of turbulent gusts to the structure. Dynamic wind effects are usually not analyzed in the time domain, but rather in the frequency domain. This transformation from measured wind time histories to frequency domain is done by first estimating the autocorrelation of the wind data. The autocorrelation function reveals obscured patterns within the measurement data, such as periodical sine functions. Carrying out a Fourier transformation for the autocorrelation then results in the power spectral density, which gives information on the distribution of gustiness on different frequencies. [7]

Large quantities of statistics have been gathered from wind. Not only velocity data has been gathered but also information about the spectral density of wind. The Van der Hoven wind spectrum is shown in Figure 8. It shows two clear peaks: the macro-meteorological peak at low frequencies, which depicts the global movement of large scale weather systems, and the micro-meteorological peak at higher frequencies, which depicts turbulent gusts etc. In designing buildings and especially in assessing their vibrations, the micro-meteorological frequency range is of interest.

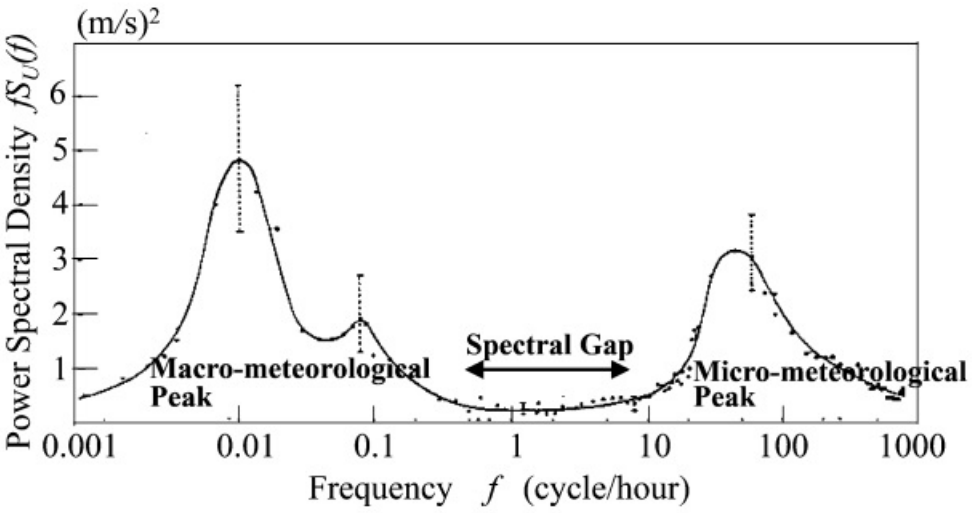

Figure 8. Wind power spectral density. [1]

Terrain features may significantly affect the local wind characteristics. An individual hill for example reduces the cross sectional area of the flow, thus choking it. As the amount of air flowing per time unit has to remain constant over the length of the flow, the flow velocity has to increase at locations of smaller cross-sectional areas. This effect causes wind velocities at the hilltop and at the windward hillside to be increased. Another common feature is a change in the governing terrain type near to the building site. When e.g. building a skyscraper near to but not exactly at the coast (say, 1km away), so that the terrain in between is of low-rise cityscape, the change from undisrupted flow over the ocean to more turbulent flow over the city may not be observable at the top level of the skyscraper. This is because the distance from the change in terrain type is too short for the boundary layer to develop to be fully representative of the new terrain category at higher altitudes. This phenomenon is illustrated in Figure 9. [2]

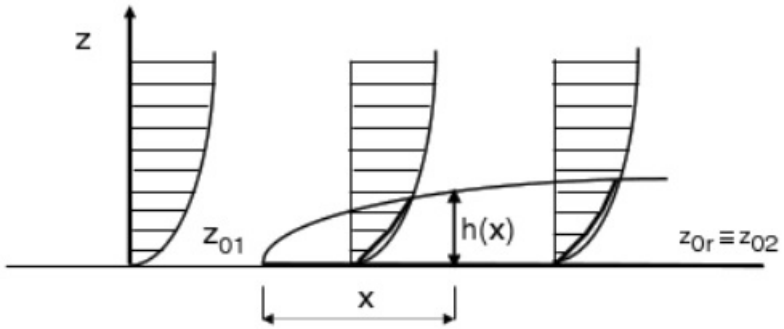

Figure 9. Effect of change of terrain roughness on wind velocity profile [2]

2.3 Structural dynamics

Many textbooks have been written on structural dynamics and the following presentation is based on [8]. As seen in previous Chapters, wind is an extremely time-dependent phenomenon and thus it produces a dynamic loading on buildings. Understanding of structural dynamics is therefore needed to analyze it. The simplest system used to portray a dynamic system is the single degree-of-freedom system (SDOF), which is depicted in Figure 10. It consists of a single mass attached to a spring and a damper moving along an axis. It's Equation of motion is written as:

$$m\ddot{x}(t) + d\dot{x}(t) + kx(t) = F(t) \tag{10}$$

where m = mass, d = damping ratio, k = spring constant, F = time-dependent external force, x = location coordinate.

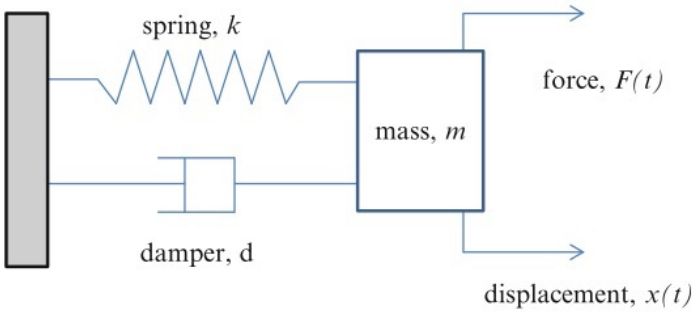

Figure 10. A single degree-of-freedom system [1]

For the natural vibration (no external loading applied, right side of eq 10 equals zero) of a SDOF an analytical solution can be easily found. First, by using the notations of dimensionless time

$$\tau = \omega_0 t \tag{11}$$

and natural angular frequency:

$$\omega_0 = \sqrt{\frac{k}{m}} \tag{12}$$

the solution can be found by using the trial function:

$$x = Ae^{\lambda\tau} \tag{13}$$

and after recombining variables and constants can be expressed as:

$$x(\tau) = Ce^{-D\tau}\cos(\nu\tau + \alpha) \tag{14}$$

where C = initial amplitude, α = phase angle and D = dimensionless damping, given as

$$D = \frac{d}{2\sqrt{mk}} \tag{15}$$

and

$$\nu = \sqrt{1 - D^2} \tag{16}$$

A graph of the solution is shown in Figure 11. It should be noted that this solution is only valid for 0≤D≤1. The coefficients C and α are to be defined from the initial or boundary conditions.

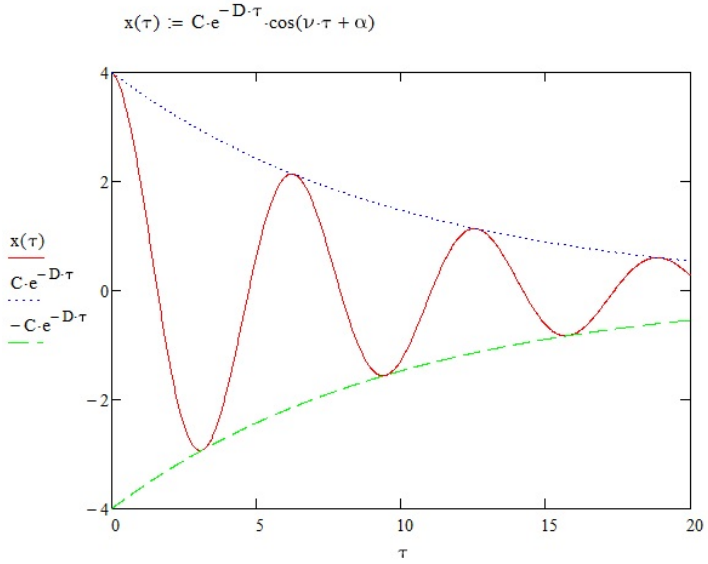

Figure 11. A viscously damped free vibration

If dynamic loading is applied to the system the situation changes slightly. The easiest type of external force to analyze is a simple harmonic loading. Now response of the system is dependent also on the loading frequency, not only on the system frequency. Also, the effect of the initial displacement will diminish with time (the homogenous solution) leaving only the particular solution to be of interest. Therefore the diminishing exponential part of the solution will drop out and only the harmonic part will remain. This leads to a reasonable trial function of:

$$x(\tau) = x_0 V_1 cos(\eta\tau - \gamma) \tag{17}$$

V_1 is the dynamic amplification factor which depends on the ratio of load frequency and system frequency and the damping ratio and can be found to be expressed as:

$$V_1 = \frac{1}{\sqrt{(1-\eta^2)^2 + 4D^2\eta^2}} \tag{18}$$

where η = ratio of the load frequency to the system natural frequency. The amplification factor is plotted in Figure 12.

The situation when the load frequency and natural frequency are the same is called resonance. With zero damping the vibration amplitude at resonance would be infinitely large. The amplitude decreases with increase of damping. Even when resonance does not occur, the response vibration of the structure will focus on its natural frequency or frequencies.

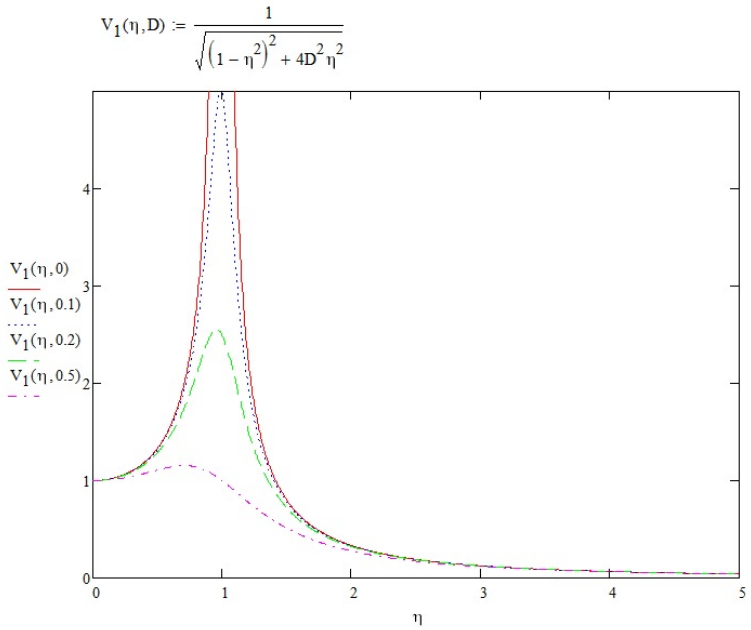

Figure 12. Dynamic amplification factor with different damping ratios.

A system with more than one degree of freedom is called a multi degree-of-freedom system (MDOF). All real buildings and structures have a large number of DOFs and should be modelled with more than one degree of freedom to gain more realistic results. A simple example of a MDOF system is a two-story frame as shown in Figure 13.

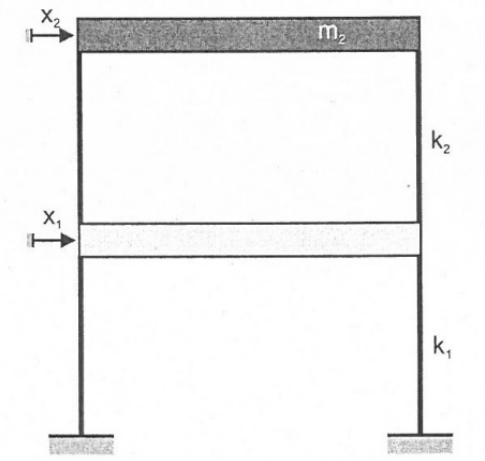

Figure 13. A two degree-of-freedom model of a two-story frame.

In MDOF systems the previously scalar values of mass and stiffness are now expressed as matrices and the displacements as vectors:

$$M = \begin{bmatrix} m_{11} & m_{12} \\ m_{21} & m_{22} \end{bmatrix} \tag{19}$$

$$K = \begin{bmatrix} k_{11} & k_{12} \\ k_{21} & k_{22} \end{bmatrix} \tag{20}$$

$$x = \begin{bmatrix} x_1 \\ x_2 \end{bmatrix} \tag{21}$$

Damping is ignored as of now and will be dealt with later on. Writing the Equation of motion with the above matrices and using a trial function similar as in expression 12 an eigenvalue problem will emerge:

$$(-\omega^2 M + K)C = 0 \tag{22}$$

The trivial solution is of course when the coefficients C are zero, which means the system stays in rest. The nontrivial solution will be obtained by solving the determinant of the part in brackets:

$$\det(-\omega^2 M + K) = 0 \tag{23}$$

which yields the natural frequencies of the system. The corresponding natural modes, expressed as the vectors Φ_1 and Φ_2, can then be calculated using the knowledge that the natural modes are independent of the actual vibration amplitudes and are only related to the ratios of the coefficients in the vectors of C. Assuming $m_1=m_2=m$ and $k_1=k_2=k$, the natural mode shapes for the 2-DOF system in question are shown in Equations 24-25 and Figure 14.

$$\phi_1 = \begin{bmatrix} 1 \\ 1.62 \end{bmatrix} \tag{24}$$

$$\phi_2 = \begin{bmatrix} 1 \\ -0.62 \end{bmatrix} \tag{25}$$

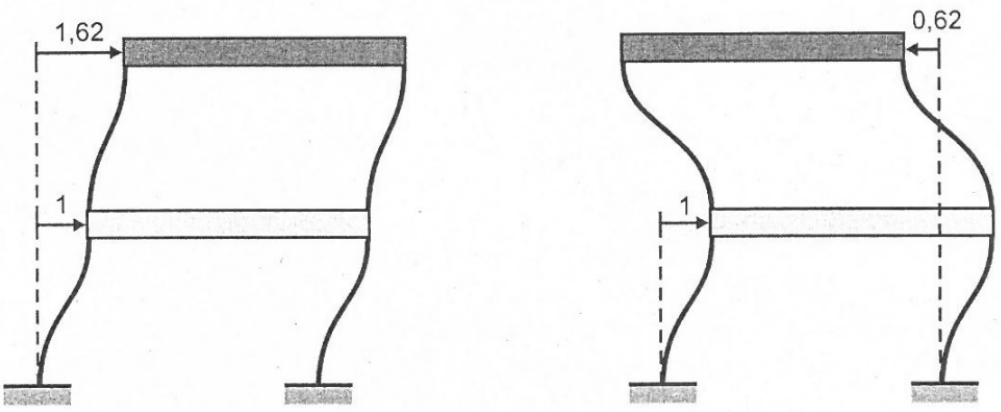

Figure 14. The natural mode shapes for the two-story frame.

Even though the mode shapes are separated, the structure will vibrate at both modes at the same time and the resulting deformations are acquired as the superposition of the different natural modes. The values of the masses and stiffness's determine what portion of the total response is due to which natural mode. Because the natural frequencies are different, the resulting free vibration will not be harmonic.

When analyzing MDOF systems, one is often interested in the contribution of different natural modes on the resulting vibration. This can be studied by the means of modal analysis. A modal matrix is the basic tool of such analysis. It is a matrix where each column is a natural mode of the structure.

$$\phi = [\phi_1 \phi_2 \dots \phi_n] \tag{26}$$

It has the property that

$$\phi^T M \phi = \begin{bmatrix} m_1^* & 0 \\ 0 & m_n^* \end{bmatrix} \tag{27}$$

$$\phi^T K \phi = \begin{bmatrix} \omega_1^2 m_1^* & 0 \\ 0 & \omega_n^2 m_n^* \end{bmatrix} \tag{28}$$

As the mass and stiffness matrices become diagonal with this transformation, the resulting n Equations of motion for n degrees of freedom become independent of each other. Therefore they can be solved separately and then combined to acquire the total response of the system. As an example, a three-story frame modelled in a similar fashion as the two-story frame in Figure 13 is loaded at every mass with a harmonic loading. By first calculating the natural frequencies and corresponding modes, performing the modal transformation and solving the resulting three differential Equations the response of the structure can be obtained. The resulting vibration of all three stories is shown in Figure 15.

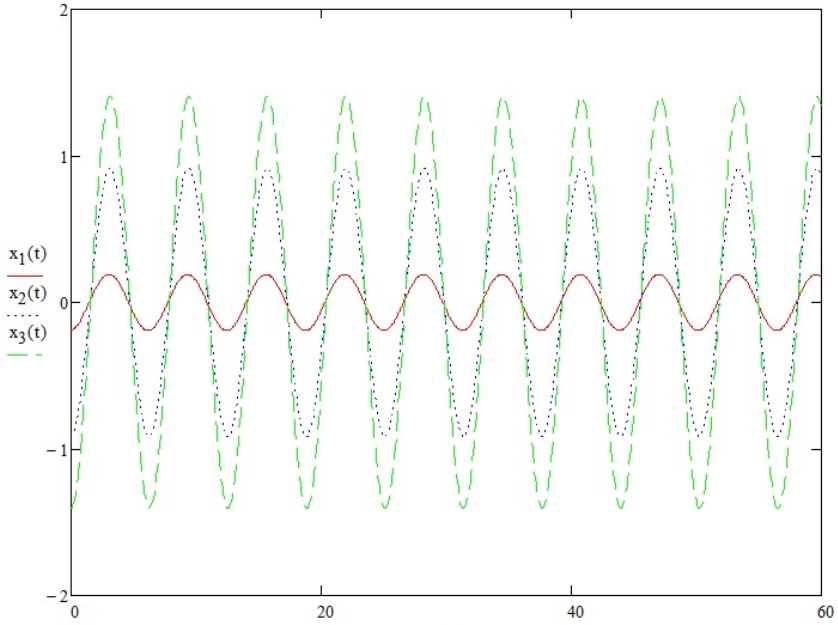

Figure 15. Steady state motion of all three stories of a three-story frame under harmonic loading.

The portions of all thee natural modes on the response as well as the total response of the third story of the system are shown in Figure 16. As can be seen, the first natural mode has by far the largest influence on the displacement response with the higher natural modes contributing only little. For this reason, all natural modes of real

buildings, which are extremely many, need not to be investigated. Instead, analyzing only the first or first few is adequate.

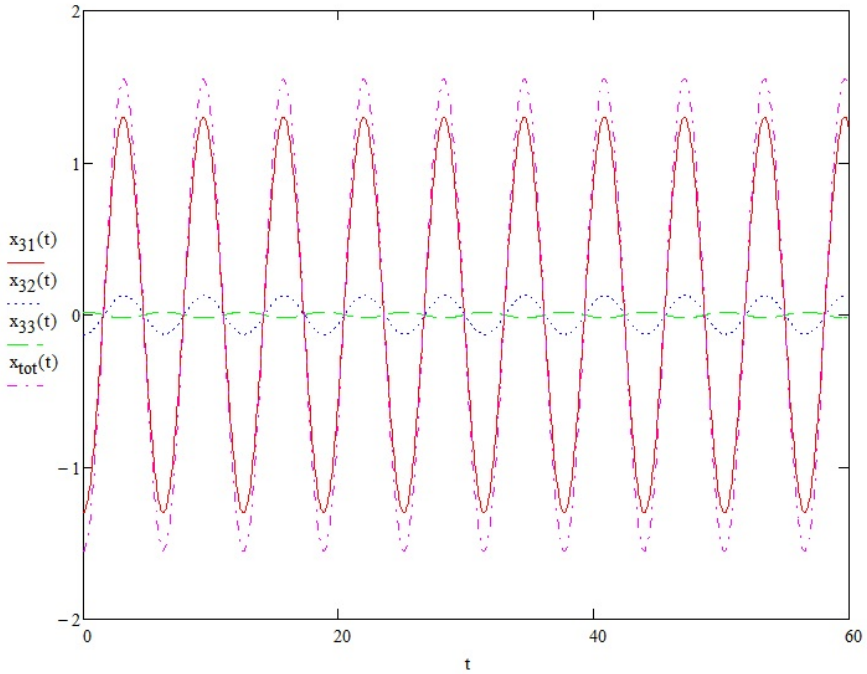

Figure 16. Total response of one degree of freedom as well as the modal components of the response.

Accounting for damping in such a system may be done by assigning separate damping coefficients to separate natural modes. These damping ratios may be defined experimentally. However, separating the original matrix-formed Equation of motion into individual natural modes becomes more complicated if the damping matrix is not related to the values of K and/or M. Methods exist for developing such damping matrices, such as the Rayleigh-damping, but whether these accurately represent the behavior of a real structure is not guaranteed.

As the system has more than one natural frequency, resonance is also possible on more than one load frequency. Usually only the lowest or lowest few natural frequencies of buildings are of interest, because they contribute the large majority of the response. Higher natural modes are usually also outside of the main portion of wind power spectrum, meaning that they contribute little to the resonant building response, as explained in the next Chapter. Therefore damping can also be taken into account merely by manually evaluating the damping ratios for the first few natural modes. [6]

2.4 Wind effects on structures

There exist several mechanisms by which wind effects structures dynamically. Buffeting is caused by the natural turbulence of wind which means that gusts of different strengths hit buildings at different locations at different times, thus directly causing a dynamic loading. Buffeting is the main excitation mechanism in along-wind vibrations and can also cause across-wind and torsional vibrations. Vortex shedding is a mechanism where vortices are shed periodically from alternating sides of the building, causing across-wind forces. Galloping is a type of aeroelasticity, where the deformations of the structure cause a change in the relative angle of attack of the wind, thus causing asymmetric pressure distributions and further amplifying the motion. Other

aeroelastic phenomena exist also, but they are relevant only for very slender structures whereas galloping is closely related to building interference, which is a focus point of this study. The vibrations in three degrees of freedom (along or across-wind and torsional) and the associated excitation mechanisms are presented in table 1. [1]

Table 1. Excitation mechanisms for different vibration modes.

	Along-wind	Across-wind	Torsion
Buffeting	x	x	x
Vortex shedding	-	x	x
Galloping	-	x	-

As illustrated in Table 1, several excitation mechanisms exist in the across-wind direction. Because turbulence is always a 3-dimensional phenomenon, natural turbulence also has a component perpendicular to the mean wind direction. This causes buffeting excitation in the across-wind direction. Vortex excitation, meaning vortices being shed alternatingly from different sides of the building, happens at all wind velocities but is especially strong at certain wind speed, called the critical wind speed, when the frequency of vortex shedding equals the natural frequency of the building. At such wind speeds vortices are shed periodically in an organized manner from different sides of the building, forming a stable vortex street in the wake of the building, also called Von Karman vortex street. Figure 17 depicts the vortex shedding phenomenon. Shedding of the vortices is usually controlled by the Strouhal law as defined by the Strouhal number

$$St = \frac{n_{st} b}{v} \tag{29}$$

Where St is the Strouhal number, n_{st} is the vortex shedding frequency, b is the building breadth and v is wind velocity. However, strong building motions may in some situations be such that they start controlling the vortex shedding instead. This phenomenon is called “lock-in”. [1]

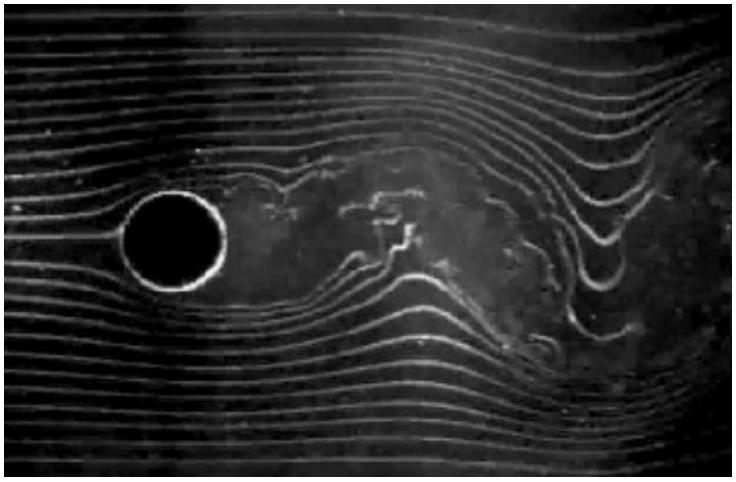

Figure 17. Vortex shedding. [1]

The third across-wind excitation mechanism to consider is galloping. If other excitation mechanisms, such as buffeting or vortex excitation, cause a building to sway in the across-wind direction, the motion of the body causes the relative angle of attack of the wind to change, as depicted in Figure 18. Thus wind which originally was perpendicular to the structure now has a component in the across-wind direction as well, notably in such a direction that for some building shapes the asymmetric pressure distribution it inflicts attempts to push the building further, amplifying the vibration. Even though aeroelastic phenomena are usually relevant only for very slender structures, two or more closely located tall buildings may be endangered to experience interference galloping.[2]

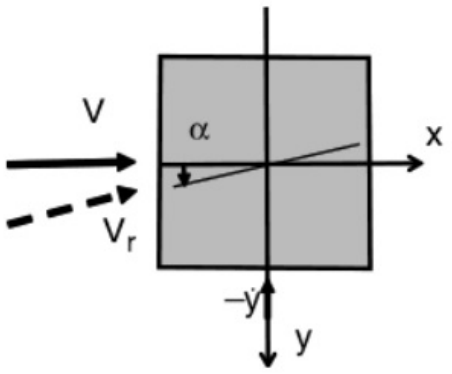

Figure 18. Change in relative wind angle of attack causing galloping excitation. [2]

An example of the effect the wind velocity has on building across-wind acceleration is shown in Figure 19, which depicts the estimated across-wind response of a super-high 150-story tower at different wind speeds. A clear bump is seen at a relatively low wind speed of slightly under 20 m/s at building top level, which indicates a vortex street phenomenon occurring. After the bump is passed, the response increases relatively linearly with wind speed. For slender buildings and structures, such as skyscrapers with high aspect ratios or chimneys, the across-wind response may be more important than the along-wind response. Vibration amplitude in the across-wind direction is usually smaller than along-wind, but acceleration values may be larger. Neighboring buildings or other obstacles may further strengthen especially the across-wind vibration.[9]

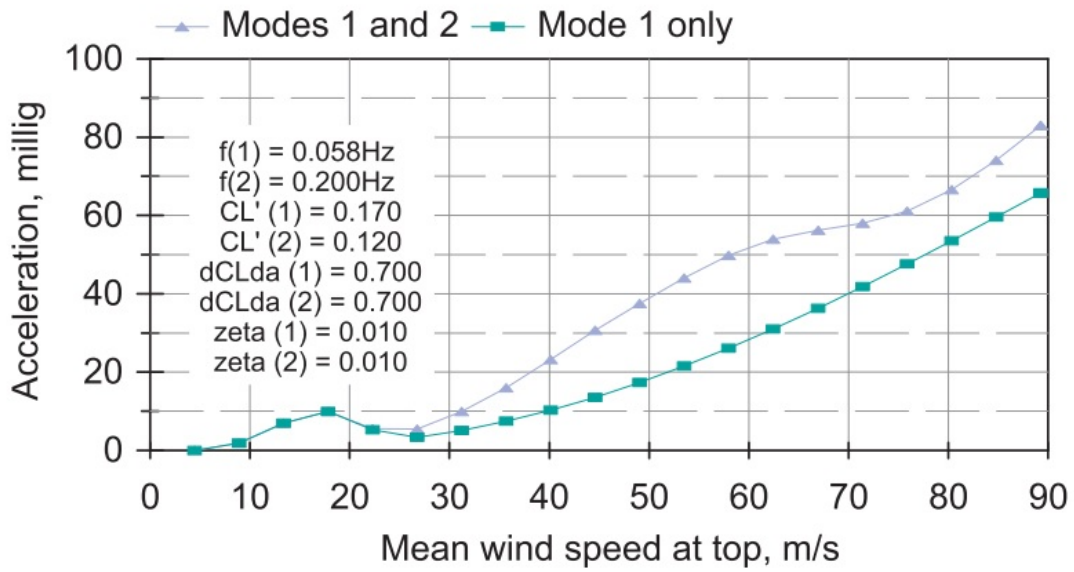

Figure 19. The estimated across-wind response of a 150-story building. [9]

As can be seen, the vortex street is a phenomenon that produces stronger than otherwise expected vibration levels at a certain wind speed, referred to as the critical wind speed. As the phenomena only occurs at very slender structures, often limited as those having an aspect ratio of larger than 6, it is mostly relevant for chimneys and other such non-building structures. Even with super-slender buildings it does not usually produce the strongest overall vibration response and is not therefore relevant for the vibration comfort criteria. Rather it is an issue related to fatigue effects of chimneys, as it occurs at very common wind speeds. The dominant building across-wind vibrations are usually caused by other excitation mechanisms, occurring at peak wind velocities. As the across-wind excitation is strongly dependent on building geometry, the building shape has an even larger effect on across-wind than on along-wind vibrations and is ever more important as the structure turns more slender.[9]

The third form of vibration that may occur is torsional vibration. As with other modes of vibration, this type of response is also fundamentally caused by fluctuating pressure differences at different parts of the building surface. These may be caused for example by buffeting of vortex excitation, but in general torsional vibrations and excitation mechanisms are so complicated that estimating their effects by any other means than wind tunnel testing is practically impossible. Some basic principles have however been identified. The possible eccentricity of the stiffening system in the building endangers the building to torsional vibrations. Buildings with a rectangular plan where the sides are of clearly different length are also more prone to torsional vibration than buildings with square or almost square plans. This is due to the fact that at a longer side the probability of uneven wind distribution is larger and the torsional stiffness of such sections is smaller than that of square sections.[1]

In general aeroelastic effects are difficult to analyze. They present complex interactions between the air and the building, where the motions of the building affect the wind flow, which then again changes the type of loading and motion induced on the building, which again affects the wind flow etc. Mostly they are only relevant for extremely slender structures, such as buildings with very large aspect ratios or light bridge decks.

Many building codes have adapted the aspect ratio of 6, meaning the building height over side length, as the limit value after the exceedance of which aeroelastic effects have to be investigated in the design.[2]

Many types of aeroelastic behavior exist. Two of them, the vortex-induced lock-in and galloping, were already mentioned earlier. Flutter is a third type which has been studied in detail. It is an even more complicated phenomenon that may occur at slender plate-like structures, such as bridge decks. It involves the structural deformations affecting the wind flow and resulting forces especially in the case of torsional vibration. The most famous example of flutter is the collapse of the Tacoma Narrows Bridge in the US in 1940, where a flutter of the deck of a suspension bridge caused the entire structure to collapse. Both galloping and flutter are examples of negative aerodynamic damping, i.e. the aerodynamic motion amplifies the vibration instead of suppressing it.[2]

Effects of neighboring buildings or other obstacles are also to consider in the design of challenging structures, especially when they may significantly affect the wind flow. This is the case in e.g. a pair or a group of skyscrapers built close to each other when rest of the surrounding terrain is low-rise. In a positive case the buildings may shield each other, but they might also redirect or concentrate wind flows so that a neighboring building actually experiences higher wind speeds than it would if it stood alone. Change of the flow direction and increase in turbulence may both expose neighboring buildings especially to across-wind and torsional vibrations. An example of the flow behavior around two closely spaced interfering buildings is shown in Figure 20. [2]

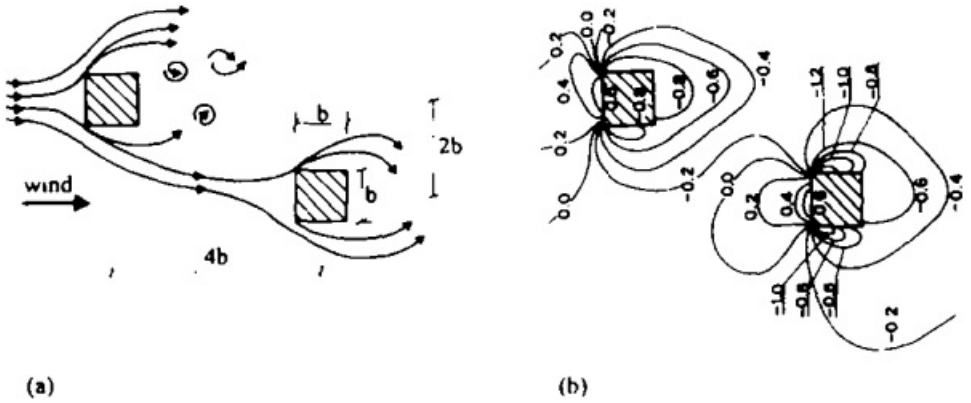

Figure 20. Example of a) the streamlines and b) the pressure distribution on two interfering buildings. In this situation a stronger negative pressure is formed on the inner side of the downstream building than on the outer side. [10]

Many mechanisms of building interaction or interference exist. These are dependent on many variables: building geometry, arrangement and dynamic properties, as well as wind profile and direction. The main excitation mechanism is wake buffeting, where the changes in turbulence of the flow cause increased buffeting response. Interference effects are also important not only for the downstream building, but they may also affect the upstream one by disrupting or altering the wake of the building, which leads to changes in vortex shedding and pressure distribution. These effects are however usually favorable. [1]

In general building interference provides a shielding effect when considering the mean wind speed. The changes in turbulence behavior may however strengthen the dynamic

part of wind and its effects, leading to vibration-related issues. Even though analyzing wind behavior becomes more complicated as the number of interacting buildings increases, the shielding effect also becomes stronger on average. Rougher terrain categories, especially in upwind direction, reduce the magnitude of interference effects. This is due to increased turbulence already present in the oncoming wind, which diminishes the effects of turbulence caused by building interference. Increase in the height of the upstream building also increases the magnitude of interference effects. Both the size and shape of the building cross-section also affect interference behavior. Some research has indicated that the larger vortices shed by larger upstream buildings increase the dynamic response of downwind buildings despite the increased amount of shielding. Orientation of the building cross-sections may also have an effect, since both or all interfering buildings don't necessarily face the wind directly at the same time (wind direction), instead some may be rotated about their vertical axis. This may expose structures especially to torsional vibrations. The spacing between the buildings is also important. The maximum distance at which interference phenomena may occur can be as large as hundreds of meters or even a kilometer in the case of tall buildings. Several researches have shown that interference produces the strongest adverse effect when the downstream building is located not exactly behind another building, as then shielding prevails and the downstream building may even behave as an aerodynamically stabilizing fin, greatly reducing vortex excitation and thus across-wind vibration of both buildings, but rather the worst case is often when the downstream building is on located at the edge of the wake produced by the upstream building. [10]

A form of interference buffeting that is also possible is that periodically shed vortices from the upwind building hit other buildings, thus producing a strong dynamical loading. The phenomenon is especially important if the natural frequency of the downstream building equals to the vortex shedding frequency of the upstream building. This type of interference buffeting is less likely to occur when the buildings are located very close to each other, because in that situation the vortices from upstream building don't have the space required to develop in an organized manner and are more likely to occur randomly. [10]

3 Methods for estimating vibration response

There are two basic categories of methods available for estimating building behavior under dynamic wind loading: simplified methods as given in building codes, design guides etc. and advanced methods. Simplified methods are usually frequency domain approaches based on wind statistics and structural properties, mainly natural frequencies, damping values and masses. They are suitable for the design of simple buildings and for preliminary estimates of more demanding structures. Advanced methods include more demanding computational analyses and wind tunnel testing. According to [11], advanced methods are required if the building is not of regular shape, it has response characteristics subjecting it to across-wind loading, vortex shedding, galloping or flutter, or if the location of the building is such that topography or neighboring buildings may cause significant interference effects.

There are several quantities that are wanted as result of wind analyses: wind pressure at different parts of the building, total wind load, deflections and accelerations. Total wind loads are used for stability calculations, making sure the building satisfies the ultimate limit state (ULS) criteria. Wind pressures (positive or negative) are needed for the design of claddings and their fastening. For total wind loads, a force coefficient method is usually applied. The oncoming wind velocity and turbulence effects are transferred to a static loading via a force coefficient, which accounts for the aerodynamics of the whole structure. For cladding design, pressure coefficients may be used. They depict the resulting wind pressure on smaller areas on the building envelope. The absolute values of pressure coefficients (which may be positive or negative) grow larger as the area considered grows smaller. This is because small scale turbulence and aerodynamic effects may cause strong very local peaks in the pressure distribution, whereas for a larger area these effects are averaged out. [1]

Deflections and accelerations are needed for the service limit state (SLS) design. Deflection limits are to make sure that no aesthetic issues arise, such as damage to secondary structures or clearly visible deformations, which might cause unnecessary concerns in building users. For vibrations, the main criterion is building acceleration. Depending on the type of building the engineer must evaluate one or more of the following building responses: along wind, across wind, torsional response and aeroelastic effects. [1]

3.1 Wind tunnel testing

Wind tunnel testing is the most widely used and reliable method for precise analysis of wind effect on buildings. Different types of analyses can be performed to obtain different results. A boundary layer wind tunnel is usually used when analyzing wind effects on buildings. In such a tunnel, wind blows in at one end of the tunnel at a constant velocity. The building model or models are usually located 15-30 m away from the air inflow, and the distance between includes roughing elements which generate a real-like boundary layer and turbulence conditions. A view from inside a boundary layer wind tunnel is shown in Figure 21. Correcting factors have to be applied to account for the scale of the model. Three different types of analyses may be performed in wind tunnels. [2]

A rigid pressure model includes a rigid building model with an adequate number of pressure sensors. These sensors then record the wind pressure at different locations on the building surface. The results may be used for the design of claddings and to compute a resulting total wind force, which may be used for design of the frame. Wind-induced vibrations cannot be analyzed by this method alone. [2]

A high frequency force balance (HFFB) analysis is performed by attaching a rigid building model on an extremely sensitive scale, which then records the time-history of resulting pressures of the scale, from which total forces and moments of the building can be calculated. The vibrational behavior of the building can also be estimated computationally from the spectra obtained from the results. HFFB method is the most widely used of all wind tunnel techniques. [2]

Most precise results are obtained from an aeroelastic building model. There are different types of aeroelastic models available but their common factor is that they all depict the building deformations at least to some extent. Thus the results obtained from such models are the most accurate ones available. A drawback of testing aeroelastic models is that the construction of such models and carrying out the tests is difficult and labor intensive, making it time consuming and expensive. [2]

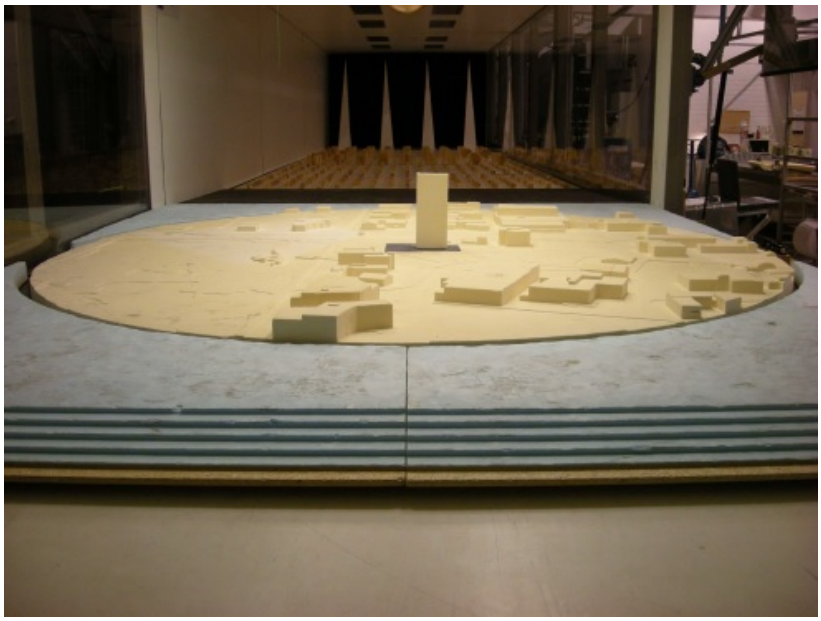

Figure 21. View inside a boundary layer wind tunnel. [7]

3.2 Computational fluid dynamics

Computational fluid dynamics (CFD) attempts to simulate the fluid flow by numerically solving the Navier-stokes equations presented in Chapter 2. The problem with this approach is that the complexity of a turbulent flow causes the required computational power to greatly exceed that available even with modern supercomputers if the size of calculation area is anywhere near that required in wind engineering applications. Therefore a different approach and some approximate methods have to be applied. [1]

The basic concept of CFD is to divide the calculation region into small elements, each of which is treated as a control volume. As the values in an element affect the values of the neighboring elements the system has to be solved iteratively starting from the initial

condition. As the problem is also time-dependent, the solution has to be updated at every time step, making the calculation heavy due to several nested iteration loops. Also, especially at highly turbulent flows the element mesh needs to be very dense to provide accurate results. [1]

To counter these problems, different turbulence models have been developed to prevent the need to solve the equations exactly. They attempt to simulate turbulence effects with additional parameters and supplementary equations, which demand less computational effort than the real equations. The drawback with this approach is that the user has to make assumptions about the problem and nature of the flow before carrying out the computation. No such turbulence model has also been developed that would yield adequately accurate results for all situations. Therefore lots of expertise is required from the user of CFD programs for the results to be at least somehow representative of the actual flow. [1]

The most commonly used turbulence models are the so-called two equation models. Several slightly differing models have been developed, but the basic one is the k-ε model. It is based on time-averaging the Navier-stokes equations, thus removing time-dependency from the problem. Instead, the k equation describes the average turbulent kinetic energy and ε the turbulent energy dissipation. Another commonly used model is the k-ω model, where ω is referred to as specific dissipation. The computation procedure in both models is fairly similar. Research and practice has shown that the k-ω model produces better results, especially at areas of negative pressure and flow reversal, but the k-ε model has better convergence rate. The abovementioned computation methods also include special wall functions to account for the small size scale effects occurring near obstacle surfaces. [1]

A promising calculation method is Large Eddy Simulation (LES). In a LES simulation large turbulent eddies are solved exactly using the actual equations from fluid mechanics and a turbulence model is only used for small scale turbulence. Time-dependent, transient results can be obtained from a LES simulation. However, the calculation costs are that much higher than with time-averaged models that as of now, LES remain purely in academic use with individual analyses carried out with supercomputers. The increased accuracy of the results and the availability of time-dependent results make LES nevertheless a very intriguing method in the near future. [1]

For vibration analysis, the major drawback of CFD calculations can be observed: with the current computer power available only static, time-averaged results can be obtained with feasible computing times. Thus recording the exact time history of wind pressure at building surface and performing a time-domain dynamic analysis, e.g. with a finite element program, is not possible. Therefore the only purely computational method for analyzing wind-induced vibrations that is in widespread use is still the spectral method presented in the next Chapter. [1]

CFD results can however be used in other ways. Time-averaged pressure coefficients may be calculated for structures of complex geometry and used in collaboration with spectral methods given in building codes. The average pressure distribution may also be used to optimize the aerodynamics of the building. Even minor changes in the building

shape may have significant effects for the flow and turbulence behavior around the structure, meaning that aerodynamic optimization can result in smaller wind pressures and loads on the building. The static CFD analysis can also be used to estimate effects of neighboring structures. By analyzing how the flow behaves around a group of structures, the possible positive or negative effects of buildings shielding or concentrating loads on each other may be estimated. An example of wind flow around two closely spaced buildings calculated with a CFD program is shown in Figure 22. The same applies also for topography, so the effect of hills or other elements may be estimated. Also the effect of buildings on wind behavior at ground level can be estimated, which can be used for assessment of pedestrian comfort. In building physics, CFD analyses made on wind behavior can be used to estimate e.g. the effectiveness of the ventilation system or heat convection from the building. [1]

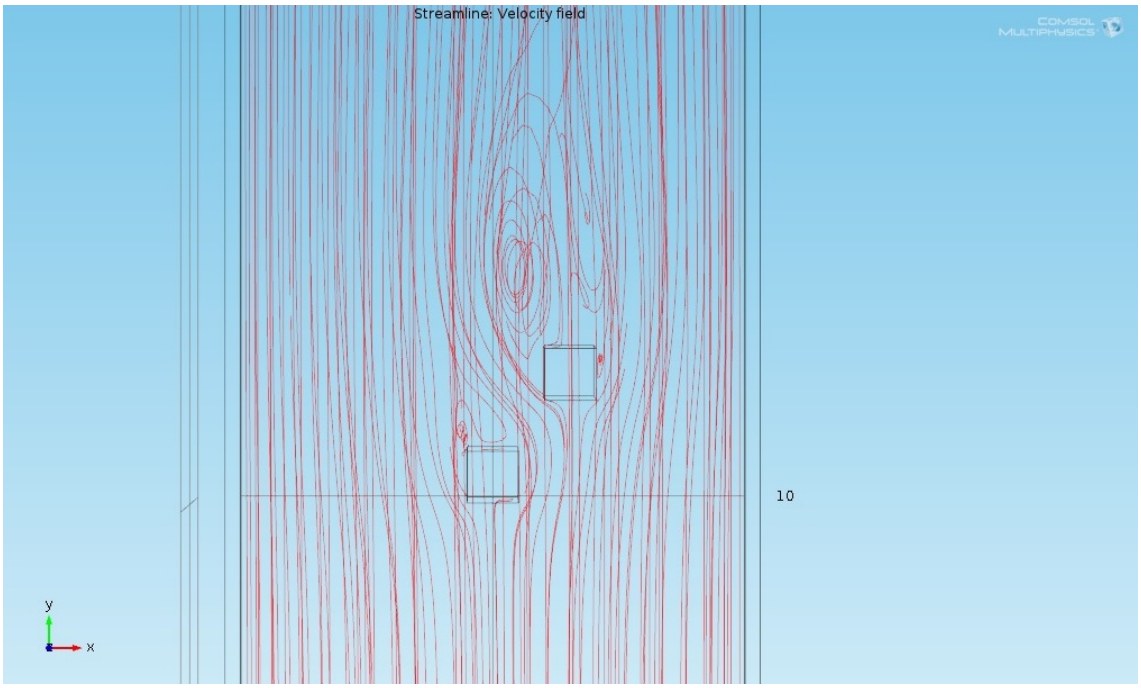

Figure 22. Wind flow around two buildings calculated with Comsol Multiphysics software using the k-ε turbulence model.

When carrying out CFD calculations using a two-equation turbulence model, the value of turbulence energy gained from the analysis may also be used to estimate turbulence phenomena. Larger turbulence kinetic energy means more turbulence in the flow, which in turn means larger possibility of vibration. In practice, this is done by using the calculated value to estimate turbulence kinetic energy in the vibration analysis. [1]

It needs to be noted that the unreliability of CFD calculations and the large effect of the input parameters and calculation settings on results make basing design decisions and calculations only on CFD results highly inadvisable. Where the standard methods given in building norms are not adequate for the design of structures, traditional wind tunnel tests still are still required. CFD calculations may serve as preliminary estimates before wind tunnel testing is carried out or for analyzing the effects of minor changes in system geometry etc. [1]

3.3 Spectral methods

Combining the information from previous Chapters, we see that along the wind direction the stationary part of wind loading, the mean wind, imposes a purely static loading on the structure and therefore does not contribute to building vibrations. The turbulent part imposes a stochastic loading on a broad spectrum of frequencies. Estimating the vibration response caused by turbulence buffeting in the along-wind direction can be carried out by spectral methods.

First, the gust spectrum is multiplied by the aerodynamic admittance function, resulting in the wind force spectrum. This is then multiplied by the mechanical admittance function depicting the natural frequencies of the building, which results in the vibration response spectrum. This procedure is depicted in Figure 23. Two different parts can be identified from the response spectrum: the background part and the resonance part. The contribution of the background part to the vibration response is small. Most of the commonly used building codes estimate the along-wind vibration by an implementation of this procedure.[1]

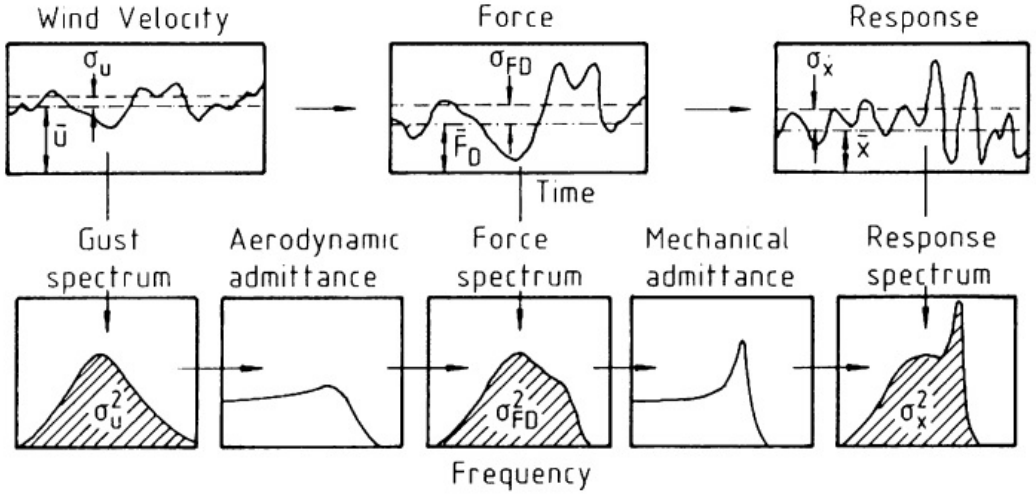

Figure 23. The spectral method [1]

3.4 Codes and guidelines

Almost all building codes provide some methods to estimate dynamic building response under wind loading. The most widely used procedure is the spectral method for along-wind vibrations, the basis of which is explained in the previous Chapter. For across-wind and torsional vibrations, the formulas may be shaped similarly as in along-wind situation, but because of the complicity of turbulence and randomness of the wind behavior, they cannot be solved analytically and these Equations are based on data gathered from wind tunnel testing. Separate estimation formulas are usually given in norms for vortex-street induced vibrations at the relevant critical wind speed. Due to the occurrence of the vortex street phenomenon at relatively low wind speeds and the fact that it is only relevant for extremely slender structures, it does not usually produce the dominant vibration acceleration value for buildings, even such that are classified as tall buildings in Finland.

The vibration assessment methods from four sources are presented below: The Eurocode, supplementary literature for the American Society of Civil Engineering

norms, the Architectural Institute of Japan guidelines and the Australian/New-Zealand building code. Of these the Eurocode and the AS/NZS standards are the only legally binding building codes whereas the AIJ guidelines are commonly accepted as useable in building practice.

Different building codes use different formulations for depicting wind profile inside the boundary layer and the standard procedure and acceptance criteria may be set for different return periods, e.g. maximum wind speed over 1-year or 5-year period. Terrain types may also be categorized differently. The methods for defining the wind speed values used in the vibration analyses are not presented here.

The basic model used in the analysis is a cantilever beam. A linear first modal shape and uniform mass distribution over building height is usually assumed. Some norms include methods to account for other modal shapes or mass distributions. Only the first natural frequency and modal shape are considered in the basic spectral method, meaning that the structural model used in the analysis can be thought of as a SDOF system as shown in Figure 24. With the assumptions of a linear modal shape and uniform mass distribution over height, the mass m will be one third of the total mass of the building.

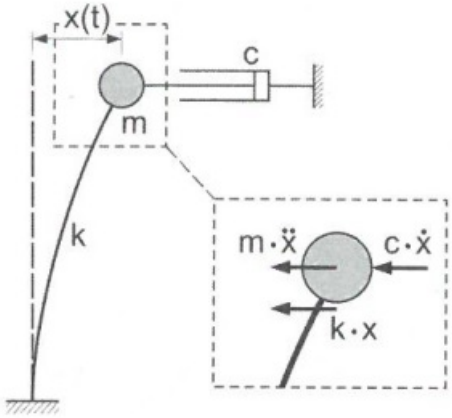

Figure 24. The structural model used in the spectral method. [6]

The building dynamic properties required in the spectral method may be defined by simplified formulas given in codes and guidelines or defined more exactly. In general it is recommended to define the natural frequencies using a relatively accurate finite element model of the building instead of the approximate formulas given in guidelines, since their accuracy is poor. This is also the commonly used practice in design, since a finite element model is almost always constructed and used for a variety of other purposes in the design process, so extracting natural frequencies from the FEA program requires very little extra work.

3.4.1 Eurocode

The eurocode is the common building code for countries of the European Union. Wind issues are dealt with in the document EN 1991-1-4 [12]. Each nation may supplement it with its own national annex, which is where e.g. the basic values for wind speed are found. The basic standard also occasionally gives two or more procedures for defining some values and the national annex may determine what method should be applied.

For along wind acceleration the EC gives two possible methods, the first of which is based on the standard Davenport spectral method explained earlier and the second is a

newer modification from it. The methods are explained in annexes B and C, respectively. For across wind or torsional vibrations no methods for calculating the accelerations are given. Instead, for vortex-street induced across wind vibrations, two methods for calculating the vibration amplitude are given in annex E and to account for torsional effects a static analysis with non-uniform wind load distribution is presented in Chapter 7. The first method for along wind acceleration is presented below.

The peak acceleration value at height z above ground is obtained by multiplying the standard deviation of the acceleration at height z,

$$\sigma_{a,x}(z) = \frac{c_f \rho b I_v(z_s) v_m^2(z_s)}{m_{1,x}} R K_x \Phi_{1,x}(z) \tag{30}$$

where $\sigma_{a,x}(z)$ = standard deviation of the along-wind acceleration, c_f = force coefficient dependent on structure geometry, ρ = air density, b = width of the structure, $I_v(z_s)$ = turbulence intensity, $v_m(z_s)$ = mean wind velocity, z_s = reference height, R = square root of the resonant response factor, K_x = non-dimensional coefficient, $m_{1,x}$ = along-wind equivalent mass and $\Phi_{1,x}(z)$ = first modal shape in along wind direction, by the peak factor (B.4)

$$k_p = \sqrt{2\ln(\nu T)} + \frac{0.6}{\sqrt{2\ln(\nu T)}} \geq 3 \tag{31}$$

where k_p = peak factor, ν = up-crossing frequency and T = averaging time for mean wind velocity which equals 600 s.

The up-crossing frequency is then defined as:

$$\nu = n_{1,x} \sqrt{\frac{R^2}{B^2 + R^2}} \geq 0.08Hz \tag{32}$$

where $n_{1,x}$ = first natural frequency of the structure in along wind direction and B = square root of the background response factor.

The background response factor is defined as

$$B^2 = \frac{1}{1 + 0.9\left(\frac{b+h}{L_s(z_s)}\right)^{0.63}} \tag{33}$$

where b = width of the structure, h = height of the structure and $L_s(z_s)$ = turbulent length scale, and the resonant response factor is defined as

$$R^2 = \frac{\pi}{2\delta} S_L(z_s, n_{1,x}) R_h(\eta_h) R_b(\eta_b) \tag{34}$$

where δ = logarithmic damping decrement, S_L = power spectral density function and R_h,R_b = aerodynamic admittance function.

The admittance functions are defined as

$$R_h = \frac{1}{\eta_h} - \frac{1}{2\eta_h^2}(1 - e^{-2\eta_h}) \tag{35}$$

$$R_b = \frac{1}{\eta_b} - \frac{1}{2\eta_b^2}(1 - e^{-2\eta_b}) \tag{36}$$

with the functions

$$\eta_h = \frac{4.6h}{L(z_s)} f_L(z_s, n_{1,x}) \tag{37}$$

$$\eta_b = \frac{4.6b}{L(z_s)} f_L(z_s, n_{1,x}) \tag{38}$$

where the non-dimensional natural frequency is

$$f_L(z, n) = \frac{nL(z)}{v_m(z)} \tag{39}$$

The non-dimensional frequency is used also in defining the power spectral density function, which gives the wind distribution over different frequencies:

$$S_L(z, n) = \frac{6.8 f_L(z, n)}{(1 + 10.2 f_L(z, n))^{5/3}} \tag{40}$$

It should be noted that the formulas given in EC for the aerodynamic admittance functions are only valid if the first modal shape does not have internal turning points. The first modal shape for tall and slender buildings can usually be expressed in the form

$$\Phi_{1,x}(z) = (\frac{z}{h})^{\xi} \tag{41}$$

The simplest case if of course when ς=1, indicating a linear shape. If we assume the first modal shape to be of the form given in Equation 38, the dimensionless factor K_x can be approximated as

$$K_x = \frac{(2\xi + 1)\{(\xi + 1)\left[\ln\left(\frac{z_s}{z_0}\right) + 0.5\right] - 1\}}{(\xi + 1)^2 \ln(\frac{z_s}{z_0})} \tag{42}$$

where z_0 = roughness length dependent on the terrain category.

Comparing the formulation of the Equations with Figure 23 clearly shows that the procedure is indeed a spectral method as explained in Chapter 2.4. The values of turbulence intensity and length scale as well as mean wind velocity are terrain-dependent and can be calculated from the eurocode. [12]

3.4.2 ASCE & literature

The American Society of Civil Engineers publishes, among many other technical publications, building standards in the USA. The wind standard is ASCE 7-10, where the latter number indicates publishing year. The norm itself gives formulas for calculating the along-wind acceleration, but many literary sources that comment and supplement the norm exist. The formulas presented below for along-wind, across-wind and torsional vibration are taken from [2].

The peak along-wind acceleration is given as:

$$a_{pk}(z) \approx 4.0 \frac{0.5\rho\mu_*^2 C_D B z}{M_1} R^{1/2} \tag{43}$$

where ρ = air density, C_D = total wind force coefficient, consisting of windward and leeward coefficients C_d=C_w+Cl, B = width of the building, z = height at which to calculate, M_1 = fundamental modal mass, R = resonant response coefficient and

$$\mu_* = \frac{V(H)}{2.5\ln(\frac{H}{z_0})} \tag{44}$$

where H = building height, V(H) = hourly mean wind speed at elevation H and z_0 = roughness length.

The resonant response factor is defined as

$$R = \frac{0.59Q^2 N_1^{-2/3}}{\varsigma_1} \frac{C_{Df}^2}{C_D^2} \frac{C(\eta_1)}{1 + 3.95N_1 \frac{B}{H}} \tag{45}$$

where N_1 = dimensionless frequency and C_{df},C = aerodynamic admittance.

$$Q = 2\ln\left(\frac{H}{z_0}\right) - 1 \tag{46}$$

The dimensionless frequency is defined as:

$$N_1 = \frac{n_1 H}{\mu_* Q} \tag{47}$$

Where n_1 = fundamental frequency.

The aerodynamic admittance functions are formulated as:

$$C_{Df}^2 = C_w^2 + C_l^2 + 2C_w C_l C(\eta_2) \tag{48}$$

$$C(\eta) = \frac{1}{\eta} - \frac{1 - e^{-2\eta}}{2\eta^2} \tag{49}$$

with the functions

$$\eta_1 = 3.55N_1 \tag{50}$$

$$\eta_2 = 12.32N_1 \frac{\Delta}{H} \tag{51}$$

where Δ = smallest of the building dimensions.

We see that even though some Equations are formulated differently and the coefficients don't exactly match, the basic method is still the same as in the Eurocode. The results obtained from the two methods are also close to each other, as will be shown in Chapter 6.

The formulas for across-wind acceleration in [2] are noticeably less complicated, as they are empirical formulas. The acceleration is defined with the help of the deflection, given as:

$$y_{pk}(z) = C[\frac{V(H)}{n_1\sqrt{A}}]^p \frac{\sqrt{A}}{\varsigma_1^{1/2}} \frac{\rho}{\rho_b} \frac{z}{H} \tag{52}$$

where C = an empirical constant which equals 0.00065, A = area of horizontal building section, p = empirical constant which equals 3.3 and ρ_b = mass of building per unit volume.

Using the deflection, the peak acceleration is then given as

$$a_{pk}(z) = (2\pi n_1)^2 y_{pk}(z) \tag{53}$$

This represents the fundamental angular frequency of the building squared times the vibration amplitude. It can also be noted that the formulas are based entirely on properties of the building and empirical constant. No representation of wind behavior is present.

Empirical formulas are presented also for estimating torsional response. They are only valid if the mass and elastic centers of the building coincide. The acceleration is approximated as:

$$a_{pk}(v) \approx \frac{7.6T_{rms}v}{\rho_b AHr_m^2} \tag{54}$$

where T_{rms} = root-mean-square torsional base moment as defined in eq 55, v = distance from the elastic center and r_m = radius of gyration.

The empirically defined root mean square value of the fluctuating base torsional moment is defined as

$$T_{rms}[V(H)] = 0.0017 \frac{1}{\varsigma_T^{\frac{1}{2}}} \rho L^4 H n_T^2 [\frac{V(H)}{n_T L}]^{2.68} \tag{55}$$

where ς_t = damping ratio in the torsional mode, n_t = natural frequency in the torsional mode and

$$L = \frac{2 * 2\frac{B^2}{8}}{\sqrt{BD}} + \frac{2 * 2\frac{B^2}{8}}{\sqrt{BD}} \tag{56}$$

The radius of gyration for rectangular horizontal cross section is given as

$$r_m = \frac{(B^2 + D^2)^{1/2}}{\sqrt{12}} \tag{57}$$

We note that similarly to the estimates of across-wind response, the formulas are based on empirical constants and building properties with no representation of wind behavior. [2]

3.4.3 AIJ

The Architectural Institute of Japan publication Recommendations for Loads on Buildings [13] is commonly used in building practice in Japan. The document includes a very thorough section on wind loads, the Chapter 6, and also a large commentary supplement. It provides formulas for estimating building acceleration in along wind, across wind and torsional modes.

The peak along wind acceleration at the top of the building is given as

$$a_{Dmax} = \frac{q_H g_{aD} B H C_H C_g' \lambda \sqrt{R_D}}{M_D} \tag{58}$$

where q_H = wind velocity pressure, B = projected breadth of the building, H = reference height, CH = wind force coefficient at height H, C_g = rms overturning moment coefficient, λ = mode correction factor, R_d = resonance factor, M_D = generalized mass of building, f_D = natural frequency of the building in along-wind direction and the peak factor:

$$g_{aD} = \sqrt{2\ln(600 f_D) + 1.2} \tag{59}$$

Assuming the first modal shape to be linear, the mode correction factor λ can be set to equal 1. The rms moment coefficient is defined as

$$C_g' = 2I_H \frac{0.49 - 0.14\alpha}{\{1 + \frac{0.63\left(\frac{\sqrt{BH}}{L_H}\right)^{0.56}}{\left(\frac{H}{B}\right)^{k}}\}} \tag{60}$$

where I_H = turbulence intensity, L_H = turbulence length scale, α = coefficient dependent on the terrain category, k = coefficient, k=0.07 if H/B≥1 and k=0.15 if H/B<1.

The resonance factor is calculated as:

$$R_D = \frac{\pi F_D}{4\zeta_D} \tag{61}$$

where ζ_D = damping ratio for along-wind vibration.

The coefficient F_D is then

$$F_D = \frac{I_H^2 F S_D (0.57 - 0.35\alpha + 2R\sqrt{0.053 - 0.042\alpha}}{{C_g'}^2} \tag{62}$$

with

$$R = \frac{1}{1 + 20\frac{f_D B}{U_H}} \tag{63}$$

where U_H = design wind speed and

$$F = \frac{4\frac{f_D L_H}{U_H}}{\{1 + 71\left(\frac{f_D L_H}{U_H}\right)^2\}^{5/6}} \tag{64}$$

and

$$S_D = \frac{0.9}{\left\{1 + 6\left(\frac{f_D H}{U_H}\right)^2\right\}^{0.5}(1 + 3\frac{f_D B}{U_H})} \tag{65}$$

As can be seen, the method is very similar to the two procedures for along-wind acceleration displayed earlier. Some equations are formulated slightly differently and with different coefficients, but the basic methodology remains the same. Unlike in the method described in Chapter 3.4.2., the across-wind acceleration formulas given by AIJ are formulated more similarly to those of along-wind acceleration, even though the wind force spectrum used is based on data gathered from wind tunnel experiments instead of real wind data. The peak across-wind acceleration is given as:

$$a_{Lmax} = \frac{q_H g_{aL} B H C'_L \lambda \sqrt{R_L}}{M_L} \tag{66}$$

with

$$g_{aL} = \sqrt{2\ln(600 f_L) + 1.2} \tag{67}$$

The variables have the same meanings as for along-wind situation, only substituting the indices D by L. The new coefficients required are

$$C'_L = 0.0082(\frac{D}{B})^3 - 0.071\left(\frac{D}{B}\right)^2 + 0.22(\frac{D}{B}) \tag{68}$$

and

$$R_L = \frac{\pi F_L}{4\zeta_L} \tag{69}$$

with the new F_L

$$F_L = \sum_{j=1}^{m} \frac{4\kappa_j(1 + 0.6\beta_j)\beta_j}{\pi} \frac{(\frac{f_L}{f_{sj}})^2}{\{1 - \left(\frac{f_L}{f_{sj}}\right)^2\}^2 + 4\beta_j^2(\frac{f_L}{f_{sj}})^2} \tag{70}$$

where κ_1, κ_2 are coefficients, κ_1=0.85 and κ_2=0.02 and m=1 if D/B<3 and m=2 if D/B≥3.

The required coefficients are

$$f_{s1} = \frac{0.12}{\{1 + 0.38\left(\frac{D}{B}\right)^2\}^{0.89}} \frac{U_H}{B} \tag{71}$$

$$f_{s2} = \frac{0.56}{\left(\frac{D}{B}\right)^{0.85}} \frac{U_H}{B} \tag{72}$$

$$\beta_1 = \frac{(\frac{D}{B})^4 + 2.3(\frac{D}{B})^2}{2.4(\frac{D}{B})^4 - 9.2\left(\frac{D}{B}\right)^3 + 18\left(\frac{D}{B}\right)^2 + 9.5\left(\frac{D}{B}\right) - 0.15} \frac{0.12}{\frac{D}{B}} \tag{73}$$

$$\beta_2 = \frac{0.28}{(\frac{D}{B})^{0.34}} \tag{74}$$

The approach for torsional vibrations is the same. The formulas are shaped in the same manner but the wind force spectrum is empirical. The maximum torsional acceleration is given as:

$$a_{Tmax} = \frac{0.6 q_H g_{aT} B^2 H C_T' \lambda \sqrt{R_T}}{I_T} \tag{75}$$

where I_T = inertia moment of the building for torsional vibration and

$$g_{aT} = \sqrt{2\ln(600 f_T) + 1.2} \tag{76}$$

The required force coefficients are [13]

$$U_T^* = \frac{U_H}{f_T \sqrt{BD}} \tag{77}$$

$$F_T = \frac{0.14 K_T^2 (U_T^*)^{2\beta_T}}{\pi} \frac{D(B^2 + D^2)^2}{L^2 B^3} \; [U_T^* \le 4.5{,}6 \le U_T^* \le 10] \tag{78}$$

$$F_T = F_{4,5} \exp\left[3.5 \, ln\left(\frac{F_6}{F_{4.5}}\right) ln\left(\frac{U_T^*}{4.5}\right)\right] \; [4.5 < U_T^* < 6] \tag{79}$$

$$K_T = \frac{-1.1\left(\frac{D}{B}\right) + 0.97}{\left(\frac{D}{B}\right)^2 + 0.85\left(\frac{D}{B}\right) + 3.3} + 0.17 \; [U_T^* \le 4.5] \tag{80}$$

$$K_T = \frac{0.077\left(\frac{D}{B}\right) - 0.16}{\left(\frac{D}{B}\right)^2 - 0.96\left(\frac{D}{B}\right) + 0.42} + \frac{0.35}{D/B} + 0.095 \; [6 \le U_T^* \le 10] \tag{81}$$

$$\beta_T = \frac{\left(\frac{D}{B}\right) + 3.6}{\left(\frac{D}{B}\right)^2 - 5.1\left(\frac{D}{B}\right) + 9.1} + \frac{0.14}{D/B} + 0.14 \; [U_T^* \le 4.5] \tag{82}$$

$$\beta_T = \frac{0.44\left(\frac{D}{B}\right)^2 - 0.0064}{\left(\frac{D}{B}\right)^4 - 0.26\left(\frac{D}{B}\right)^2 + 0.1} + 0.2 \; [6 \le U_T^* \le 10] \tag{83}$$

3.4.4 Australian/New-Zealand standard

The joint Australian/New-Zealand standard AS/NZS 1170-2 [14] provides methods for calculating wind-induced accelerations in along-wind and across-wind directions. The specialty of the along-wind method is the applied boundary layer wind profile, which unlike in other norms is not defined either as the power-law method or the logarithmic method, but rather based on a more complicated wind profile and given as values at 12 separate heights, between which linear interpolation is used.

The along-wind acceleration is given as:

$$a_{max} = \frac{3}{m_{0\,h^2}} \frac{\rho_{air} g_R I_h \sqrt{\frac{SE_t}{\zeta}}}{1 + 2 g_v I_h} \{C_w \sum_{z=0}^{h} [V_{des}(z)]^2 b_z z \Delta z - C_l [V_{des}(h)]^2 \sum_{z=0}^{h} b_z z \Delta z \tag{84}$$

where m_0 = average mass per unit height, ρ_{air} = air density, V_{des} = design wind speed, bz = average building breadth, Δz = height of the building section, ζ = damping ratio, I_h = turbulence intensity, C_w, C_l = windward and leeward wind force coefficients and g_v = peak factor for upwind velocity fluctuations.

As can be seen, the formulation is again similar to all the other implementations of the spectral method presented earlier, with the exception of the integration of windward velocity over building height. This method also enables accounting for changing building shape over height, as the building breadth is inside the summation term. The peak factor for resonant response, calibrated for a 10-minute averaged velocity, is given as:

$$g_R = \sqrt{2 \ln(600 n_a)} \tag{85}$$

where n_a = first natural frequency along-wind.

The size reduction factor is given as:

$$S = \frac{1}{\left[1 + \frac{3.5 n_a h (1 + g_v I_h)}{V_{des}}\right]\left[1 + \frac{4 n_a b_{0h} (1 + g_v I_h)}{V_{des}}\right]} \tag{86}$$

And the turbulence spectrum as

$$E_t = \frac{\pi N}{(1 + 70.8 N^2)^{5/6}} \tag{87}$$

where N = non-dimensional reduced frequency.

The across-wind acceleration is given as:

$$a_{max} = \frac{1.5bg_R}{m_0}\left[\frac{0.5\rho_{air}V_{des}^2}{(1+g_vI_h)^2}\right]K_m\sqrt{\frac{\pi C_{fs}}{\zeta}} \quad (88)$$

where K_m = mode shape correction factor and C_{fs} = crosswind force spectrum coefficient, dependent on turbulence conditions and building geometry. [14]

3.4.5 Effects of neighboring buildings

Due to complexity of the air flow around a group of buildings, estimating the effects of neighboring buildings by computational methods alone is difficult. For the case of one or two buildings some approximate formulas and procedures exist, but for a larger number of interacting buildings more exact methods have to be applied. In practice this means wind tunnel testing. Several different approximation methods for building interference have been developed and are found in literature and research articles, but relatively little of this information has been adopted in building codes, mainly due to uncertainties and lack of testing of these developed methods. [1]

The Eurocode gives some guidance on the case of a single tall building surrounded by lower buildings. An instruction is given to approximate the resulting wind velocity on structures surrounding the tall building, which yields increased velocities due to channeling of wind on the surrounding structures. The code also states that for a tall building located in terrain category IV, the surrounding low-rise buildings cause the wind to behave as if the ground was at the building roof level. Therefore the wind profile may be lifted upwards from the actual ground level, producing a positive effect for the tall building. [12]

The AIJ recommendation for loads on buildings gives a method for approximating the situation of two tall buildings. The graphs displayed in Figure 25 represent a coefficient for the response of a tall building located downstream from another tall building in along-wind and across-wind direction, with the placing of the buildings given as function of their dimensions. The terrain category also has an effect on the response, because at terrain categories with more turbulence present, the increased natural turbulence diminishes the added effect of a single tall building. [13]

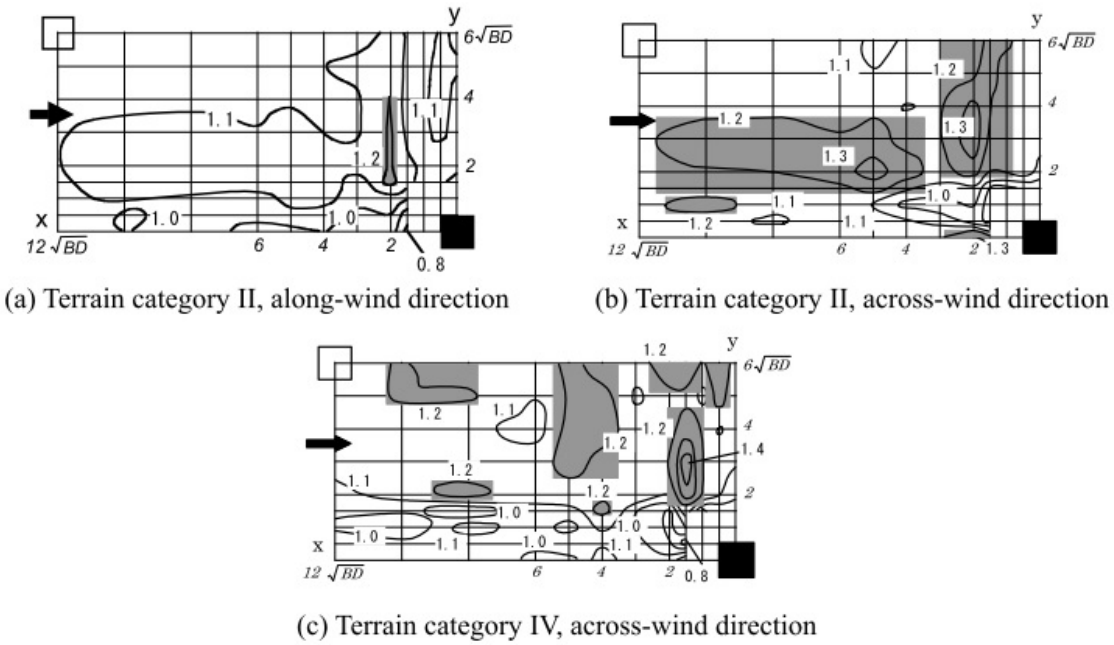

(a) Terrain category II, along-wind direction

(b) Terrain category II, across-wind direction

(c) Terrain category IV, across-wind direction

Figure 25. The effect of a neighboring tall building on building response. Note that the terrain categories stated in the picture are those of the AIJ recommendations and do not directly correspond with those given in other norms. [13]

The Australian/New-Zealand wind standard AS/NZS 1170-2 allows the use of a shielding multiplier in definition of the design wind speed. Buildings located within a 45° sector with a radius of 20h may be considered to provide shielding up to the height of their own roof level. The value of the shielding multiplier varies between 0.7-1.0 and it is defined based on the value of a shielding parameter: [14]

$$s = \frac{I_s}{\sqrt{h_s b_s}} \tag{89}$$

where I_s = average spacing of shielding buildings, h_s = average roof height of shielding buildings and b_s = average breadth of shielding buildings.

$$I_s = h(\frac{10}{n_s} + 5) \tag{90}$$

where h = height of the building to be shielded and n_s = number of shielding buildings.

Many more approximation methods can be found in scientific research articles. The graphs in Figures 26 and 27 depict the mean drag or lift interference factor for two rectangular buildings located either directly after or directly next to each other and mean along-wind and dynamic along- and across-wind for two buildings with a varying location. It can be seen that these graphs, which are based on experiment results, very often show interference factors smaller than one, which indicates a shielding effect. This effect is used in the Australian/New-Zealand standard, whereas the AIJ guideline presented earlier has a conservative attitude and only gives factors larger than or equal to unity. However, when evaluating the shielding parameter given in the AS/NZS standard, it quickly becomes noticeable that to obtain a shielding multiplier smaller than

unity, more than one shielding buildings have to generally be present (or the single building has to be huge compared to the building to be shielded).

Developing more comprehensive estimate functions is made difficult not only by the large number of variables included and the nonlinearity of their effects, but also by the labor intensity and resulting scarcity of experiment results from wind tunnel tests. In addition to traditional methods for formulating estimate functions an alternative approach is provided by Artificial Neural Networks (ANN). These are so-called learning computer algorithms used in developing functions describing nonlinear multi-variable problems. Such algorithms are first “trained” by existing experiment data to provide estimates that match with experiment results. They can then be used to estimate a situation for which tests have not been carried out. In the study of building interference this means training the algorithms with the limited data available from existing wind tunnel tests for selected building configurations and then using the ANN to estimate the resulting interference phenomena for a different configuration. Such an analysis could be used in early planning stages to find an optimal building configuration to minimize wind effects and maximize the utilization of shielding effects. The resulting designs need of course to be verified by carrying out comprehensive wind tunnel testing. [10]

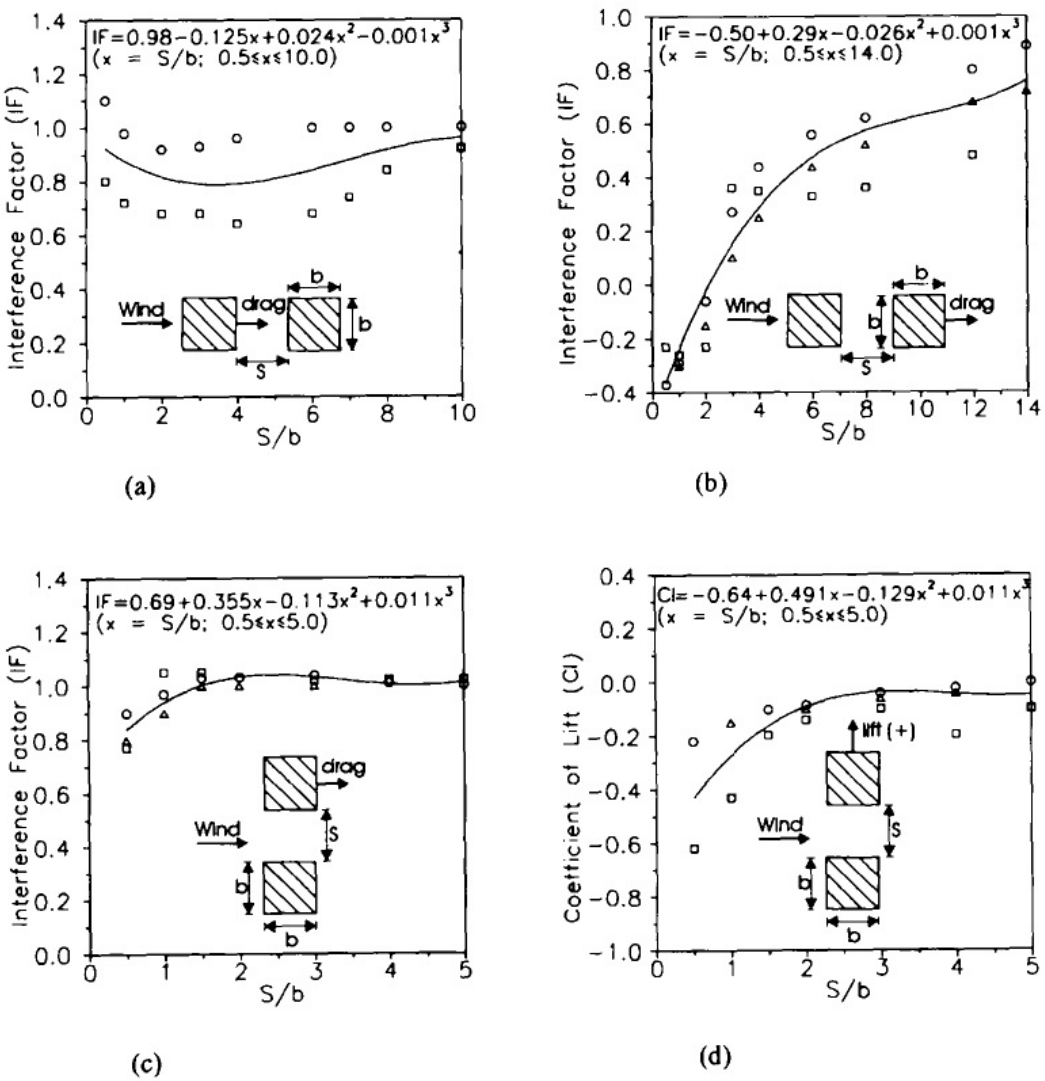

Figure 26. Mean drag or lift interference factor for two rectangular buildings [10]

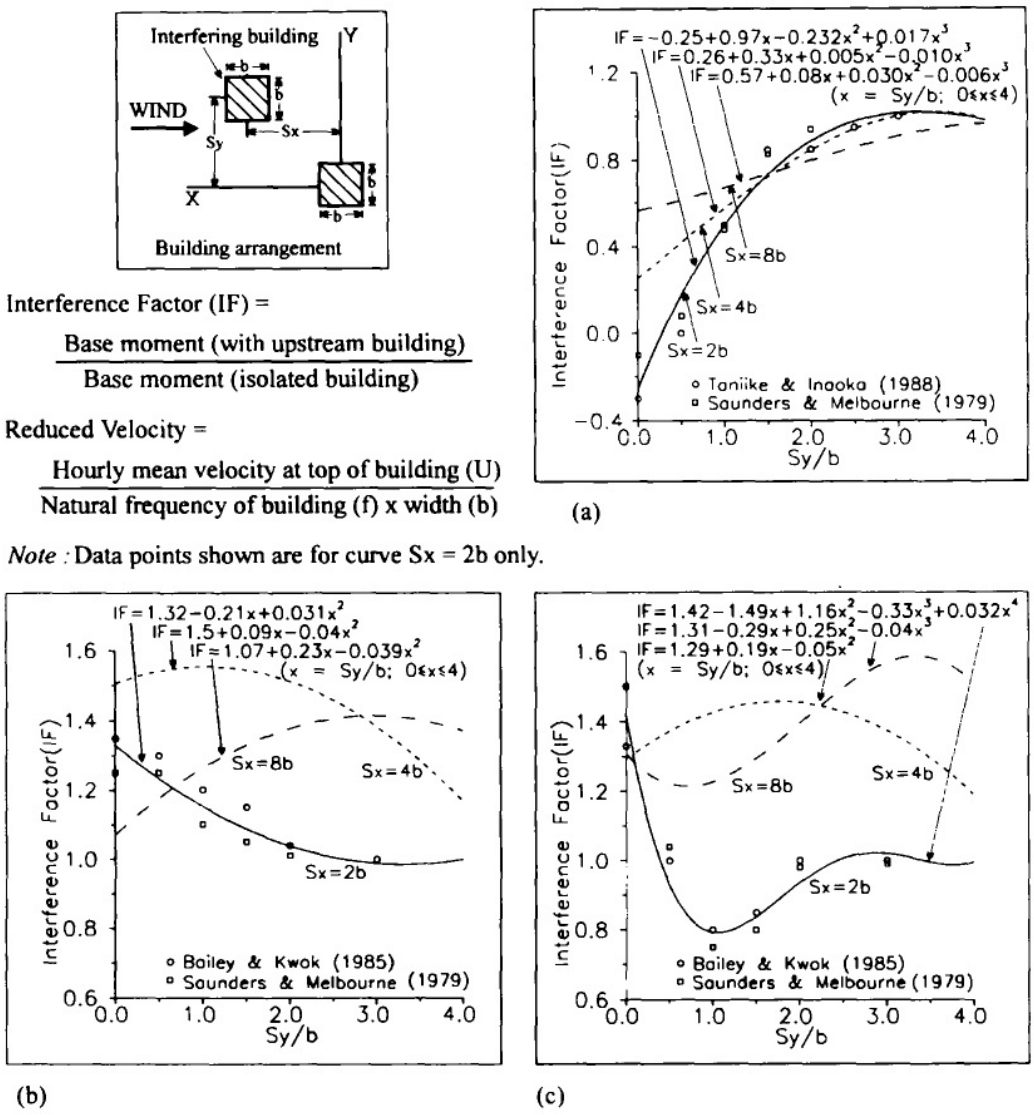

Figure 27. Mean along-wind and dynamic along- and across-wind interference factors for two buildings [10]

3.5. Other methods

Other methods for assessing wind-induced effects on buildings have also been developed and experimented with. Due to the price and time consumption of wind-tunnel testing, developing computational methods has been of interest. Varying levels of success have been achieved but widespread use of other methods than the ones described in previous Chapters is rare.

The basis of most of these methods is performing a dynamic finite element analysis, i.e. carrying out the analysis in time domain. The main advantage of such an analysis is the possibility of direct superposition of wind loading with other loads, which would enable dimensioning the structure and individual members more precisely than with the spectral methods. All higher vibration modes would also automatically be accounted for in such an analysis, unlike in the spectral method. The time history of stresses inside members would also be useful for estimating fatigue. [2]

The main difficulty with this approach is defining the loading. For such an analysis, time-dependent wind pressure distribution on the building envelope is needed. Obtaining such data is not trivial. First of all, the pressure distribution has to be precise enough, i.e. the loading time history needs to be defined for adequately many points. This large number of different time-dependent loadings makes the calculation heavy. The second problem is obtaining a time-history of the load in the first place. As wind is a stochastic process, the load history would have to represent all possible wind conditions. As in the planning stage the building is obviously not physically there and the wind conditions are greatly dependent on the surrounding terrain and structures, direct measurements of wind velocities for the new building are not available and generating such load histories is impossible without wind tunnel measurements. [2]

As explained in Chapter 2, recorded wind histories are transformed into frequency domain by a Fourier transformation to obtain the frequency spectrum. This spectrum is given e.g. in building codes. This spectrum can be transformed back into time domain via a reverse Fourier transformation. This transformation is not trivial however, as it requires the use of a random generator for determining the Fourier coefficients for the transformation. Such transformations are usually performed with MATLAB or other numerical computation software. The resulting time histories of the general wind spectrum are then combined with the local pressure coefficients on the building surface, obtained either from CFD calculations or wind tunnel tests, to acquire the final wind load. This can then be input into FEA software for the dynamic analysis. [2]

A further problem with this approach is defining the loading in across-wind direction. Even though generalized along-wind forces could be derived from wind data with a statistical distribution, the same does not apply for across-wind loads. The pressure distribution and time history on building sides is dependent on the turbulent flow and vortices generated by the building itself and is practically impossible to be estimated without wind tunnel testing. Therefore estimating across-wind or torsional vibrations with this method is even more difficult than along-wind vibrations. [2]

Another method that has been proposed is the Database Assisted Design (DAD). It utilizes the recorded time-histories of wind pressures on building envelope gained from wind tunnel experiments. This enables a time-domain vibration analysis to be performed. However, the advantages of this type of dynamic analysis may be counterweighed by the larger amount of labor needed compared to e.g. direct vibration assessment by the HFFB method. An attempt to eliminate the need of wind tunnel testing in this sort of approach is to gather extensive databases from earlier wind tunnel experiments. The existing data could be utilized in the design of new buildings if the building shape and local wind climate are similar to the old buildings. [2]

The ultimate type of computational vibration analysis would be a complete fluid-structure interaction simulation. In such an analysis the elements of CFD calculation for the air flow and dynamic FEM analysis for the structure would be combined in single software, which could then simulate the dynamic behavior of the structure under time-dependent wind loading. In theory, such analysis would reveal all aspects of building behavior under wind, even aeroelastic effects. In practice such analyses and software lies currently far beyond our reach. First of all, the computational power required would be immense. Second, even the theories of numerical computation still have difficulties

with many issues in such analyses, the most important of which is the interface between the CFD element mesh and the FE mesh. [2]

4 Comfort criteria of wind induced vibrations

As stated above, the main criterion for assessing whether the building motions are acceptable is the acceleration. People are sensitive to accelerations in building motion, but motion can also be perceived by other senses, such as sounds and visual cues. Motion perception is also very individual, with the threshold of perception varying greatly. Therefore setting one specific value as a limit for acceptable building motion is difficult. [1]

Motion perception is also not only dependent on the acceleration magnitude alone. Several studies have shown that the perception limit for acceleration is dependent on the vibration frequency. This correlation is also not linear. According to most research a certain frequency interval is more easily perceived than higher or lower frequencies. This information has been adopted in many building codes. [1]

Motion perception is also dependent on the type of activity people are exhibiting, time of day, mood etc. Limit values for acceleration have traditionally been recommended to be lower in residential than office buildings, because people at the office are more active than when sleeping at home and are thus less affected by small vibration levels. Research has also shown that people sense vibrations more easily when lying down than in other positions. Some new research however shows that even vibrations at the limit of perception may have a negative impact on work efficiency as the exposure time grows (e.g. at the end of a work day). [1]

The concept of exposure time has not traditionally been incorporated in building codes. It is a phenomenon strongly related to local climatic conditions. As the vibrations exceeding the perception limit usually occur only at peak wind speeds, the exposure time is dependent on the duration of the high wind speeds. For some geographic locations, short periods of peak wind speeds occurring very locally are typical whereas others are characterized by longer-lasting high wind speeds prevailing over large regions. Obviously, considering the effect of exposure time is more crucial at latter regions. [15]

Motion is also perceived via sounds and visual aspects. Things such as oscillating lamps hanging from the ceiling, glasses clinging against each other in the cupboard or rattling façade claddings all cause a perception of building motion and have a negative impact on occupant comfort. Minor details in the façade shape or surface material may also amplify the volume of wind “whistling” around the structure, which also increases perception of strong winds and possibly motion. Some of these effects can be eliminated by the proper design of secondary structures and interior design, e.g. by proper cladding design. [2]

Whether motion perception limit or the amount of discomfort caused by motion is also culture or ethnicity-related is another uncertain issue. A thorough research on this topic has not been made. It is known that gender affects motion perception. Women are on average more sensitive to building motions than men. The possible effect of age is largely unknown.

Different norms and guidelines for assessing vibration acceptability have been developed since the 1970’s. These limit values are mostly based on three types of

experiments: field experiments and surveys on wind-excited tall buildings, motion simulator and shake table experiments on test subjects and field experiments in artificially excited buildings. Field experiments in real buildings obviously provide most realistic results, but the unwillingness of building owners to provide their property for use in such experiments makes the amount of test result very limited. Much more extensive laboratory experiments can and have been made. A basic test set up of such experiments is to attach a real-size room model on a motion simulator or shake table, run different motion patterns on the machinery and record what observations people in the room have made on the motion. These experiments have studied the effect of different variables, which have been presented above, on motion perception. Limit values have then been set based on a chosen level of motion perception, e.g. 10% or 30% of the people perceive motion or consider it disturbing. [1]

The first building code to include criteria for building acceleration was the National Building Code of Canada (NBCC), which in 1977 simply suggested 1% of gravity acceleration (≈0.1 m/s^2) for residential buildings and 3% for office buildings as the acceptable limit values. Nowadays most design codes account for the frequency dependency of vibration perception. Some codes, such as the AIJ guidelines, give values for different perception levels instead of one single limit value, leaving the designer and/or owner of the building to assess the acceptable vibration level based on the type of building and its intended use. Frequency-dependent vibration limit curves from some norms and building codes are presented in Figures 28 and 29. [16]

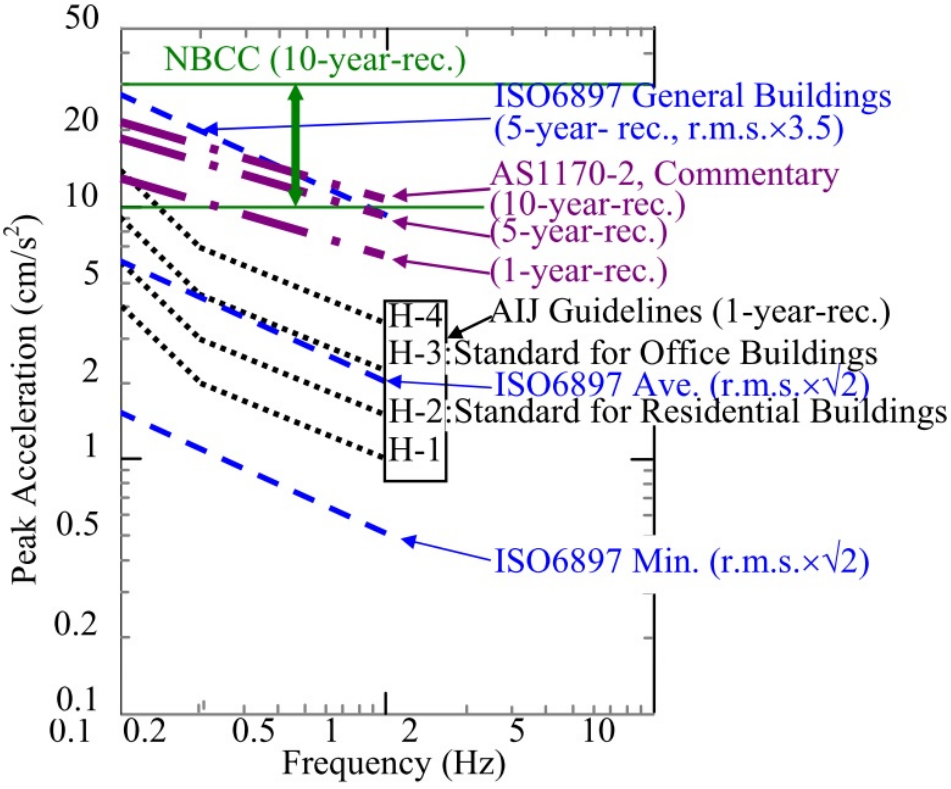

Figure 28. Frequency-dependent limit values for peak wind-induced acceleration according to different norms and guidelines [16]

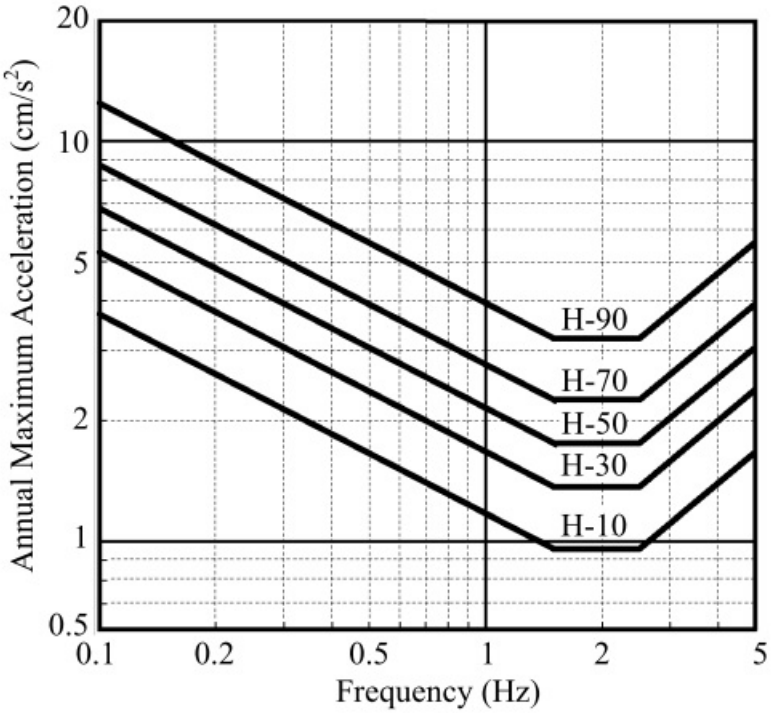

Figure 29. Different vibration perception thresholds according to AIJ guidelines 2004. [16]

Due to the frequency dependency of the acceptance criteria, acceleration values associated with different vibration modes have to be estimated separately. A reasonable first estimate is to assume vibration occurs mostly on the first natural mode in each direction, i.e. two translational and one torsional mode, and the effect of higher vibration modes is negligible. However, especially if the natural frequencies of higher modes are close to those of the first modes, their contribution may be significant. If vibration measurements are carried out using the HFFB method, as usually is the case in tall buildings, the different modal components may be identified from the response and their acceptability evaluated. [1]

Assessing torsional vibration modes includes additional difficulties. Some research has shown that people are more sensitive to torsional vibrations than translational vibrations. However, literature and research on the subject is hard to find. Limit values based on magnitude of angular velocity have been suggested, but no generally accepted acceptance criteria exist. [1]

When assessing the acceptable limit value for vibration acceleration, a key factor is the recurrence period. As explained in Chapter 2, wind velocities are based on measurements and statistical assessments based on them. The mean recurrence period means how often a certain wind speed value, and thus the resulting acceleration value, will be exceeded at a given probability. The limit values from different norms may be given for different recurrence periods, e.g. 1, 5 or 10 year period. These values need to be scaled to represent the same period in order for a comparison of the acceptance criteria to be possible. This can be done by converting the wind velocity used in calculating the acceleration to represent the desired recurrence interval. The conversion is dependent on the wind velocity distribution, which again is dependent on geography and the statistical model used. Therefore the conversions given in different sources are

not equal. The eurocode provides the following formula for a coefficient converting the basic wind speed with 50 year mean recurrence interval (MRI), corresponding to a yearly exceedance probability of 0.02, to represent a desired exceedance probability:

$$c_{prob} = \left(\frac{1 - Kln(-\ln(1-p))}{1 - Kln(-\ln(0.98))}\right)^n \quad (91)$$

where p = annual probability of exceedance, K = shape parameter depending on the extreme-value distribution and n = exponent.

The recommended values for K and n are 0.2 and 0.5, respectively, but different values may be specified in national annexes. It should be noted that a direct conversion into 1-year MRI is not possible with this formula. Other sources, such as the AIJ recommendations or British standards, provide conversion formulas that are capable of such conversions.

The limit values from different guidelines, given for different MRI, may also be scaled for comparison. The ISO 6987 [17] guidelines presents a conversion factor of 0.72 for conversion from 5-year to 1-year recurrence period. For example, for vibration at frequency 0.2 Hz, the ISO 6897 gives an acceptable rms acceleration of 0.05 m/s^2 for regular buildings with 5-year MRI. Multiplying this with a peak factor of 3.5 (which is a reasonable estimate) and the 1-year conversion coefficient of 0.72 yields an acceleration limit value of 0.126 m/s^2. Comparing this to the AIJ guideline motion perception curves of Figure 29, it can be seen that the acceptable acceleration value according to the ISO standard represents a clearly perceivable vibration. The standard itself defines this as the value at which no more than 2% of building occupants located where the motions are at their largest comment adversely about the motion. [17] The AS/NZS 1170-2 commentary limit value for 1-year MRI shown in Figure 28 is close to the ISO value, whereas the Canadian limit of 0.1m/s^2 for residential buildings with 10-year MRI is noticeably stricter at this frequency level.

The averaging times for wind speeds may also differ in norms. Most norms, e.g. the eurocode, use a 10-minute averaged wind speed with a 50 year recurrence period as the basic wind speed value. However, the method presented in Chapter 3.4.2, for example, uses a one-hour mean wind speed in calculation of the acceleration values. As the averaging time is used for defining the peak gust factor, the averaging time obviously has an effect on the resulting peak acceleration values. An hourly mean value needs to be scaled up to represent a 10-minute mean value. Some European countries also previously used hourly mean values and have now adapted a factor of 1.06 to scale the values. [18]

5 Design parameters affecting wind-induced vibrations

There are several different structural systems commonly used in high-rise construction. The first division in types of structural solutions applied depends on the main load-bearing material of the frame: steel, concrete or a combination of these two. Different frame designs are suitable for different materials. Concrete buildings usually include walls and steel buildings trusses to resist horizontal loads. Rigid frames may be constructed of either of the two materials. Typical for high-rise construction is a combination of different systems, e.g. a concrete core housing elevator shafts and staircases at the center of the building and steel trusses or rigid frames at the sides. Details of the frame, such as joint design, are also important in defining the properties of the entire system.

As shown in Chapter 2.3, the main properties affecting the dynamic behavior of a structure are its mass, stiffness and damping, whereas shape of the building affects the aerodynamics and thus the loading imposed on the structure by wind. Concrete structures inherently have larger mass than steel structures making them less prone to vibrations, but besides the choice of material, possibilities of affecting the mass of the structure are limited. Due to the nature of high-rise construction, minimizing the self-weight is usually always desirable and thus adding passive mass to the building is out of the question. The overall design of the building may affect the distribution of the mass however, which has some effect. This leaves the engineer with the possibilities of affecting the aerodynamics, stiffness and damping of the building, the latter of which is practically only realizable by the use of special damping devices discussed in Chapter 5.4.

5.1 Stiffness

Stiffness is the property most easily affected by the structural engineer. The design and dimensioning of the stiffening system can be carried out relatively exactly by modern design tools, such as finite element analysis programs. For wind design of tall buildings the goal is always to maximize stiffness within the boundaries set by architecture and economic issues. In addition to the acceleration limit values other serviceability limit state requirements, such as peak deflection or inter-story drift limits may also set the limiting minimum value for stiffness. [2]

Stiffness should always be defined as exactly as possible, e.g. the stiffness reduction caused by concrete cracking should be taken into account, since its effect is large. A simple method to account for cracking effects is to use a reduced stiffness value, e.g. by 50%, for members which may be considered to be cracked, such as plates. Structural members that are always under compression, e.g. columns, may be considered uncracked. Concrete cracking also has an effect on structural damping. Estimating joint stiffness is also crucial, especially in steel buildings, where the division between a hinge and rigid connection is not so clear. Foundation elasticity may also need to be included in the stiffness estimates. [2]

In addition to the stiffness of the main structural frame, buildings always have a varying amount of so-called “hidden stiffness”. This means the increase in stiffness caused by secondary structures, such as interior walls or claddings. For vibration control, their effect is positive, so the usual practice of excluding them from the calculations is an assumption on the safe side. [2]

5.2 Damping

As explained in 2.3, damping means the dissipation of energy from the system. In buildings, damping is caused by a variety of different mechanisms. Damping occurs e.g. as aerodynamic damping, structural damping or foundation damping. Estimating the damping of a building in the design phase can be done simply by using a building type dependent value given in norms. The eurocode, for example, gives separate values for steel, concrete and timber buildings. Other norms may further separate different building types, e.g. steel buildings constructed using welded or bolted joints. Therefore significantly affecting the vibration behavior of the structure by attempting to increase structural damping is difficult. However, damping always has a positive effect on building behavior, so maximizing it is always recommended. The exact damping ratio of a building may be defined by measurements after the building is finished. [19]

Different damping values should also be used for the ultimate limit state design used in assessing the effects of seismic loads and in service limit state design in assessing wind effects. In SLS design the structure is supposed to remain intact and serviceable, whereas in earthquake situation the only goal is to prevent the building from collapsing. The latter approach enables the use of e.g. energy dissipation in plastic deformation, which is unacceptable in SLS design. Therefore smaller damping values need to be used for design of buildings against wind than for against earthquakes. Another reason for the possibility of using larger damping values for ULS design is the joint slip, described later. [19]

Aerodynamic damping is caused by building motion relative to air. The viscosity of the fluid resists building motion causing damping. Due to the complex motions of the air flow surrounding the building, estimating the value of aerodynamic damping is difficult. Air flow also gives rise to the possibility of negative aerodynamic damping ratio, i.e. the air doesn't suppress building vibrations but rather amplifies them. For along-wind vibrations the aerodynamic damping value is usually positive, indicating a damping effect. For across-wind vibrations, negative values may be observed, indicating vibration amplification. [19]

Structural damping is caused by several different mechanisms. These include friction in micro-cracks in the material itself, friction between structural members of the frame and friction with secondary structures. The amount of structural damping is therefore greatly dependent on the structure. Concrete structures generally have higher damping values due to cracking and the friction caused by these cracks. Prestressed concrete, which is usually designed to not crack under normal circumstances, therefore has lower damping value than normal reinforced concrete. Some guidelines, for example German DIN-norms, also differentiate steel structures based on joint type. The justification for this is that bolted joints allow some movement, and thus friction, in the joint, which gives them higher damping values than welded joints. [19]

Foundation damping presents the dissipation of vibration kinetic energy into the ground below. As the soil is always somewhat elastic, motion of the building causes movement in the soil also. This means transfer of kinetic energy from building vibration to soil motion and thus damping. The magnitude of soil damping is dependent on the soil type, foundation size and geometry and also the loading, because different loading types

(vertical, horizontal, overturning moment) produce different deformations and tensions in the soil, thus altering the energy dissipation.[19]

Damping is also dependent on the type of motion the building is exhibiting. Larger vibration amplitude leads to larger damping values up to a certain threshold. This is because at small amplitudes no motion, or slip, occurs between structural members or secondary structures, meaning that damping will increase with amplitude as slip starts to occur. When the amplitude is large enough for slip to occur at all joints, the damping value has reached its peak. It should be noted that slip occurring in joints may also decrease the natural frequency due to reduction in stiffness. The frequency itself is also important. Since the natural frequency in general decreases with building height and the higher the building is, the smaller is the effect of foundation damping, it can be said that damping decreases as building height increases.[1]

As the slip between the frame and secondary structures in important, the design and amount of these structures obviously is therefore important. For example, hotels and residential buildings generally have higher damping values compared to office buildings, especially open-plan offices, due to larger amount of interior walls. [19]

Damping values given in different norms and guidelines for steel and concrete buildings are presented in Figures 30 and 31. As can be seen, there is large scatter in the values, which is to be expected considering the amount of uncertainty related to estimating damping.

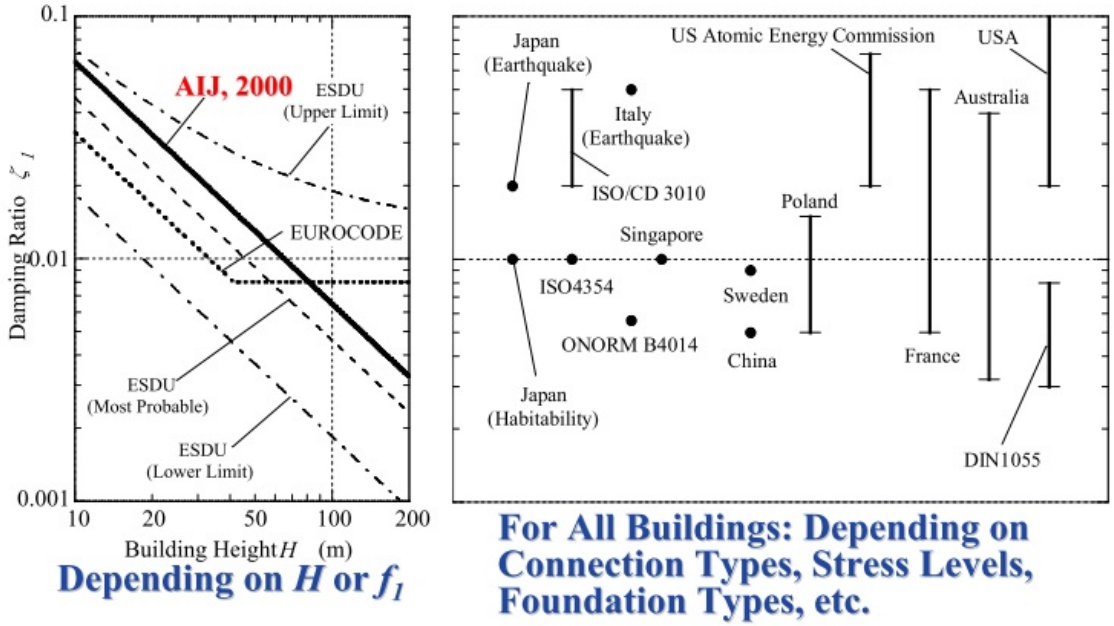

Figure 30. Damping values given for steel buildings by different norms. [19]

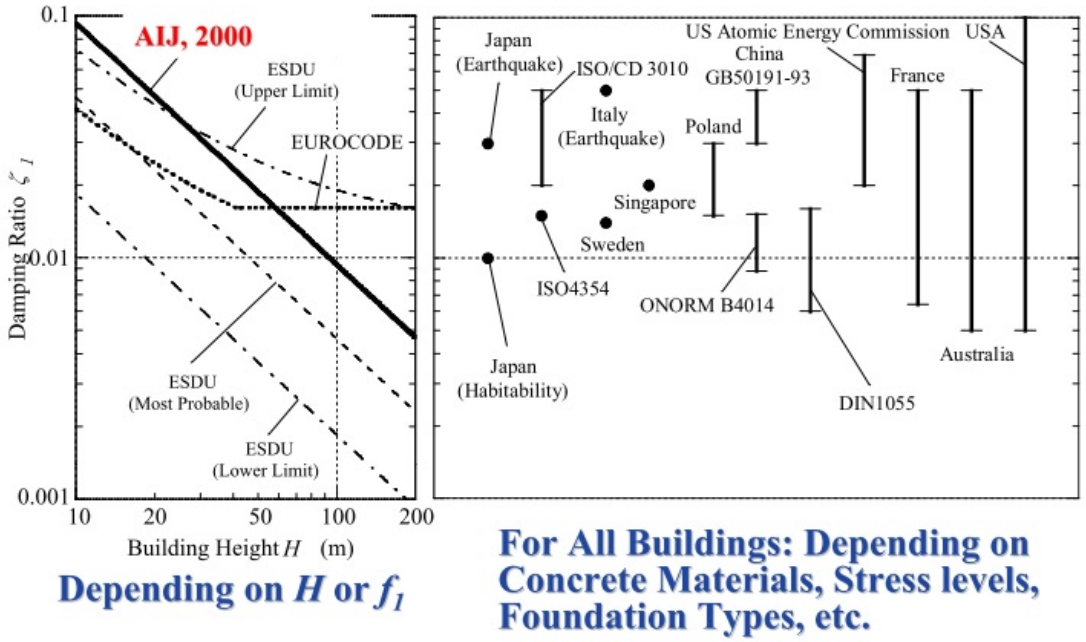

Figure 31. Damping values given for reinforced concrete buildings by different norms. [19]

5.3 Aerodynamics

As seen in previous Chapters, the building size and shape play an important role in defining the wind flow behavior around the building. This in turn means that the pressures imposed on the building by the flow are dependent on the building itself. Aerodynamic optimization is therefore crucial in economical design of high-rise buildings.

As stated in previous Chapters, for tall structures the dominant vibration phenomenon may often be the across-wind vibration. One approach to minimize this effect is breaking the shape of the building. If the building were of a regular rectangular (or circular) section, the fluctuating vortex shedding would occur at (almost) the same frequency along the entire building height. Thus making the shape more irregular, e.g. by the building turning slimmer as height increases, breaks up the regular vortex shedding pattern, leading to the fluctuating across-wind forces being out of phase with each other. This greatly reduces the across-wind vibrations. Such a design is also favorable because the mass center of the building will move lower and the surface area exposed to high wind speeds at high altitudes will be smaller. [1]

Another feature to avoid are sharp edges. They lead to large negative pressures on the leeward side, which sets higher requirements for cladding elements and exposes the structure to stronger vortex shedding in the wake. For example the corners of the Taipei 101 building are chamfered for this reason, which lead to significant reduction in the design wind load. The effect of corner rounding on the drag coefficient is illustrated in Figure 32 and some possible improvements to a square building plan are shown in Figure 33. [1]

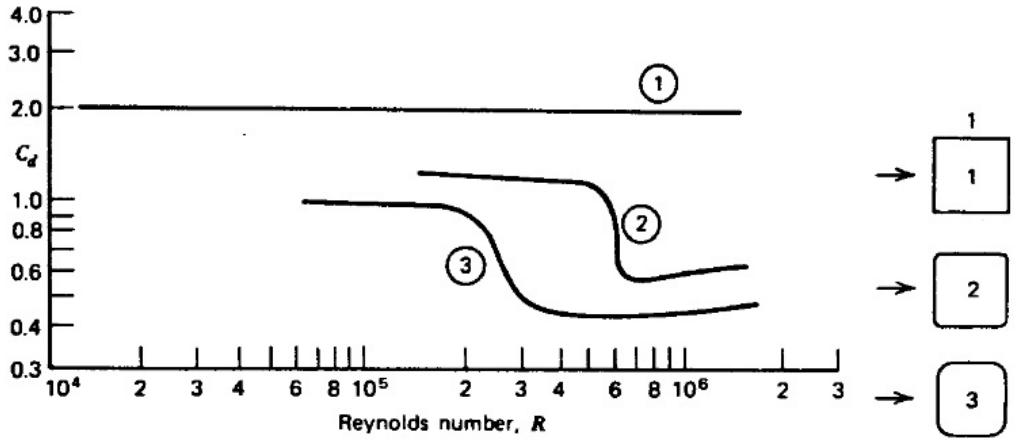

Figure 32. The effect of corner rounding on drag coefficient with different Reynolds numbers. [20]

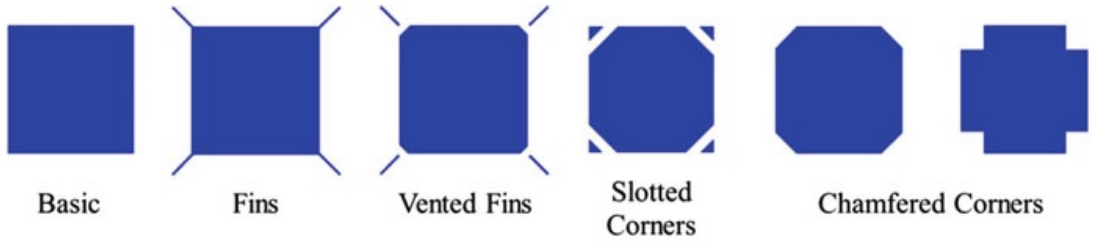

Figure 33. Aerodynamic modifications to a square building shape [1]

One solution commonly used in chimneys is spoilers. Even though they may slightly increase the surface are subjected to wind load, they may, if designed correctly, provide such a reduction in vortex shedding that their implementation is recommended. The use of spoilers in buildings is not very common mainly due to architectural reasons. [9]

Another possibility is to add openings or porosity to the building. They also aim to disrupt the creation of large or periodical vortices. The design of the Shanghai World Financial Center is aimed partly to utilize this effect. Many conceptual skyscraper designs also include openings or grooves cut at the corners of the sides of the building to achieve the same effect. [9]

The phenomena mentioned above are merely examples of the effects of aerodynamics, which is a complicated field of engineering in itself. Even very small details may have a large effect on aerodynamic behavior. Aerodynamic optimization has traditionally been carried out by wind tunnel testing, but CFD analyses are emerging as an alternative or at least as a supplement for them, enabling preliminary aerodynamic design at a lower cost than wind tunnel experiments. Aerodynamic optimization requires strong interaction between the architect and the engineer, which may not always be trouble-free. [9]

5.4 Vibration control devices

Commonly used vibration control devices include Energy Dissipative Devices (EDD) and Tuned Mass Dampers (TMD). EDDs are added between two points in the structure (or between the structure and the ground) that move in relation to each other. Such dampers simply add damping to the overall system and their analysis is thus relatively simple. A typical damper element used is a viscous damper, where a piston is moving

inside a cylinder filled with oil and the damping effect is caused by friction of moving the oil. EDDs may also be constructed from special polymer materials, where hysteresis effects of the material are the main working principle. Such elements are referred to as viscoelastic dampers. Viscous dampers are also usually included in tuned mass damper arrangements. [1]

As stated, viscous dampers need to be positioned so that they are connected to two points which are not stationary with each other. The problem in designing such systems comes from the very large number of possible damper arrangements: different damper types with different properties may be used, they may be positioned on different places, on one or more floor levels etc. Finding the optimal damper configuration is thus possible only with an adequate level of practical experience or optimization algorithms. One possible arrangement is to position the dampers between the lower chord of a truss and the column to which the truss is connected, as depicted in Figure 34. Thus, when the columns deflect, the damper elements start working. Such a system was employed e.g. in the World Trade Center twin towers in New York City. Other arrangements that have been utilized include e.g. positioning damper elements as diagonals on frames, examples of which are shown in Figure 35.

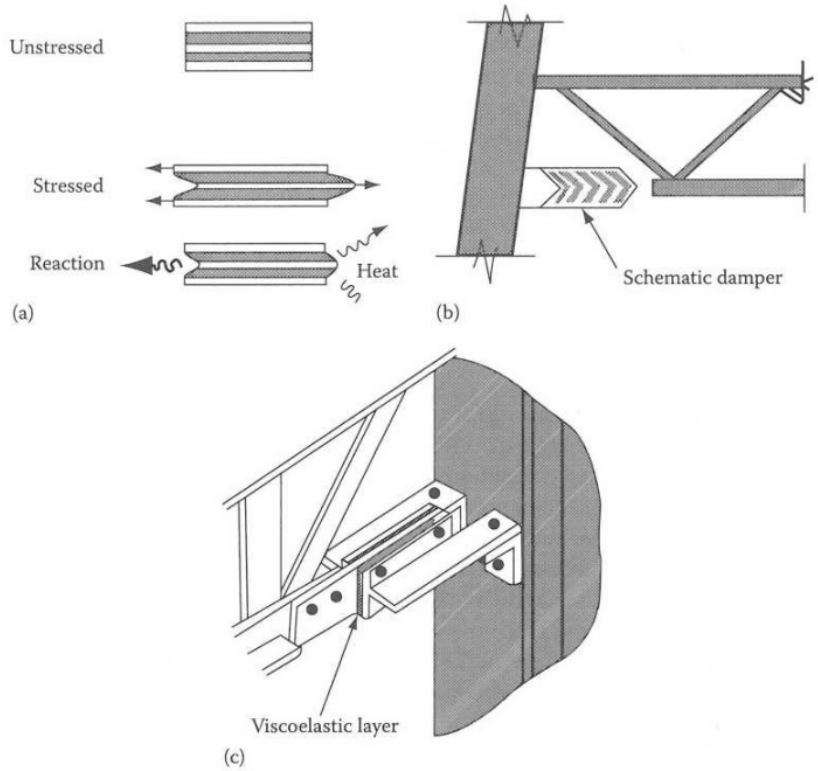

Figure 34. Arrangement of viscous dampers in the WTC twin towers [24]

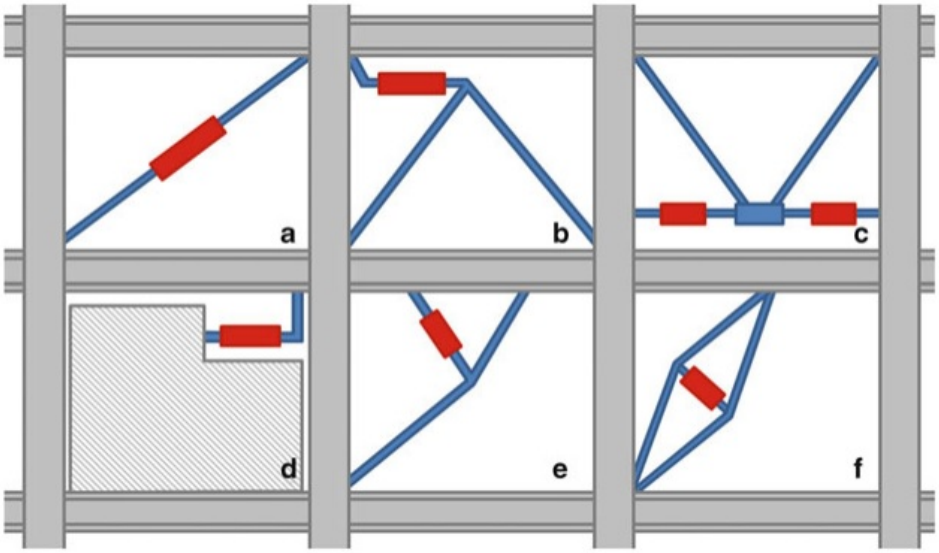

Figure 35. Different possibilities for positioning dampers as diagonals within a frame. [1]

Tuned mass dampers are also commonly implemented vibration control devices. They can be divided into passive and active TMDs. Passive TMDs function entirely mechanically whereas active dampers are electrically controlled. Both have been used in high-rise buildings, but passive ones are more common.

The working principle of a tuned mass damper can be understood by analyzing a SDOF system, as presented in Chapter 2. The amplification factor for the dynamic loading is as in Figure 12. Considering a two-degree of freedom system as shown in Figure 36, a similar graph depicting the dynamic amplification factor can be plotted for both masses (degrees of freedom) and is shown in Figure 37.

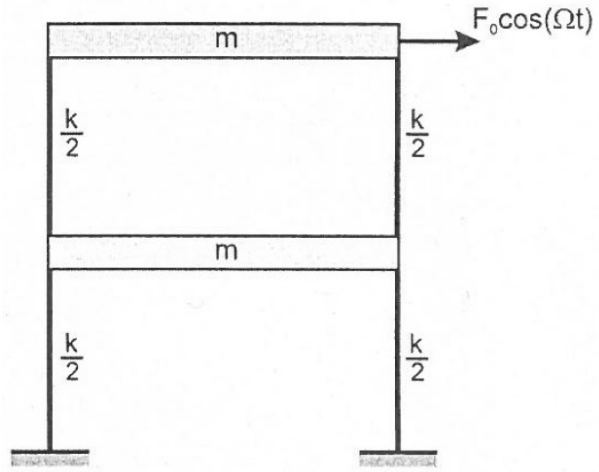

Figure 36. A two-story frame under harmonic loading.

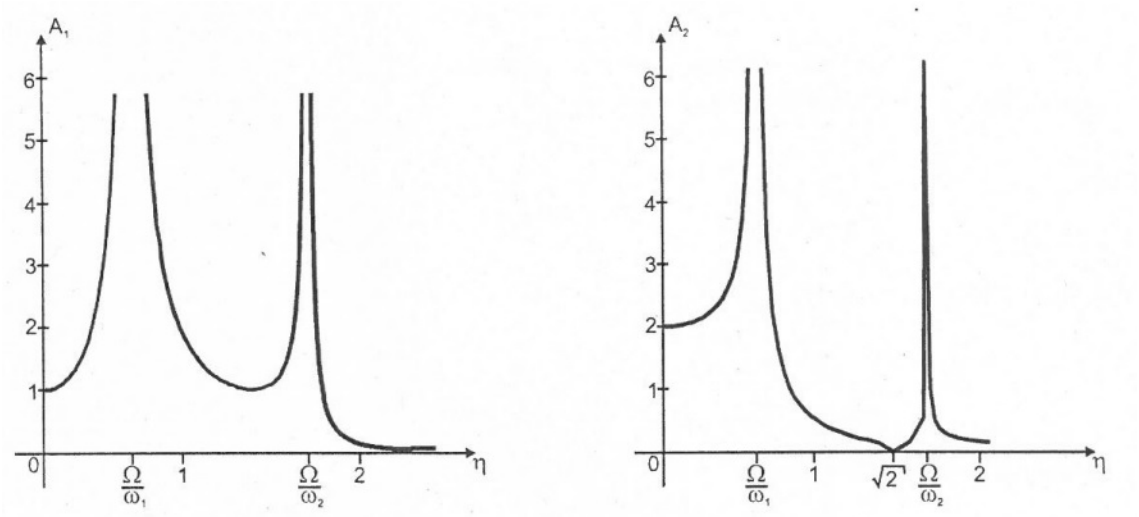

Figure 37. Amplification factors for both degrees of freedom.

It can be seen that the 2-DOF system has two natural frequencies and thus resonance is possible on two separate load frequencies. It can also be seen that at a certain load frequency the displacement of the top story drops to zero and only the bottom story is vibrating. The amplification factor for the bottom story is 1, meaning that the entire load is acting on the damper.

A usual arrangement of a TMD is to attach an additional mass via spring and damper to the original structure, as in Figure 38. The desired working frequency of a TMD, which is usually one of the natural frequencies of the building, is achieved by a correct ratio of stiffness k and mass m. TMDs are most efficient when located at the position of maximum motion amplitude in the building, meaning that they are usually located near to building top level.

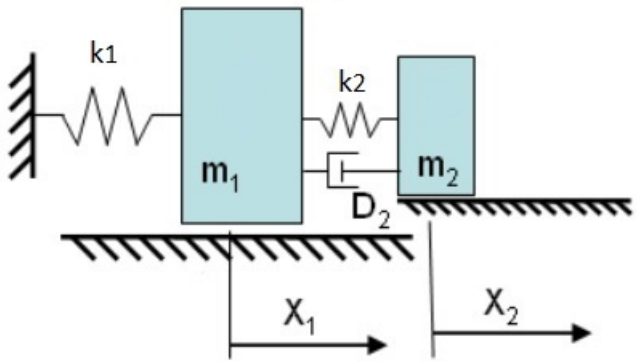

Figure 38. A TMD configuration where an additional mass m_2 is attached with a spring and damper to the original mass.

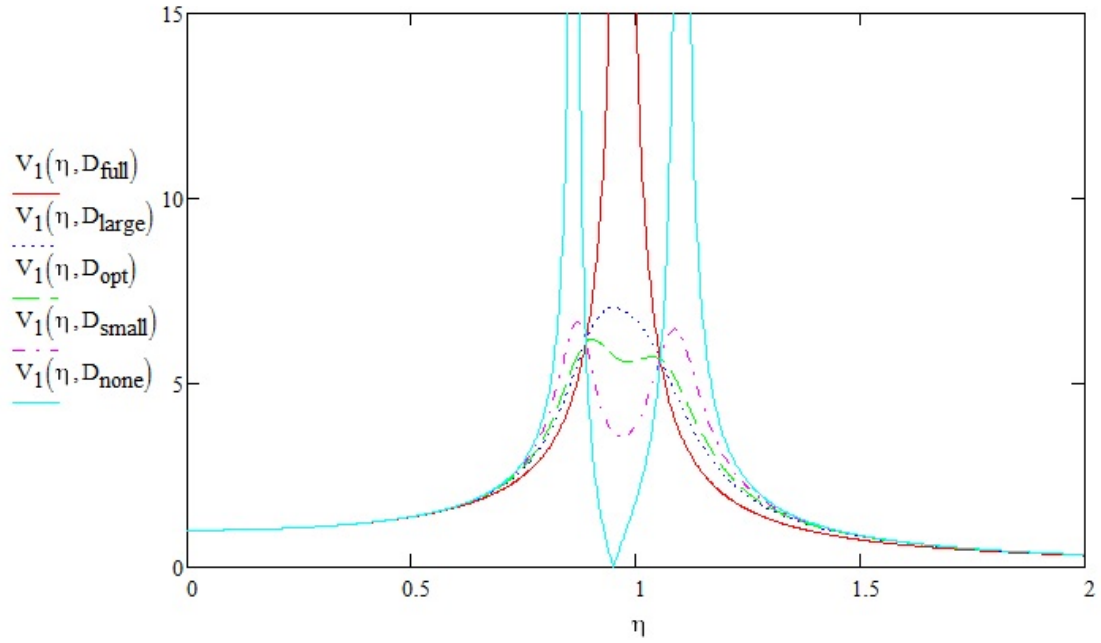

Figure 39. Vibration amplitude for the original mass with TMD attached with different damping values of the TMD arrangement.

Even though the tuned mass damper effect is irrelevant of the mass m and stiffness k themselves, only of their ration, a choice of too small m leads to two major issues. First, the vibration amplitude of the TMD grows to unreasonably large values. Second, the smaller the mass the closer the emerging new resonance frequencies are to the original frequency. Estimates for a suitable damper mass are found in literature.

TMD elements used in practice often incorporate damper elements between the original system and the damper. Most importantly these dampers reduce the amplitude of resonance vibration, because the resulting vibration is more damped than in the original system and thus the amplitude stays smaller. Choice of the damping amount D is not trivial, i.e. larger damping is not automatically better. Too small amount of damping of course does not provide the desired level of energy dissipation, but a too large damping value hinders the motion between the original structure and the new mass, thus eliminating the desired TMD effect. Guidance for optimizing the values of k, m and D can be found in literature. Figure 39 shows the amplification factor for a SDOF system with a TMD attached to it with different damping values for the damper between the original system and damper mass. The masses and stiffness's of both, original system and mass are constants in the graphs. [6]

In practice tuned mass dampers can be built out of a variety of different arrangements. The most famous TMD applied in a high-rise building is probably the pendulum on top of the Taipei 101 tower. It consists of a large ball assembled from steel plates which acts as the vibrating mass and viscous dampers attached to it. Many different arrangements exist also. The John Hancock Tower in Boston includes two steel and lead masses attached to springs and dampers sliding on a lubricated metal bed at the opposite sides of the building. Their main task is to protect the building from torsional vibration. A representation of the TMD arrangement in Citicorp Center in New York is shown in Figure 40. Some TMDs use fluids, such as water, as the vibrating mass. The advantage of this type of assembly is that the internal friction of the moving water also acts as a

damper. Fluid-based TMDs may come in the forms of e.g. sloshing tanks or liquid columns. [1]

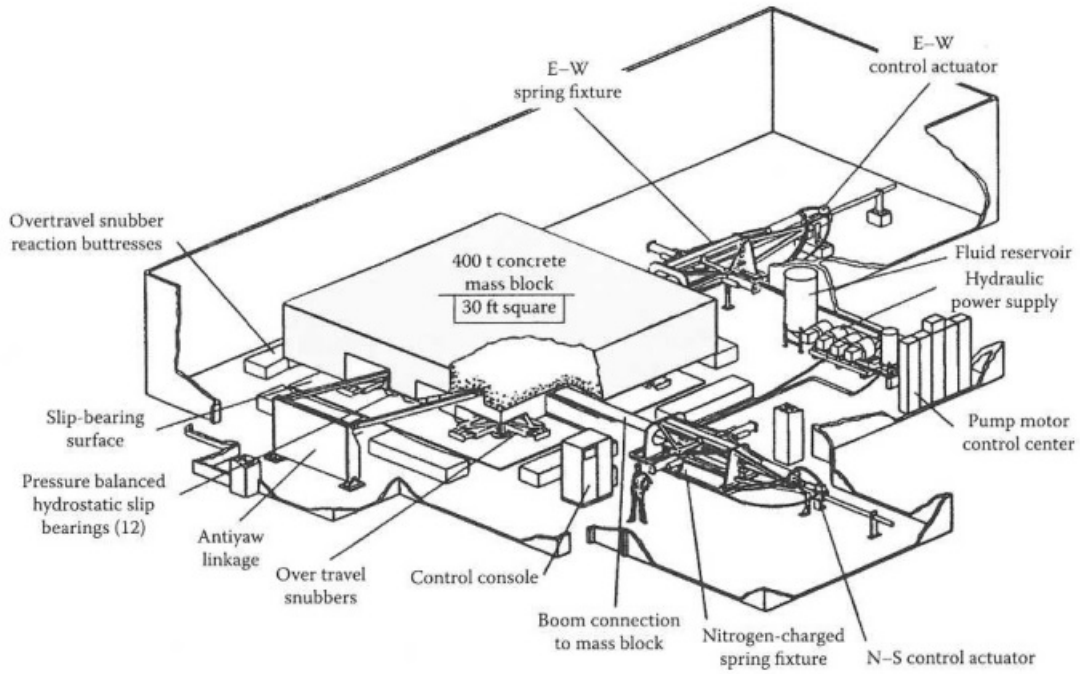

Figure 40. The tuned mass damper arrangement of Citicorp Center in New York [21]

Active tuned mass dampers are basically electronically controlled TMDs. They are linked to acceleration sensors in the building and they respond to building vibrations according to a given algorithm. In theory they are better suited for random vibrations, such as those causes by wind, because of their adaptability, but they have one major drawback. They require electricity to function and during extreme storm conditions, such as hurricanes, electricity blackouts are not uncommon. Therefore an active TMD always needs a reliable backup power source, or otherwise the usability or even structural integrity of the building may be jeopardized. [1]

Additional dampers and tuned mass dampers may be used as an original part of the design of a high-rise building, but more often they are used as supplements to existing buildings. Due to the inaccuracy of stiffness and damping predictions, design flaws or change of building use the desired vibration limits may be exceeded. In such a situation changes to the main frame of the existing building, which mainly defines the stiffness and mass of the structure, are often difficult and expensive to make, which makes installing additional dampers the most cost-effective solution. Negative effects of damper arrangements include their price, costs of maintenance, loss of useable space within the building and occupant comfort issues, such as operating noise.

Effectiveness of EDD or TMD arrangements also depends on the original building. In steel buildings, where the structural damping is small, they are generally more effective than in concrete buildings, where structural damping is larger. As an example of the effectiveness of such systems the TMD arrangement of Crystal Tower in Osaka, Japan reduced wind-induced response by approximately 50%. [1]

5.5 Vibration induced fatigue

Fatigue as a phenomenon means that when a time-dependent varying load is affecting a structural element, the maximum capacity of the element decreases as the number of load cycles increases and failure can occur at a loading significantly lower than the original capacity. The magnitude of the fatigue effect depends mainly on the magnitude of the maximum load (as a ratio of the maximum initial load carrying capacity), the amplitude of the load variation and the number of load cycles. Different types of fatigue loading histories are shown in Figure 41. Different materials also have different fatigue behavior. Fatigue effects in steel have been studied in detail, but in concrete structures not so much.

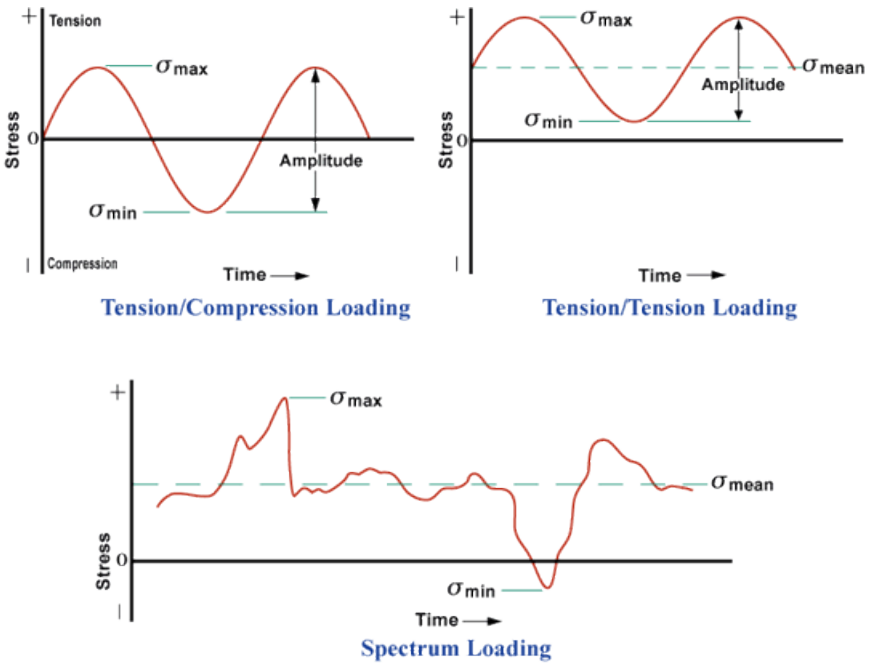

Figure 41. Different types of fatigue load histories.

The main problems accompanied with assessing the fatigue durability under wind loading is again related to the stochastic nature of wind and the difficulty of determining the loading history. Peak values for wind loads and accompanied vibrations occur only seldom, but vibrations present at lower wind speeds result in a frequently repeating dynamic loading, which may impose a fatigue loading on the structure. Whether fatigue is to be taken into account in the design depends on the materials and the frequency and magnitude of the stresses caused by the loading. Usually fatigue effects are not relevant for main load bearing members but rather for secondary structures, such as fastening elements of claddings. Another fatigue-relevant aspect in the design of chimneys and other extremely slender structures is vortex induced vibrations in the across-wind direction. The formation of a stable Von Karman vortex street in the wake of such a structure may lead to strong vibration at very frequently occurring wind speeds, inducing strong fatigue effects. [22]

Fatigue effects of wind loading may be differentiated into two categories: fatigue induced by gusts and fatigue induced by resonance vibrations. The difference of these two is represented in Figure 42. Because the number of stronger gusts is small compared to those required for fatigue effects to occur, only the resonance vibrations are relevant for fatigue. Therefore the fatigue assessment of structural members should

be carried out by assessing the number of resonance vibration cycles occurring during a strong wind of given duration, not by the amount of gusts occurring during a given time period. [22]

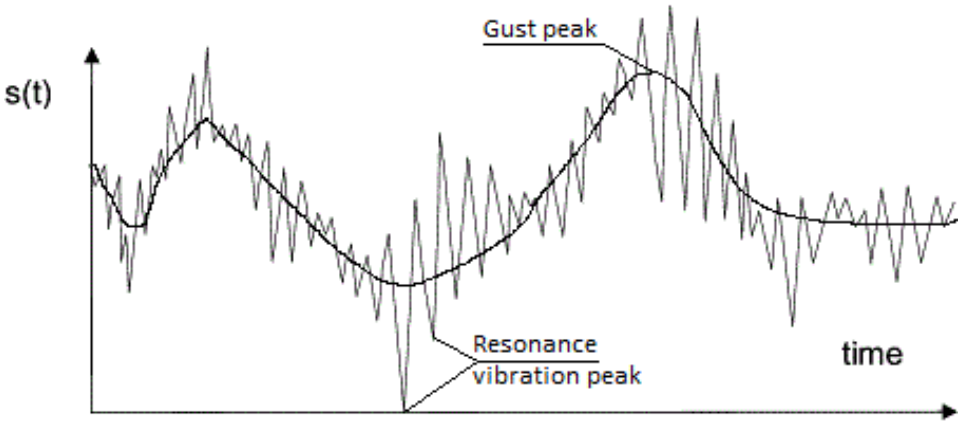

Figure 42. Fatigue load cycles caused by gust cycles and resonance vibration cycles.

The Eurocode deals with fatigue from wind-induced vibrations only by giving an estimate of how many times any percentage of the maximum wind load for a mean recurrence period of 50 years will be reached during that same time. The graph for this estimate is presented in Figure 43. The calculation of number of load cycles due to resonance vibration has to be carried out by other means. [12]

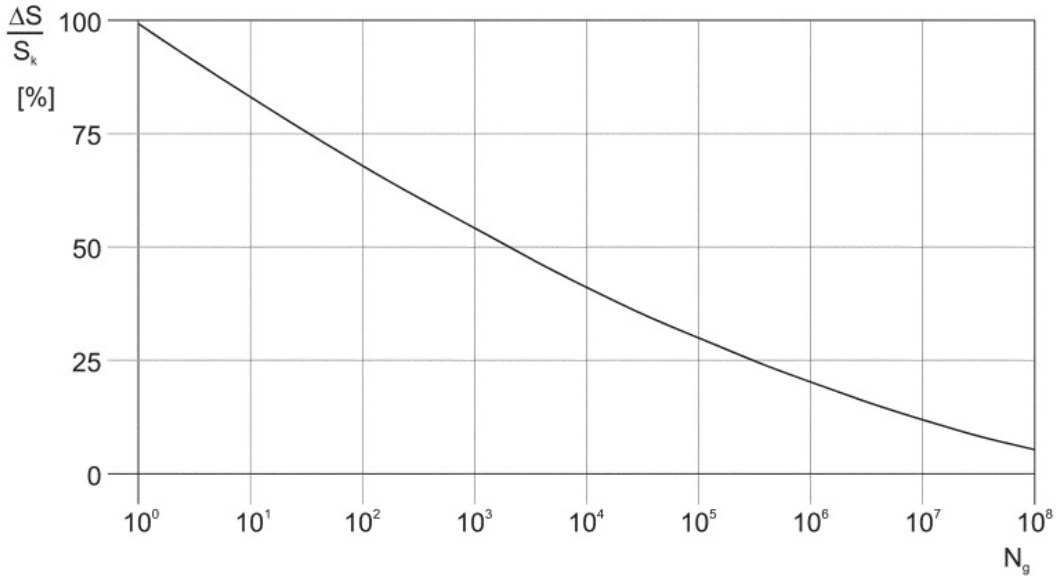

Figure B.3 Number of gust loads N_g for an effect $\Delta S/S_k$ during a 50 years period

Figure 43. Eurocode estimate for the number of different load magnitudes for wind loading. [12]

Fatigue loading may occur not only in structural members but on joints also. This becomes significant for vibration control assessment if the stiffness of the joints is reduced as number of load cycles increase. The occurrence of such stiffness change naturally changes the dynamic properties of the entire building, which may make the previously acceptable vibration levels to grow unacceptably large. Such phenomena has not been detected to be significant in existing buildings built using generally accepted connection designs and materials, but the possibility needs to be taken into account when developing new materials and structural solutions.

6 Case study on a mid-rise office building

To test the abovementioned analysis techniques a similar building as studied in [23] has been used. The building is a 137 m tall reinforced concrete structure to be built in Helsinki and used as an office building with a concrete core housing the elevator shafts as the main horizontal load resisting structure. Columns are round with diameters ranging from 700 to 900 mm. Floors are concrete slabs. All members are of concrete C50/60.

A 3-dimensional finite element model of the building has been made using the program RFEM from the company Dlubal. The model consists only of the main load bearing frame without secondary structures modelled. Connections between structural members have been modelled as rigid and foundations as hinged. Views from the model as well as the building floor plan are shown in Figures 44 and 45.

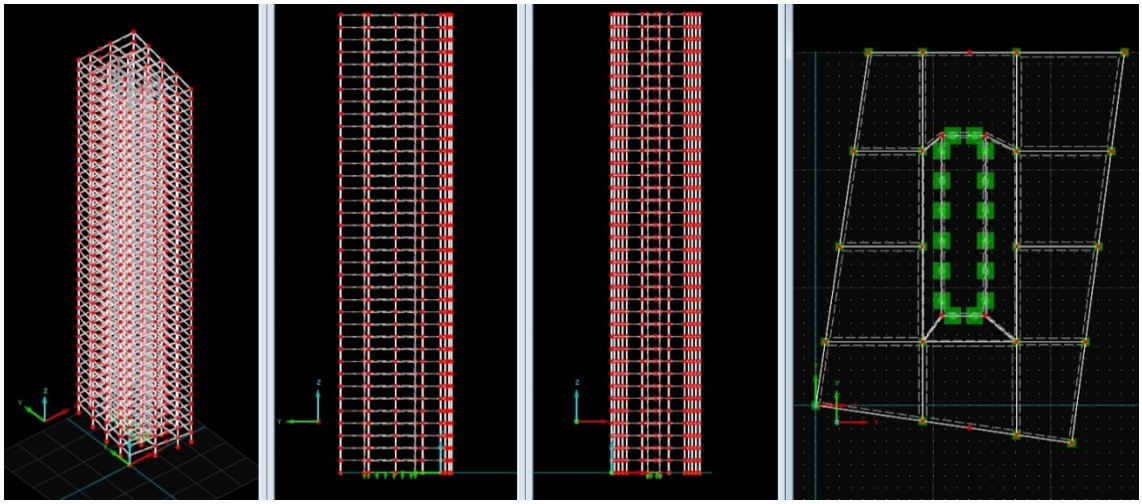

Figure 44. The finite element model

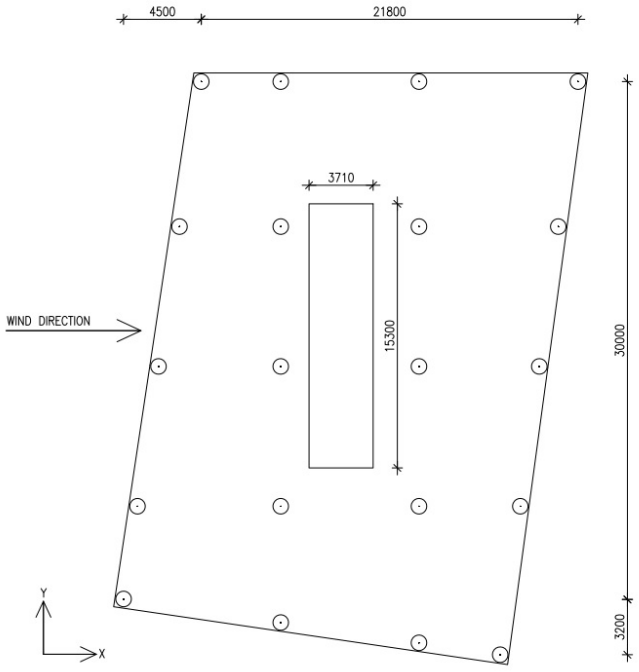

Figure 45. Building floor plan

The model has first been used for calculation of the natural frequencies and corresponding natural mode shapes. The first two natural modes are translational motion in x and y-directions with the natural frequencies of 0.20 Hz and 0.34 Hz, respectively. The third mode represents torsional vibration with the frequency 0.48 Hz. Visualizations of the mode shapes are given in Figure 46. The terrain category used is category II according to the eurocode. Design wind speed has been calculated using the eurocode and Finnish national annex for a 5 year mean recurrence period and has the value of 28.3 m/s at the building top. A damping ratio of 0.01 has been used for all vibration modes. Masses used in the analysis are self-weight of the structure multiplied by a factor of 1.2 to account for the self-weight of secondary structures. The initial data used in the calculations have been gathered in table 2.

Table 2. Initial values used in the calculations

Parameter	Value
Terrain category, eurocode	2
Basic wind speed, 5-year MRI	18,8 m/s
Wind speed at building top, 5-year MRI	28.3 m/s
Floor mass	888.9 t
First natural frequency, along-wind	0.20 Hz
First natural frequency, across-wind	0.34 Hz
First natural frequency, torsion	0.48 Hz
Damping ratio, all vibration modes	1%

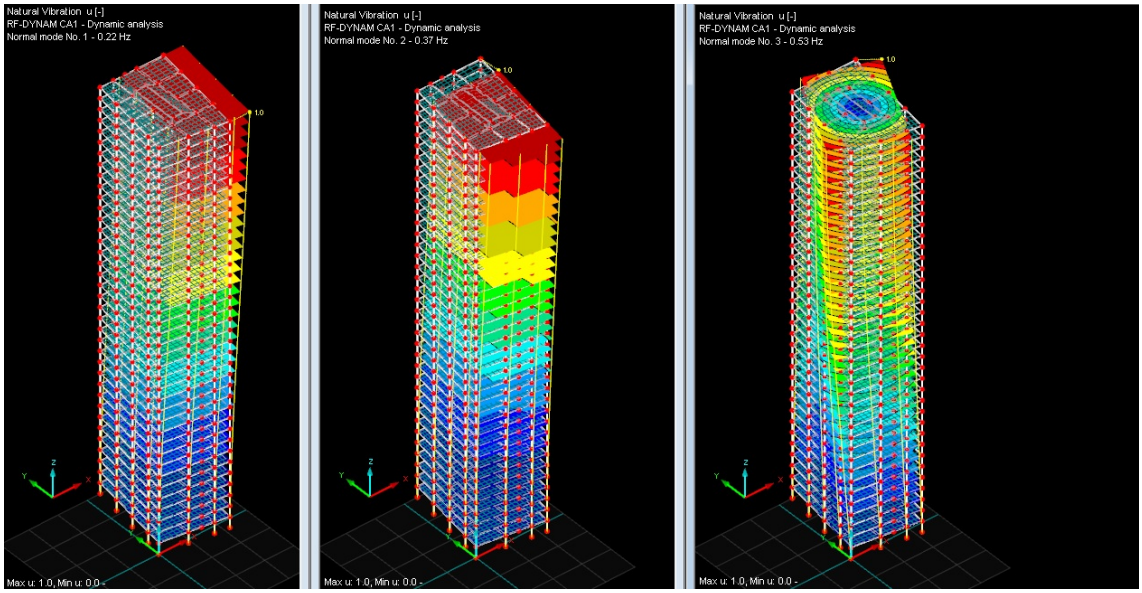

Figure 46. Lowest vibration modes for the structure.

Vibration assessment using the codes and guidelines presented in Chapter 3 has then been made using these values. The results for peak acceleration are as shown in table 3:

Table 3. Acceleration values calculated with different guidelines using 5-year MRI

Code/guideline	Along-wind [m/s^2]	Across-wind [m/s^2]	Torsion [m/s^2]
EC	0.087	-	-
AIJ	0.100	0.123	0.084
AS/NZS	0.05	0.068	-
(ASCE)/literature	0.06	0.102	0.097

It can be seen that the variation in results is relatively large, 100% in the along-wind direction. Reflecting to the vibration acceptance criteria presented in Chapter 4 and especially Figure 28, it can be seen that vibration levels are acceptable for an office building. The structure fulfills the AS/NZS 1170-2 and ISO6897 criteria for 5-year recurrence period. Carrying out the AIJ guidelines calculations with 1-year recurrence period for the design wind speed also shows the AIJ criteria for office buildings to be fulfilled. Because wind speed for a 1-year recurrence period is not defined in the eurocode, the value has been defined using the British standard BS 6399-2:1997 [24], which gives a value of 0.749 for the probability coefficient.

Another type of analysis performed for the structure is a dynamic finite element analysis in the time domain. A full time-history analysis has been carried out instead of e.g. a computationally less demanding modal analysis because of the limitations of the software used. The loading time history has been obtained from a Japanese wind tunnel database gathered by the Tokyo Polytechnic University, accessible at [25]. The database includes wind pressure coefficient time histories at a large number of measuring points on building envelope for a number of different building shapes at different wind conditions. For this study, the data for a rectangular building with breadth:depth:height ratio of 1:1:4 and wind direction perpendicular to the building side was used. The model scale used is 1:400 and the model size 0.1x0.1x0.4 m, which represents a building with dimensions 40x40x160 m. The terrain category used in the experiments is category II of the AIJ guidelines, which is described as “Open, few obstructions, grasslands, agricultural field”. Since the AIJ guidelines uses the power law in defining the wind speed profile, the terrain category is defined by the exponent of the power law instead of the roughness length used in the logarithmic law applied in the eurocode, it cannot be linked directly to categories in other norms. Estimation of the descriptions and exemplary pictures of the categories reveals it to be roughly equal to category II of the eurocode. The turbulence intensity calculated from the data also corresponds closely to the values calculated based on the eurocode category II, with a value of 0.128 gained from the wind tunnel data and 0.126 from the eurocode at 140m height. The data includes wind measurements on 400 points on the building surface (100 measurements per building side, roof not included) made with a frequency of 1 kHz, i.e. 1000 measurements per second, and using a basic wind speed of 11.3 m/s, which corresponds to the wind speed at 10m height at building scale. No averaging procedure for noise removal has been used. The time history of wind pressure coefficient at one measurement point is presented as an example in Figure 47.

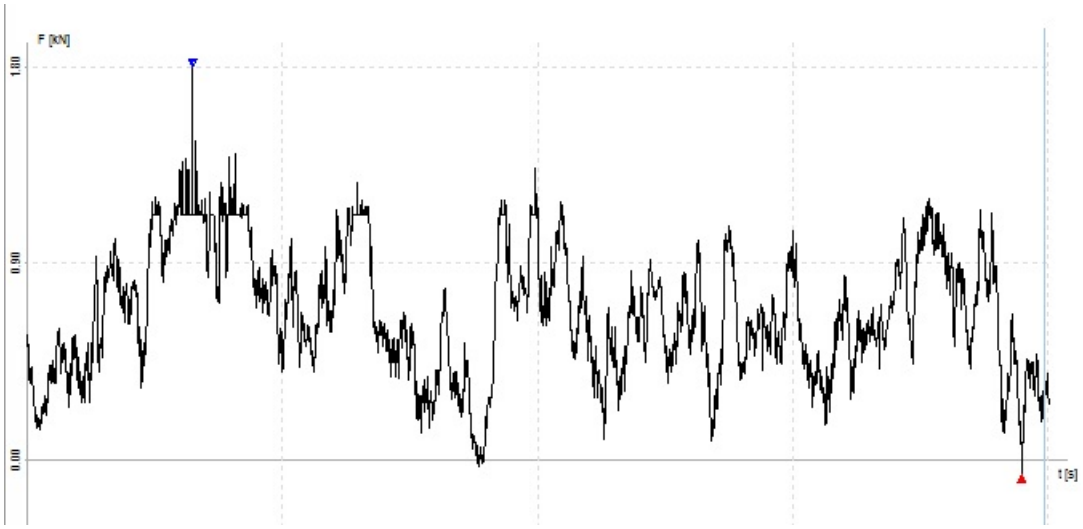

Figure 47. Wind pressure coefficient time history at one measurement point.

In order to use this data as loading in the finite element analysis, it has to first be converted from model scale to real building scale, which means scaling the time step with the formula

$$\Delta t_p = \frac{D_p}{D_m}\frac{V_m}{V_p}\Delta t_m \tag{92}$$

where D_p = length at prototype scale, D_m = length at model scale, V_m = wind velocity at model scale, V_p = wind velocity at prototype scale and t_m = time interval at model scale. This results in a building scale time step of 0.24 s.

The given wind pressure coefficients are converted to pressures using the Equation

$$p = \frac{1}{2} C_p \rho V_H^2 \tag{93}$$

where C_p = pressure coefficient, ρ = air density and V_H = free flow wind velocity and to forces with the tributary areas. These load histories are then used in the dynamic analysis. The self-weight of the concrete members multiplied by 1.2 is used as mass in the calculation. Damping is estimated by the Rayleigh model, using the natural angular frequencies of the two first vibration modes calculated by RFEM and the damping ratio of 0.01 for both modes in estimating the Rayleigh damping parameters:

$$\beta = \frac{2(\varsigma_1\omega_1 - \varsigma_2\omega_2)}{\omega_1^2 - \omega_2^2} \tag{94}$$

$$\alpha = 2\varsigma_1\omega_1 - \beta\omega_1^2 \tag{95}$$

The resulting damping matrix is then given in the form:

$$C = \alpha M + \beta K \tag{96}$$

where M = mass matrix and K= stiffness matrix.

For the analysis performed in this study, 200 different loading points and corresponding time histories have been used. The analysis has been run for the duration of 600 seconds using a time step of 0.1 s. The time step used in a dynamic analysis should normally be ≤(1/20f), which means that the increment used is slightly too large if the natural frequency of the torsional mode is considered. This is accepted because a shorter time step would result in increased computational times, which are long already with the used calculation parameters. Because the load value is defined at a larger time interval as used in the analysis, linear interpolation is used to acquire load values between the defined points. The parameters used in the analysis are gathered in table 4.

Table 4. Parameters used in the analysis

Parameter	Value
Time step	0.1 s
α	0.016 1/s
β	0.00601 s
Mass	1.2 * self-weight

Nodal accelerations and deformations have been recorded from selected nodes at different locations of the building. Results are presented as time history graphs. The results for accelerations and displacements in x- and y-directions of a node at the top corner of the building are shown in Figures 48-51:

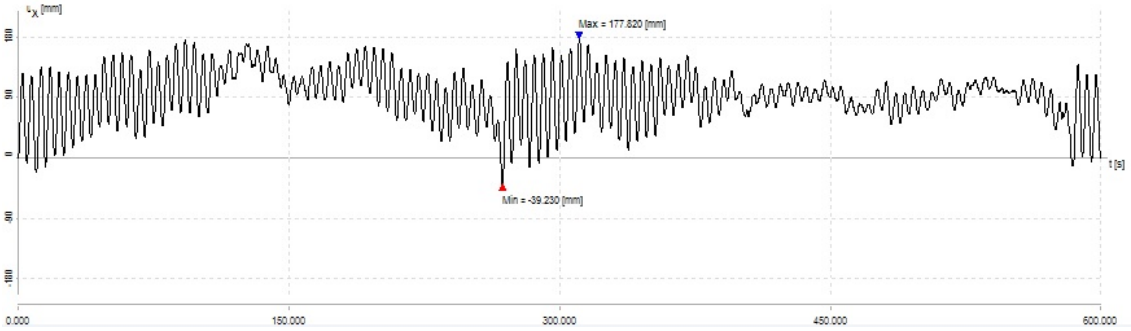

Figure 48. Displacement in the X direction

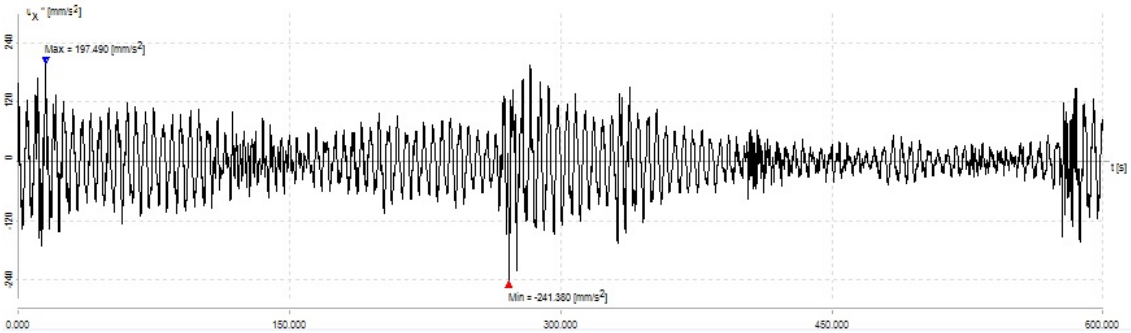

Figure 49. Acceleration in the X direction

Figure 50. Displacement in the Y direction

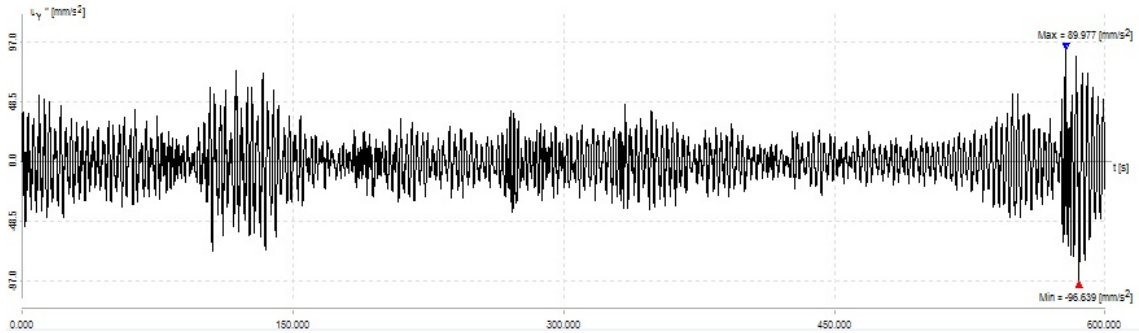

Figure 51. Acceleration in the Y direction

The resulting displacement in the X-direction is in line with the values calculated in the normal service limit state design while the displacement in y-direction remains small, as expected. The peak acceleration of 0.09 m/s^2 in the y-direction also matches well with the result from the guidelines. The peak acceleration value of 0.241 m/s^2 in the x-direction is however something unexpected, as it is much above what could be expected based on the approximations by the guideline methods.

Possible sources of error in the dynamic analysis presented are numerous. First of all, the wind pressure data used was measured for a rectangular building with given side ratios, whereas the building to be designed is not exactly of the same shape nor does it have exactly the same side ratios. The lack of noise reduction from the measurements may cause actually non-existing peaks to be present in the data. The reduction of loading points and corresponding load time histories from 400 to 200 may also increase the amount of coherence in the loading, thus causing the dynamic response to be stronger than it should be. The need to run the calculation for at least duration of 10min leads to the necessity to use a time increment slightly larger than otherwise recommended due to limitations of computational power available. Predicting damping by the Rayleigh model is also a possible source of error, as such damping models are only approximates at the best. The possibility of numerical errors embedded within the RFEM calculation procedure also exists. Measurement errors in the original wind tunnel data are also always possible.

Since wind tunnel data for exactly the building to be analyzed is not available within this study and the correctness of the experiments from which the data is extracted cannot be validated, these possibilities for the source of error cannot be confirmed nor ruled out. The possibility of too large time increment in the dynamic analysis was studied by calculating the response of the building on a smaller time interval using several values of time increment ranging from 0.01 s-0.1 s, but no large change in the

results was observed. The calculations were also carried out using only 100 load points and histories. An increase of approximately 5% in the acceleration value was observed, which makes the possibility that an increase of load points from the original 200 would cause a major decrease in the response very unlikely. It also shows that the reduced computational cost of using only 100 loading histories would cause such a minor error in the results that the use of 200 points is rather uneconomical from a design practice point of view. The correctness of the used damping parameters was verified by evaluating the decay of the free vibration occurring after the loading has stopped. The analysis was also carried out with Rayleigh damping coefficients corresponding to first and second mode damping ratios of 5%, but the results were still noticeably larger than the guideline values. Different finite element meshes were also studied as well as the acceleration values in a larger number of nodes surrounding the nodes at the top of the building in order to rule out the possibility of local acceleration peaks due to the finite element calculation procedure. Therefore the most likely source of the unexpectedly large along-wind acceleration value is errors in wind tunnel data used or the noise present within, errors in the calculation procedure within the analysis software or a vastly larger than expected contribution of higher vibration modes. A difference in the terrain category and resulting difference in turbulence intensity may also be possible.

One possibility is also that the results acquired from the time domain analysis are not incorrect. It is possible that an unusually strong turbulent gust has occurred in the wind tunnel at that time, which lies outside the boundaries of the statistical distribution of wind data on which the guideline assessment methods are based. However, the experimental nature of the time-domain analysis method compared to decades of successful utilization of spectral methods in design practice makes this possibility rather improbable, and some sort of error in the analysis procedure remains the likely cause of the result.

Performing this type of dynamic analysis presents also many other issues which make it impractical as a standard design procedure. First of all, carrying out the pressure measurements in wind tunnel is more time-consuming and expensive than the standard HFFB procedure due to the required equipment (large number of pressure sensors) and the manual labor needed to attach them. In addition to this comes the time and effort required for the finite element analyses, which need to be carried out for an adequate number of wind directions. A single analysis requires several hours with a standard desktop computer, and setting up the analysis may take even longer even if the finite element model itself would be readily made. Assessing the acceptability of the results is also difficult, as only a maximum acceleration value is obtained as a result, without the knowledge of to which vibration mode, and respective frequency, it is related to. A spectral analysis of the results would therefore be necessary to exactly interpret the results. A simple first estimate is of course to assume only the first vibration mode to be relevant, but such simplifications do not fit in the philosophy of carrying out such analysis in the first place, as the objective would be to gain more exact results. Therefore the analysis procedure becomes rather cumbersome and in the current context has more value as a subject of academic interest than as a design method used in work practice. An area where such procedure could be a valid design method is the design of special structures or structural elements with complex geometries where the HFFB technique cannot be applied, such as canopies.

For the sake of academic interest possibilities for a further reduction of vibration response have been studied. Two different modification possibilities have been investigated: adding stiffening steel trusses to the outer perimeter of the structure and adding a damper system. These approaches reflect the options of modifying the stiffness or the damping of the structure, respectively. The effects of both modifications have been studied using the guideline calculation methods presented earlier.

The added stiffening trusses are steel members positioned as shown in Figure 52. The resulting natural frequencies in the three first vibrational modes are 0.233 Hz for the along-wind vibration, 0.358 Hz for the across-wind vibration and 0.558 Hz for the torsional vibration. The resulting acceleration values are shown in table 5.

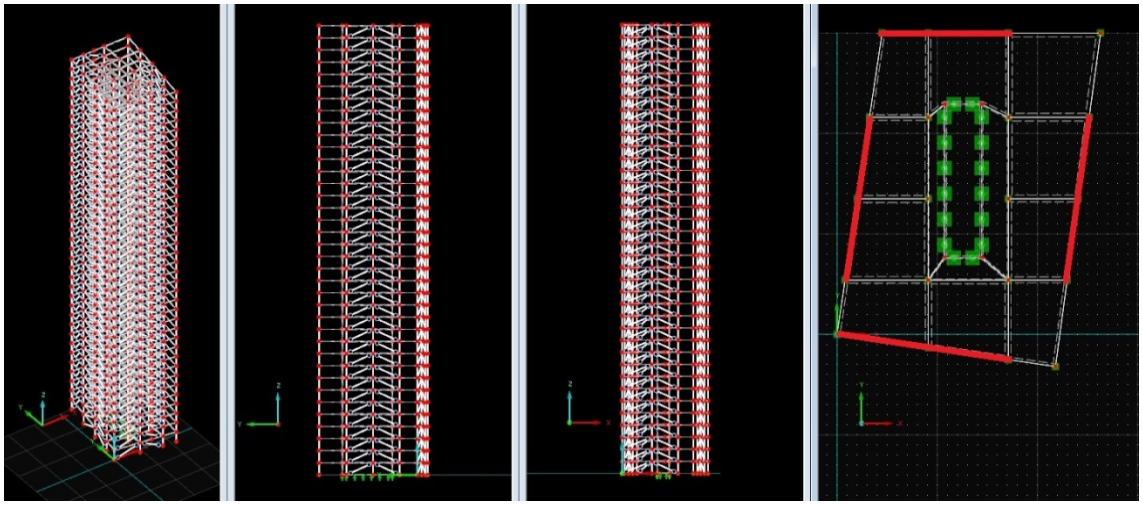

Figure 52. Finite element model with added truss system

Table 5. Acceleration values with added truss system

Code/guideline	Along-wind [m/s^2]	Across-wind [m/s^2]	Torsion [m/s^2]
EC	0.076	-	-
AIJ	0.087	0.116	0.073
AS/NZS	0.043	0.069	-
(ASCE)/literature	0.05	0.095	0.088

It can be seen that the acceleration values have decreased due to the added stiffness, but only by approximately 10%. It should also be noted that reflecting to the acceptance criteria of Chapter 4 the increase in natural frequency diminishes the effect of reduced peak acceleration value, because in most norms the allowed value also decreases with increased frequency. Therefore a further improved stiffening system would be needed to provide a truly significant improvement in vibration behavior. Such a system would not only increase the costs of the building but also provide further architectural challenges.

As an alternative to increasing the stiffness of the structure an increase in damping has also been considered. If an additional damper arrangement is installed to the structure doubling the damping ratio to 2%, the resulting building acceleration values are as presented in table 6.

Table 6. Acceleration values with added damper system

Code/guideline	Along-wind [m/s^2]	Across-wind [m/s^2]	Torsion [m/s^2]
EC	0.064	-	-
AIJ	0.071	0.087	0.059
AS/NZS	0.035	0.048	-
(ASCE)/literature	0.042	0.072	0.069

A noticeable decrease of up to 30% is observed in the acceleration predictions, which is a significantly better result than obtained with the truss system adding stiffness. Because the added damping has little effect on vibration frequency, the system has no negative effect on the acceptable peak acceleration values.

It should be noted that installing a damper system in such a building is most likely not a very cost-efficient solution even though it yields good results. Damper systems are normally not applied to such buildings. The costs of the system as well as the negative architectural and other effects overweight the benefits. The possibility of manufacture mistakes or breaking of the damper equipment also makes the system less reliable than simply added frame stiffness. Designing and optimizing a damper system is also a difficult task.

7 Conclusions

The study and the calculations performed in this work have shown that wind induced vibrations are an important aspect and have to be accounted for in the design of buildings which are classified as tall buildings in Finland. Especially in the case of apartment buildings the vibration levels may grow unacceptably large even if the ultimate limit state criteria or other service limit state criteria were fulfilled.

Some key characteristics of wind have been described and the difficulties in analyzing wind have been identified. Different analysis techniques for estimating wind effects on buildings have been described and compared with each other. A large variance in the results obtained from different guidelines based on the same basic principle has been observed, which emphasizes the unreliability and approximate nature of such calculation methods. However, their ease of use makes them suitable for preliminary analyses. The problems and limitations still affiliated with more advanced computational methods have been identified, most notably problems associated with reliability and the too large amount of work required for performing dynamic finite element analyses as a reasonable design method.

The importance of assessing across-wind vibrations is also noted, as they may often result in the largest acceleration values. As carrying out the preliminary estimation calculations given in the guidelines presented requires very little work using readily made calculation sheets, it is recommended that they are carried out whenever it is suspected that wind-induced vibrations in the across-wind direction may need to be considered. The ASCE criteria for when wind tunnel tests need to be performed are recommended for assessing the sufficiency of guideline calculation methods.

The difficulty of assessing the acceptability criteria for wind-induced vibrations has also been addressed. A single limit value cannot be stated and there is noticeable scatter in the acceptance criteria given in different norms, as shown in Chapter 4. Also the inability of the Eurocode methods to perform wind speed conversion to 1-year recurrence interval should be noted, as it forces such conversions to be based on other norms. In general, the decision of acceptance has to be made based on a diverse assessment of the building, its dynamic behavior and intended use. Many unknown factors are also included in the process, including the difficulties in predicting the exact response of the building and the vibration perception threshold of its users, as large variance is observed within people, depending on a large number of variables.

Different aspects of structural design which affect the vibration behavior of a building and the means available for a structural engineer to control vibrations have been described. Emphasis on the large influence of damping is highlighted. The possibilities and drawbacks of additional damping devices have also been described.

The large influence of pre-planning stage on the economical aspect of a tall building is also emphasized. In addition to the aerodynamic shape of the building, which should be discussed together with the architect in an early planning stage, the importance of interference effects and topography should also be taken into account. Considering wind effects already as a part of urban planning stage does not only provide possibilities for optimizing the interference effects but also to assess pedestrian comfort. These are also the areas where recent advancements in computational wind engineering, mainly in

CFD calculations, currently have the most implementation possibilities, as the CFD estimates can be used in the pre-planning stage before more expensive wind tunnel experiments are carried out.

Possible areas of future research in the field in general include the development of computational wind engineering, which could in the future replace wind tunnel testing. For this purpose both numerical methods introduced in this work, CFD and dynamic FEM, require further development. There exists also room for development of guideline estimation methods especially for across-wind and torsional vibrations. The ever increasing amount of wind tunnel results available may also enable the development of more advanced guideline methods for estimating interference effects. As a more local future development target evaluation of the accuracy of different guideline methods in Finnish wind conditions and with Finnish construction practices can be made when more actual experience from tall buildings is acquired.

In general, the goals set for the thesis were partially fulfilled. The guideline methods found from literature were found to be suitable for use in the planned mid-rise projects in Finland and working Mathcad calculation sheets utilizing them were created. Different acceptance criteria were found from literature. The ISO 6897 criteria are suitable as a minimum requirement for vibration control. Stricter limits may be set if desired or deemed necessary because of e.g. planned building use. Experiments with the dynamic finite element analysis showed that the method is possible to be used but not very practical. The results obtained were also partly not those expected, the reasons of which would require further research. It may however be more useful in the design of such structures where the geometry or the situation otherwise prevent the use of other wind-tunnel methods.

References

[1] Tamura, Y. & Kareem, A. Advanced structural wind engineering, 1st ed. Tokyo, Japan: Springer Japan, 2013. 410s. ISBN 978-4-431-54337-4

[2] Simiu, E. Design of buildings for wind: A guide for ASCE 7-10 standard users and designers of special structures, 2nd ed. Hoboken, New Jersey, USA: John Wiley & Sons, 2011. 338s. ISBN 978-0-470-46492-2

[3] Frei, W. Comsol Blog, 16.09.2013. Available at http://www.comsol.com/blogs/which-turbulence-model-should-choose-cfd-application/ [cited 27.02.2015]

[4] Bar-Meir, G. Basics of fluid mechanics. Genick Bar-Meir, 2002. 398s. Free textbook.

[5] Siikonen, T. Laskennallisen virtausmekaniikan ja lämmönsiirron perusteet. Aalto University, 2013. Lecture notes.

[6] Stempniewski, L. & Haag, B. Baudynamik-Praxis, 1st ed. Berlin, Germany: Bauwerk Verlag GmbH, 2010. 254s. ISBN 978-3-89932-264-4

[7] Savolainen, M. Vaakamittaustekniikan kehittäminen korkeiden rakennusten värähtelytarkasteluun. Diplomityö. Teknillinen Korkeakoulu. Espoo, 2009. 115s.

[8] Schweizerhof, K. & Seelig, T. Grundlagen der Baudynamik. Karlsruhe Institute of Technology, 2011. Lecture notes.

[9] Irwin, P.A. Wind engineering challenges of the new generation of super-tall buildings. Journal of wind engineering and industrial aerodynamics, 2009. Vol 97, s. 328-334. ISSN 0167-6105

[10] Khanduri, A.C. & Stathopoulos, T. & Bedard, C. Wind-induced interference effects on buildings – a review of the state-of-the-art. Engineering structures, 1998. Vol 20, s. 617-630. ISSN 0141-0296

[11] ASCE 7-10. Minimum Design Loads of Buildings and Other Structures. American Society of Civil Engineers. Reston, Virginia, USA, 2010. 608s.

[12] SFS-EN 1991-1-4. Eurocode 1: Actions on structures. Part 1-4: General actions. Wind actions. Helsinki: Finnish standards association, 2011. 254s.

[13] Recommendations for loads on buildings, Architectural institute of Japan. Tokyo, 2004.

[14] AS-NZS 1170-2. Structural design actions – Part 2: Wind actions. Sydney: Standards Australia Limited / Wellington: Standards New Zealand, 2011. 96s.

[15] Lamb, S. & Kwok, K.C.S. & Walton, D. A longitudinal field study of the effects of wind-induced building motion on occupant wellbeing and work performance. Journal of wind engineering and industrial aerodynamics, 2014. Vol 133, s. 39-21. ISSN 0167-6105

[16] Tamura, Y. Wind resistant design of tall buildings in Japan. NASCC Pacific Structural Steel Conference 24-27 March 2004, Proceedings. 20s.

[17] ISO 6897. Guidelines for the evaluation of the response of occupants of fixed structures, especially buildings and off-shore structures, to low-frequency

horizontal motion (0.063 to 1Hz). International Organization for Standardization, 1984. 8s.

[18] Cook, N. Designers guide to EN 1994-1-4 Eurocode 1 – Actions on structures, general actions, Part 1-4: Wind actions. 1st ed. London, United Kingdom: Thomas Telford Limited, 2007. 74s. ISBN 978-0-7277-3152-4

[19] Tamura, Y. Damping in buildings, lecture notes. Tokyo Polytechnic University. Available at http://www.wind.arch.t-kougei.ac.jp/info_center/ITcontent/tamura/10.pdf [cited 24.02.2015]

[20] Buresti, G. Bluff-body aerodynamics, lecture notes. University of Pisa, 2000. Available at http://www.mech.kth.se/courses/5C1211/BluffBodies.pdf [cited 03.03.2015]

[21] Kortelainen, P. Korkeiden rakennusten vaste tuulikuormituksessa. Diplomityö. Tampereen teknillinen yliopisto. Tampere, 2012. 153s.

[22] Holmes, J.D. Fatigue life under along-wind loading – closed form solutions. Engineering structures, 2002. Vol 24, s. 109-114. ISSN 0141-0296

[23] Castell-Rüdenhausen, H. Evaluation of wind load resistance of tall buildings. Diplomityö. Teknillinen Korkeakoulu. Espoo, 2012. 116s.

[24] BS 6399-2:1997. British Standard. Loading for buildings – Part 2: Code of practice for wind loads. London: British Standards Institution, 1997. 102s.

[25] Wind Pressure Database for High-Rise Building, Tokyo Polytechnic University. Available at http://www.wind.arch.t-kougei.ac.jp/system/eng/contents/code/tpu [cited 27.01.2015]

Appendix 1

Along-wind acceleration, according to EN 1991-1-4

Basic wind speed	$v_m := 28.3\frac{m}{s}$
Projected breadth of building:	$b := 34.6m$
Reference height:	$h := 137m$
Air density	$\rho := 1.25\frac{kg}{m^3}$
Terrain category	$C_{Ter} := 2$
Mass of building per unit height	$m_z := 1.2{\cdot}2.002 \times 10^5\ \frac{kg}{m}$
First natural frequency along-wind	$n := 0.20Hz$
Wind force coefficient Cf at H	$c_f := 1.3$
Damping ratio along-wind	$D := 0.01$

$$\delta_s := \frac{2\cdot\pi\cdot D}{\sqrt{1-D^2}} = 0.063$$

$z_s := h$

$$z_0 := \begin{cases} (0.003m) & \text{if } C_{Ter} = 0 \\ (0.01m) & \text{if } C_{Ter} = 1 \\ (0.05m) & \text{if } C_{Ter} = 2 \\ (0.3m) & \text{if } C_{Ter} = 3 \\ (1m) & \text{if } C_{Ter} = 4 \end{cases} \qquad z_{min} := \begin{cases} (1m) & \text{if } C_{Ter} = 0 \\ (1m) & \text{if } C_{Ter} = 1 \\ (2m) & \text{if } C_{Ter} = 2 \\ (5m) & \text{if } C_{Ter} = 3 \\ (10m) & \text{if } C_{Ter} = 4 \end{cases}$$

$k_I := 1 \qquad c_0 := 1$

$$I_v := \begin{cases} \dfrac{k_I}{c_0\cdot\ln\left(\dfrac{h}{z_0}\right)} & \text{if } h \geq z_{min} \\ \left(\dfrac{k_I}{c_0\cdot\ln\left(\dfrac{z_{min}}{z_0}\right)}\right) & \text{if } h < z_{min} \end{cases} = 0.126$$

$\zeta := 1$

$\Phi(z) := \left(\dfrac{z}{h}\right)^{\zeta}$

Appendix 1

$$m_e := \frac{\int_0^h m_z \cdot \Phi(z)^2 \, dz}{\int_0^h \Phi(z)^2 \, dz} = 2.402 \times 10^5 \frac{kg}{m}$$

$\delta_d := 0$

$$\delta_a := \frac{c_f \cdot \rho \cdot b \cdot v_m}{2 \cdot n \cdot m_e} = 0.017$$

$\delta := \delta_s + \delta_a + \delta_d$

$z_t := 200m$

$L_t := 300m$

$$\alpha := 0.67 + 0.05 \cdot \ln\left(\frac{z_0}{m}\right) = 0.52$$

$$L := \begin{cases} \left[L_t \cdot \left(\frac{h}{z_t}\right)^{\alpha}\right] & \text{if } h \geq z_{min} \\ \left[L_t \cdot \left(\frac{z_{min}}{z_t}\right)^{\alpha}\right] & \text{if } h < z_{min} \end{cases} = 246.403\,m$$

$$f_L := \frac{n \cdot L}{v_m} = 1.741$$

$$S_L := \frac{6.8 \cdot f_L}{\left(1 + 10.2 \cdot f_L\right)^{\frac{5}{3}}} = 0.089$$

$$B := \sqrt{\frac{1}{1 + 0.9 \cdot \left(\frac{b + h}{L}\right)^{0.63}}} = 0.763$$

$$\eta_b := \frac{4.6 \cdot b}{L} \cdot f_L = 1.125$$

$$\eta_h := \frac{4.6 \cdot h}{L} \cdot f_L = 4.454$$

$$R_h := \frac{1}{\eta_h} - \frac{1}{2 \cdot \eta_h^2} \cdot \left(1 - e^{-2 \cdot \eta_h}\right) = 0.199$$

$$R_b := \frac{1}{\eta_b} - \frac{1}{2 \cdot \eta_b^2} \cdot \left(1 - e^{-2 \cdot \eta_b}\right) = 0.536$$

$$R := \sqrt{\frac{\pi^2}{2 \cdot \delta} \cdot S_L \cdot R_h \cdot R_b} = 0.77$$

Appendix 1

$$K_x := \frac{(2\cdot\zeta + 1)\cdot\left[(\zeta + 1)\cdot\left(\ln\left(\frac{z_s}{z_0}\right) + 0.5\right) - 1\right]}{(\zeta + 1)^2\cdot\ln\left(\frac{z_s}{z_0}\right)} = 1.5$$

$$\sigma_{a.x} := \frac{c_f\cdot\rho\cdot b\cdot I_v\cdot v_m^{\,2}}{m_e}\cdot R\cdot K_x\cdot\Phi(h) = 0.027\,\frac{m}{s^2}$$

$$\nu := \max\left[\left(n\cdot\sqrt{\frac{R^2}{B^2 + R^2}}\right), 0.08Hz\right] = 0.142\,\frac{1}{s}$$

$$T := 600s$$

$$k_p := \max\left[\left(\sqrt{2\cdot\ln(\nu\cdot T)} + \frac{0.6}{\sqrt{2\cdot\ln(\nu\cdot T)}}\right), 3\right] = 3.183$$

$$a := \sigma_{a.x}\cdot k_p = 0.087\,\frac{m}{s^2}$$

$$a = 0.087\,\frac{m}{s^2}$$

Appendix 2

Along-wind, across-wind and torsional deflection and acceleration, according to sec 19.6.1-3 of "Design of buildings for Wind: A Guide for ASCE 7-10 Standard Users and Designers of Special Structures (2nd edition)"

specific mass of air	$\rho := 1.25\frac{kg}{m^3}$
specific mass of building	$\rho_b := 1.2 \cdot 251.571\ \frac{kg}{m^3}$
roughness length	$z_0 := 0.05m$
building height	$H := 137m$
buildings width	$B := 34.6m$
buildings depth	$D := 23m$
pressure coefficient, windward	$C_w := 0.8$
pressure coefficient, leeward	$C_l := 0.5$
fundamental natural frequency along wind	$n_1 := 0.20Hz$
fundamental natural frequency across-wind	$n_2 := 0.34Hz$
damping ratio	$\zeta_1 := 0.01$
mean hourly wind speed	$V := \frac{28.3}{1.06}\frac{m}{s}$
height at which to calculate:	$z := H$
fundamental natural frequency, torsional	$n_T := 0.48Hz$
damping ratio, torsional	$\zeta_T := 0.01$

Along-wind

$$M_1 := \frac{B \cdot D \cdot H \cdot \rho_b}{3} = 1.097 \times 10^7\,kg$$

$$\Delta := \min(H, B, D) = 75.459 \cdot ft$$

$$\mu := \frac{V}{2.5 \cdot \ln\left(\frac{H}{z_0}\right)} = 4.426 \cdot \frac{ft}{s}$$

$$Q := 2 \cdot \ln\left(\frac{H}{z_0}\right) - 1 = 14.831$$

$$J := 0.78 \cdot Q^2 = 171.578$$

$$B_z := \frac{6.71 \cdot Q^2}{1 + 0.26\frac{B}{H}} = 1.385 \times 10^3$$

$$N_1 := \frac{n_1 \cdot H}{\mu \cdot Q} = 1.369$$

$$C_D := C_w + C_l = 1.3$$

Appendix 2

$$\eta_1 := 3.55 \cdot N_1 = 4.861$$

$$\eta_2 := 12.32 \cdot N_1 \cdot \frac{\Delta}{H} = 2.832$$

$$C(\eta) := \frac{1}{\eta} - \frac{1 - e^{-2\eta}}{2 \cdot \eta^2}$$

$$C(\eta_1) = 0.185 \qquad C(\eta_2) = 0.291$$

$$C_{Df} := C_w^2 + C_l^2 + 2 \cdot C_w \cdot C_l \cdot C(\eta_2) = 1.123$$

$$R := \frac{0.59 \cdot Q^2 \cdot N_1^{-\frac{2}{3}}}{\zeta_1} \cdot \frac{C_{Df}}{C_D^2} \cdot \frac{C(\eta_1)}{1 + 3.95 \cdot N_1 \cdot \frac{B}{H}} = 545.386$$

$$x := \frac{0.5 \cdot \rho \cdot \mu^2 \cdot C_D \cdot B}{M_1 \cdot (2 \cdot \pi \cdot n_1)^2} \cdot \left[J + 3.75 \cdot (B_Z + R)^{0.5} \right] = 3.259 \times 10^{-3} \frac{1}{m} \cdot ft$$

$$a := 4.0 \cdot \frac{0.5 \cdot \rho \cdot \mu^2 \cdot C_D \cdot B}{M_1} \cdot R^{0.5} = 1.429 \times 10^{-3} \frac{1}{m} \cdot \frac{ft}{s^2}$$

Across-wind

$$A := B \cdot D = 795.8\, m^2$$

$$p := 3.3$$

$$C := 0.00065$$

$$y := C \cdot \left(\frac{V}{n_2 \cdot \sqrt{A}} \right)^p \cdot \frac{\sqrt{A}}{\zeta_1^{0.5}} \cdot \frac{\rho}{\rho_b} \cdot \frac{1}{H} = 5.331 \times 10^{-4} \frac{1}{m} \cdot ft$$

$$a_y := (2 \cdot \pi \cdot n_2)^2 \cdot y = 2.433 \times 10^{-3} \frac{1}{m} \cdot \frac{ft}{s^2}$$

Torsion

$$L := \frac{2 \cdot 2 \cdot \frac{B^2}{8}}{\sqrt{B \cdot D}} + \frac{2 \cdot 2 \cdot \frac{D^2}{8}}{\sqrt{B \cdot D}} = 100.377 \cdot ft$$

$$r_m := \frac{(B^2 + D^2)^{0.5}}{\sqrt{12}} = 39.349 \cdot ft$$

$$T_{rms} := 0.0017 \cdot \frac{1}{\zeta_T^{0.5}} \cdot \rho \cdot L^4 \cdot H \cdot n_T^2 \cdot \left(\frac{V}{n_T \cdot L} \right)^{2.68} = 2.151 \times 10^3 \cdot kip \cdot ft$$

$$v := \sqrt{\left(\frac{B}{2} \right)^2 + \left(\frac{D}{2} \right)^2} = 68.155 \cdot ft$$

$$a_T := \frac{7.6 \cdot T_{rms}}{\rho_b \cdot A \cdot H \cdot r_m^2} = 4.682 \times 10^{-3} \cdot \frac{1}{s^2}$$

Appendix 2

Along-wind	Across-wind	Torsion
$x_z := x \cdot z = 0.136 \cdot m$	$y_z := y \cdot z = 0.022 \cdot m$	
$a_{x.z} := a \cdot z = 0.06 \cdot \frac{m}{s^2}$	$a_{y.z} := a_y \cdot z = 0.102 \cdot \frac{m}{s^2}$	$a_{T.v} := a_T \cdot v = 0.097 \cdot \frac{m}{s^2}$

Appendix 3

Along-wind, across-wind and torsional acceleration, according to Architectural Institute of Japan recommendations for loads on buildings chapter 6.10

Design wind speed	$U_H := 28.3\frac{m}{s}$
Projected breadth of building:	$B := 34.6m$
Projected depth of building:	$D := 23m$
Reference height:	$H := 137m$
Wind force coefficient Cd at H	$C_H := 1.3$
Mass of building per unit height	$m_Z := 1.2 \cdot 2.002 \times 10^5 \frac{kg}{m}$
Terrain category	$C_{Ter} := 2$
Air density	$\rho := 1.25\frac{kg}{m^3}$
First natural frequency along-wind	$f_D := 0.20Hz$
Damping ratio along-wind	$\zeta_D := 0.01$
First natural frequency across-wind	$f_L := 0.34Hz$
Damping ratio across-wind	$\zeta_L := 0.01$
First natural frequency in torsion	$f_T := 0.48Hz$
Damping ratio in torsion	$\zeta_T := 0.01$

Along wind

$$Z_G := \begin{cases} (250m) \text{ if } C_{Ter} = 1 \\ (350m) \text{ if } C_{Ter} = 2 \\ (450m) \text{ if } C_{Ter} = 3 \\ (550m) \text{ if } C_{Ter} = 4 \\ (650m) \text{ if } C_{Ter} = 5 \end{cases} \quad \alpha := \begin{cases} (0.1) \text{ if } C_{Ter} = 1 \\ (0.15) \text{ if } C_{Ter} = 2 \\ (0.2) \text{ if } C_{Ter} = 3 \\ (0.27) \text{ if } C_{Ter} = 4 \\ (0.35) \text{ if } C_{Ter} = 5 \end{cases} \quad Z_b := \begin{cases} (5m) \text{ if } C_{Ter} = 1 \\ (5m) \text{ if } C_{Ter} = 2 \\ (10m) \text{ if } C_{Ter} = 3 \\ (20m) \text{ if } C_{Ter} = 4 \\ (30m) \text{ if } C_{Ter} = 5 \end{cases}$$

$$L_H := \begin{cases} \left[100 \cdot \left(\frac{H}{30m}\right)^{0.5} m\right] \text{ if } 30m < H \le Z_G \\ 100m \text{ if } H \le 30m \end{cases} = 213.698\,m$$

$$k := \begin{cases} 0.07 \text{ if } \frac{H}{B} \ge 1 \\ 0.15 \text{ if } \frac{H}{B} < 1 \end{cases}$$

Appendix 3

$$I_{rZ} := \begin{cases} \left[0.1\cdot\left(\frac{H}{Z_G}\right)^{-\alpha-0.05}\right] & \text{if } Z_b < H \le Z_G \\ \left[0.1\cdot\left(\frac{Z_b}{Z_G}\right)^{-\alpha-0.05}\right] & \text{if } H \le Z_b \end{cases} \qquad E_r := \begin{cases} \left[1.7\cdot\left(\frac{H}{Z_G}\right)^{\alpha}\right] & \text{if } Z_b < H \le Z_G \\ \left[1.7\cdot\left(\frac{Z_b}{Z_G}\right)^{\alpha}\right] & \text{if } H \le Z_b \end{cases}$$

$E_I := 1 \qquad E_g := 1 \qquad E_H := E_r \cdot E_g = 1.477$

$K_D := 1 \qquad \lambda_U := \frac{U_{500}}{U_0} =$ ▮

$k_{rW} := 0.63\cdot(\lambda_U - 1)\cdot\ln(r) - 2.9\lambda_U + 3.9 =$ ▮

$U_{H2} := U_0 \cdot K_D \cdot E_H \cdot k_{rW} =$ ▮

$q_H := \frac{1}{2}\cdot\rho\cdot U_H^{\,2} = 500.556\,\text{Pa}$

$E_{gI} := \frac{E_I}{E_g} = 1$

$I_H := I_{rZ}\cdot E_{gI} = 0.121$

$$C_g := 2\cdot I_H \cdot \frac{0.49 - 0.14\alpha}{1 + \frac{0.63\left(\frac{\sqrt{B\cdot H}}{L_H}\right)^{0.56}}{\left(\frac{H}{B}\right)^{k}}} = 0.087$$

$$R := \frac{1}{1 + 20\cdot\frac{f_D\cdot B}{U_H}} = 0.17$$

$$F := \frac{4\cdot\frac{f_D\cdot L_H}{U_H}}{\left[1 + 71\left(\frac{f_D\cdot L_H}{U_H}\right)^2\right]^{\frac{5}{6}}} = 0.087$$

$$S_D := \frac{0.9}{\left[1 + 6\cdot\left(\frac{f_D\cdot H}{U_H}\right)^2\right]^{0.5}\cdot\left(1 + 3\cdot\frac{f_D\cdot B}{U_H}\right)} = 0.202$$

$$F_D := \frac{I_H^{\,2}\cdot F\cdot S_D\cdot\left(0.57 - 0.35\alpha + 2R\cdot\sqrt{0.053 - 0.042\alpha}\right)}{C_g^{\,2}} = 0.02$$

$$R_D := \frac{\pi F_D}{4\cdot\zeta_D} = 1.566$$

Appendix 3

$$\beta := 1$$

$$\lambda := 1 - 0.4\cdot\ln(\beta) = 1$$

$$g_{aD} := \sqrt{2\cdot\ln\left(600\cdot\frac{f_D}{Hz}\right)} + 1.2 = 3.283$$

$$M_D := \int_0^H m_Z\cdot\left(\frac{Z}{H}\right)^{2\cdot\beta} dZ = 1.097\times 10^7\,kg$$

$$a_{Dmax} := \frac{q_H\cdot g_{aD}\cdot B\cdot H\cdot C_H\cdot C_g\cdot\lambda\cdot\sqrt{R_D}}{M_D} = 0.1\,\frac{m}{s^2}$$

Across wind

$$M_L := M_D$$

$$\kappa_1 := 0.85 \qquad \kappa_2 := 0.02$$

$$OK_1 := \frac{H}{\sqrt{B\cdot D}} \le 6 = 1$$

$$OK_2 := 0.2 \le \frac{D}{B} \le 5 = 1$$

$$OK_3 := \frac{U_H}{f_L\sqrt{B\cdot D}} \le 10 = 1$$

$$f_{s1} := \frac{0.12}{\left[1 + 0.38\cdot\left(\frac{D}{B}\right)^2\right]^{0.89}}\cdot\frac{U_H}{B} = 0.085\,\frac{1}{s}$$

$$f_{s2} := \frac{0.56}{\left(\frac{D}{B}\right)^{0.85}}\cdot\frac{U_H}{B} = 0.648\,\frac{1}{s} \qquad \beta_2 := \frac{0.28}{\left(\frac{D}{B}\right)^{0.34}} = 0.322$$

$$\beta_1 := \frac{\left(\frac{D}{B}\right)^4 + 2.3\cdot\left(\frac{D}{B}\right)^2}{\left[2.4\cdot\left(\frac{D}{B}\right)^4 - 9.2\cdot\left(\frac{D}{B}\right)^3 + 18\left(\frac{D}{B}\right)^2 + 9.5\left(\frac{D}{B}\right) - 0.15\right]} + \frac{0.12}{\left(\frac{D}{B}\right)} = 0.282$$

$$F_L := \left[\frac{4\cdot\kappa_1\cdot\left(1+0.6\beta_1\right)\cdot\beta_1}{\pi}\cdot\frac{\left(\frac{f_L}{f_{s1}}\right)^2}{\left[1-\left(\frac{f_L}{f_{s1}}\right)^2\right]^2 + 4\cdot{\beta_1}^2\cdot\left(\frac{f_L}{f_{s1}}\right)^2}\right] \text{ if } \frac{D}{B} < 3 \qquad = 0.025$$

$$\left[\left[\frac{4\cdot\kappa_1\cdot\left(1+0.6\beta_1\right)\cdot\beta_1}{\pi}\cdot\frac{\left(\frac{f_L}{f_{s1}}\right)^2}{\left[1-\left(\frac{f_L}{f_{s1}}\right)^2\right]^2 + 4\cdot{\beta_1}^2\cdot\left(\frac{f_L}{f_{s1}}\right)^2} \ldots + \frac{4\cdot\kappa_2\cdot\left(1+0.6\beta_2\right)\cdot\beta_2}{\pi}\cdot\frac{\left(\frac{f_L}{f_{s2}}\right)^2}{\left[1-\left(\frac{f_L}{f_{s2}}\right)^2\right]^2 + 4\cdot{\beta_2}^2\cdot\left(\frac{f_L}{f_{s2}}\right)^2}\right]\right] \text{ if } \frac{D}{B} \ge 3$$

Appendix 3

$$R_L := \frac{\pi \cdot F_L}{4 \cdot \zeta_L} = 1.977$$

$$C_L := 0.0082 \cdot \left(\frac{D}{B}\right)^3 - 0.071 \cdot \left(\frac{D}{B}\right)^2 + 0.22 \cdot \left(\frac{D}{B}\right) = 0.117$$

$$g_{aL} := \sqrt{2 \cdot \ln\left(600 \cdot \frac{f_L}{Hz}\right)} + 1.2 = 3.44$$

$$a_{Lmax} := \frac{q_H \cdot g_{aL} \cdot B \cdot H \cdot C_L \cdot \lambda \cdot \sqrt{R_L}}{M_L} = 0.123 \frac{m}{s^2}$$

Torsion

$$C_T := \left[0.0066 + 0.015 \cdot \left(\frac{D}{B}\right)^2\right]^{0.78} = 0.034$$

$L := \max(B, D) = 34.6\,m$

$U_T := 4.5$

$$K_{45} := \begin{cases} \left[\dfrac{-1.1 \cdot \left(\frac{D}{B}\right) + 0.97}{\left(\frac{D}{B}\right)^2 + 0.85 \cdot \left(\frac{D}{B}\right) + 3.3} + 0.17\right] & \text{if } U_T \le 4.5 \\ \left[\dfrac{0.077\left(\frac{D}{B}\right) - 0.16}{\left(\frac{D}{B}\right)^2 - 0.96 \cdot \left(\frac{D}{B}\right) + 0.42} + \dfrac{0.35}{\frac{D}{B}} + 0.095\right] & \text{if } 6 \le U_T \le 10 \end{cases} = 0.225$$

$$\beta_{45} := \begin{cases} \left[\dfrac{\left(\frac{D}{B}\right) + 3.6}{\left(\frac{D}{B}\right)^2 - 5.1 \cdot \left(\frac{D}{B}\right) + 9.1} + \dfrac{0.14}{\frac{D}{B}} + 0.14\right] & \text{if } U_T \le 4.5 \\ \left[\dfrac{0.44 \cdot \left(\frac{D}{B}\right)^2 - 0.0064}{\left(\frac{D}{B}\right)^4 - 0.26 \cdot \left(\frac{D}{B}\right)^2 + 0.1} + 0.2\right] & \text{if } 6 \le U_T \le 10 \end{cases} = 1.044$$

$$F_{45} := \frac{0.14 \cdot {K_{45}}^2 \cdot {U_T}^{2 \cdot \beta_{45}}}{\pi} \cdot \frac{D \cdot \left(B^2 + D^2\right)^2}{L^2 \cdot B^3} = 0.072$$

$U_T := 6$

$$OK_4 := \frac{U_H}{f_T \sqrt{B \cdot D}} \le 10 = 1$$

$$OK := OK_1 \cdot OK_2 \cdot OK_3 \cdot OK_4 = 1$$

$$ERRORS := \begin{cases} 0 & \text{if } OK = 1 \\ 1 & \text{otherwise} \end{cases} = 0$$

Appendix 3

$$K_6 := \begin{cases} \left[\dfrac{-1.1\cdot\left(\frac{D}{B}\right)+0.97}{\left(\frac{D}{B}\right)^2+0.85\cdot\left(\frac{D}{B}\right)+3.3}+0.17\right] & \text{if } U_T \le 4.5 \\ \left[\dfrac{0.077\left(\frac{D}{B}\right)-0.16}{\left(\frac{D}{B}\right)^2-0.96\cdot\left(\frac{D}{B}\right)+0.42}+\dfrac{0.35}{\frac{D}{B}}+0.095\right] & \text{if } 6 \le U_T \le 10 \end{cases} = 0.135$$

$$\beta_6 := \begin{cases} \left[\dfrac{\left(\frac{D}{B}\right)+3.6}{\left(\frac{D}{B}\right)^2-5.1\cdot\left(\frac{D}{B}\right)+9.1}+\dfrac{0.14}{\frac{D}{B}}+0.14\right] & \text{if } U_T \le 4.5 \\ \left[\dfrac{0.44\cdot\left(\frac{D}{B}\right)^2-0.0064}{\left(\frac{D}{B}\right)^4-0.26\cdot\left(\frac{D}{B}\right)^2+0.1}+0.2\right] & \text{if } 6 \le U_T \le 10 \end{cases} = 1.242$$

$$F_6 := \frac{0.14\cdot K_6^{\,2}\cdot U_T^{\,2\cdot\beta_6}}{\pi}\cdot\frac{D\cdot\left(B^2+D^2\right)^2}{L^2\cdot B^3} = 0.097$$

$$U_T := \frac{U_H}{f_T\cdot\sqrt{B\cdot D}} = 2.09$$

$$K_T := \begin{cases} \dfrac{-1.1\cdot\left(\frac{D}{B}\right)+0.97}{\left(\frac{D}{B}\right)^2+0.85\cdot\left(\frac{D}{B}\right)+3.3}+0.17 & \text{if } U_T \le 4.5 \\ \left[\dfrac{0.077\left(\frac{D}{B}\right)-0.16}{\left(\frac{D}{B}\right)^2-0.96\cdot\left(\frac{D}{B}\right)+0.42}+\dfrac{0.35}{\frac{D}{B}}+0.095\right] & \text{if } 6 \le U_T \le 10 \\ 1 & \text{otherwise} \end{cases} = 0.225$$

$$\beta_T := \begin{cases} \left[\dfrac{\left(\frac{D}{B}\right)+3.6}{\left(\frac{D}{B}\right)^2-5.1\cdot\left(\frac{D}{B}\right)+9.1}+\dfrac{0.14}{\frac{D}{B}}+0.14\right] & \text{if } U_T \le 4.5 \\ \left[\dfrac{0.44\cdot\left(\frac{D}{B}\right)^2-0.0064}{\left(\frac{D}{B}\right)^4-0.26\cdot\left(\frac{D}{B}\right)^2+0.1}+0.2\right] & \text{if } 6 \le U_T \le 10 \\ 1 & \text{otherwise} \end{cases} = 1.044$$

Appendix 3

$$F_T := \begin{cases} \left[\frac{0.14 \cdot {K_T}^2 \cdot {U_T}^{2 \cdot \beta_T}}{\pi} \cdot \frac{D \cdot \left(B^2 + D^2\right)^2}{L^2 \cdot B^3}\right] & \text{if } 6 \le U_T \le 10 = 0.015 \\ \left[\frac{0.14 \cdot {K_T}^2 \cdot {U_T}^{2 \cdot \beta_T}}{\pi} \cdot \frac{D \cdot \left(B^2 + D^2\right)^2}{L^2 \cdot B^3}\right] & \text{if } U_T \le 4.5 \\ \left(F_{45} \cdot \exp\left(3.5 \ln\left(\frac{F_6}{F_{45}}\right) \cdot \ln\left(\frac{U_T}{4.5}\right)\right)\right) & \text{if } 4.5 < U_T < 6 \end{cases}$$

$$R_T := \frac{\pi \cdot F_T}{4 \cdot \zeta_T} = 1.146$$

$$I_Z := \frac{m_Z \cdot \left(B^2 + D^2\right)}{12} = 3.456 \times 10^7 \, m \cdot kg$$

$$I_T := \int_0^H I_Z \cdot \left(\frac{Z}{H}\right)^{2 \cdot \beta} dZ = 1.578 \times 10^9 \, m^2 \cdot kg$$

$$g_{aT} := \sqrt{2 \cdot \ln\left(600 \cdot \frac{f_T}{Hz}\right) + 1.2} = 3.539$$

$$a_{dmax} := 0.6 \cdot \frac{q_H \cdot g_{aT} \cdot B^2 \cdot H \cdot C_T \cdot \lambda \cdot \sqrt{R_T}}{I_T} = 4.051 \times 10^{-3} \, \frac{1}{s^2}$$

$$a_{Tmax} := a_{dmax} \cdot \sqrt{\left(\frac{B}{2}\right)^2 + \left(\frac{D}{2}\right)^2} = 0.084 \, \frac{m}{s^2}$$

Along-wind	Across-wind	Torsion
$a_{Dmax} = 0.1 \cdot \frac{m}{s^2}$	$a_{Lmax} = 0.123 \cdot \frac{m}{s^2}$	$a_{Tmax} = 0.084 \cdot \frac{m}{s^2}$

ERRORS = 0

Along-wind and across-wind acceleration, according to standard AS/NZS 1170.2:2011

specific mass of air	$\rho_{air} := 1.25 \frac{kg}{m^3}$
specific mass of building	$\rho_b := 1.2 \cdot 251.571 \frac{kg}{m^3}$
terrain category	$c_{terrain} := 2$
building height	$H := 137m$
buildings width	$B := 34.6m$
buildings depth	$D := 23m$
pressure coefficient, windward	$C_w := 0.8$
pressure coefficient, leeward	$C_l := -0.5$
fundamental natural frequency along wind	$n_1 := 0.20Hz$
fundamental natural frequency across-wind	$n_2 := 0.34Hz$
damping ratio along wind	$\zeta_1 := 0.01$
damping ratio across wind	$\zeta_2 := 0.01$
mean hourly wind speed	$V := 28.3 \frac{m}{s}$
height at which to calculate:	$z_h := H$

Along-wind

Appendix 4

$$M_1(z) := \begin{cases} 0.99 \text{ if } 0 \le z \le 3 \\ \left[0.99 + \left(\frac{1.05 - 0.99}{5 - 3}\right)(z - 3)\right] \text{ if } 3 < z \le 5 \\ \left[1.05 + \left(\frac{1.12 - 1.05}{10 - 5}\right)(z - 5)\right] \text{ if } 5 < z \le 10 \\ \left[1.12 + \left(\frac{1.16 - 1.12}{15 - 10}\right)(z - 10)\right] \text{ if } 10 < z \le 15 \\ \left[1.16 + \left(\frac{1.19 - 1.16}{20 - 15}\right)(z - 15)\right] \text{ if } 15 < z \le 20 \\ \left[1.19 + \left(\frac{1.22 - 1.19}{30 - 20}\right)(z - 20)\right] \text{ if } 20 < z \le 30 \\ \left[1.22 + \left(\frac{1.24 - 1.22}{40 - 30}\right)(z - 30)\right] \text{ if } 30 < z \le 40 \\ \left[1.24 + \left(\frac{1.25 - 1.24}{50 - 40}\right)(z - 40)\right] \text{ if } 40 < z \le 50 \\ \left[1.25 + \left(\frac{1.27 - 1.25}{75 - 50}\right)(z - 50)\right] \text{ if } 50 < z \le 75 \\ \left[1.27 + \left(\frac{1.29 - 1.27}{100 - 75}\right)(z - 75)\right] \text{ if } 75 < z \le 100 \\ \left[1.29 + \left(\frac{1.31 - 1.29}{150 - 100}\right)(z - 100)\right] \text{ if } 100 < z \le 150 \\ \left[1.31 + \left(\frac{1.32 - 1.31}{}\right)(z - 150)\right] \text{ if } 150 < z \le 200 \end{cases}$$

$$M_2(z) := \begin{cases} 0.91 \text{ if } 0 \le z \le 5 \\ \left[0.91 + \left(\frac{1 - 0.91}{10 - 5}\right)(z - 5)\right] \text{ if } 5 < z \le 10 \\ \left[1 + \left(\frac{1.05 - 1}{15 - 10}\right)(z - 10)\right] \text{ if } 10 < z \le 15 \\ \left[1.05 + \left(\frac{1.08 - 1.05}{20 - 15}\right)(z - 15)\right] \text{ if } 15 < z \le 20 \\ \left[1.08 + \left(\frac{1.12 - 1.08}{30 - 20}\right)(z - 20)\right] \text{ if } 20 < z \le 30 \\ \left[1.12 + \left(\frac{1.16 - 1.12}{40 - 30}\right)(z - 30)\right] \text{ if } 30 < z \le 40 \\ \left[1.16 + \left(\frac{1.18 - 1.16}{50 - 40}\right)(z - 40)\right] \text{ if } 40 < z \le 50 \\ \left[1.18 + \left(\frac{1.22 - 1.18}{75 - 50}\right)(z - 50)\right] \text{ if } 50 < z \le 75 \\ \left[1.22 + \left(\frac{1.24 - 1.22}{100 - 75}\right)(z - 75)\right] \text{ if } 75 < z \le 100 \\ \left[1.24 + \left(\frac{1.27 - 1.24}{150 - 100}\right)(z - 100)\right] \text{ if } 100 < z \le 150 \\ \left[1.27 + \left(\frac{1.29 - 1.27}{200 - 150}\right)(z - 150)\right] \text{ if } 150 < z \le 200 \end{cases}$$

Appendix 4

$$M_3(z) := \begin{cases} 0.83 \text{ if } 0 \le z \le 5 \\ \left[0.83 + \left(\frac{0.83 - 0.83}{10 - 5}\right)(z - 5)\right] \text{ if } 5 < z \le 10 \\ \left[0.83 + \left(\frac{0.89 - 0.83}{15 - 10}\right)(z - 10)\right] \text{ if } 10 < z \le 15 \\ \left[0.89 + \left(\frac{0.94 - 0.89}{20 - 15}\right)(z - 15)\right] \text{ if } 15 < z \le 20 \\ \left[0.94 + \left(\frac{1 - 0.94}{30 - 20}\right)(z - 20)\right] \text{ if } 20 < z \le 30 \\ \left[1 + \left(\frac{1.04 - 1}{40 - 30}\right)(z - 30)\right] \text{ if } 30 < z \le 40 \\ \left[1.04 + \left(\frac{1.07 - 1.04}{50 - 40}\right)(z - 40)\right] \text{ if } 40 < z \le 50 \\ \left[1.07 + \left(\frac{1.12 - 1.07}{75 - 50}\right)(z - 50)\right] \text{ if } 50 < z \le 75 \\ \left[1.12 + \left(\frac{1.16 - 1.12}{100 - 75}\right)(z - 75)\right] \text{ if } 75 < z \le 100 \\ \left[1.16 + \left(\frac{1.21 - 1.16}{150 - 100}\right)(z - 100)\right] \text{ if } 100 < z \le 150 \\ \left[1.21 + \left(\frac{1.24 - 1.21}{200 - 150}\right)(z - 150)\right] \text{ if } 150 < z \le 200 \end{cases}$$

$$M_4(z) := \begin{cases} 0.75 \text{ if } 0 \le z \le 5 \\ \left[0.75 + \left(\frac{0.75 - 0.75}{10 - 5}\right)(z - 5)\right] \text{ if } 5 < z \le 10 \\ \left[0.75 + \left(\frac{0.75 - 0.75}{15 - 10}\right)(z - 10)\right] \text{ if } 10 < z \le 15 \\ \left[0.75 + \left(\frac{0.75 - 0.75}{20 - 15}\right)(z - 15)\right] \text{ if } 15 < z \le 20 \\ \left[0.75 + \left(\frac{0.80 - 0.75}{30 - 20}\right)(z - 20)\right] \text{ if } 20 < z \le 30 \\ \left[0.80 + \left(\frac{0.85 - 0.80}{40 - 30}\right)(z - 30)\right] \text{ if } 30 < z \le 40 \\ \left[0.85 + \left(\frac{0.90 - 0.85}{50 - 40}\right)(z - 40)\right] \text{ if } 40 < z \le 50 \\ \left[0.90 + \left(\frac{0.98 - 0.90}{75 - 50}\right)(z - 50)\right] \text{ if } 50 < z \le 75 \\ \left[0.98 + \left(\frac{1.03 - 0.98}{100 - 75}\right)(z - 75)\right] \text{ if } 75 < z \le 100 \\ \left[1.03 + \left(\frac{1.11 - 1.03}{150 - 100}\right)(z - 100)\right] \text{ if } 100 < z \le 150 \\ \left[1.11 + \left(\frac{1.16 - 1.11}{200 - 150}\right)(z - 150)\right] \text{ if } 150 < z \le 200 \end{cases}$$

Appendix 4

$$M_z(z) := \begin{cases} M_1(z) & \text{if } c_{terrain} = 1 \\ M_2(z) & \text{if } c_{terrain} = 2 \\ M_3(z) & \text{if } c_{terrain} = 3 \\ M_4(z) & \text{if } c_{terrain} = 4 \end{cases}$$

$$I_1(z) := \begin{cases} 0.171 & \text{if } 0 \le z \le 3 \\ \left[0.171 + \left(\frac{0.165 - 0.171}{5 - 3}\right)(z - 3)\right] & \text{if } 3 < z \le 5 \\ \left[0.165 + \left(\frac{0.157 - 0.165}{10 - 5}\right)(z - 5)\right] & \text{if } 5 < z \le 10 \\ \left[0.157 + \left(\frac{0.152 - 0.157}{15 - 10}\right)(z - 10)\right] & \text{if } 10 < z \le 15 \\ \left[0.152 + \left(\frac{0.147 - 0.152}{20 - 15}\right)(z - 15)\right] & \text{if } 15 < z \le 20 \\ \left[0.147 + \left(\frac{0.140 - 0.147}{30 - 20}\right)(z - 20)\right] & \text{if } 20 < z \le 30 \\ \left[0.140 + \left(\frac{0.133 - 0.140}{40 - 30}\right)(z - 30)\right] & \text{if } 30 < z \le 40 \\ \left[0.133 + \left(\frac{0.128 - 0.133}{50 - 40}\right)(z - 40)\right] & \text{if } 40 < z \le 50 \\ \left[0.128 + \left(\frac{0.118 - 0.128}{75 - 50}\right)(z - 50)\right] & \text{if } 50 < z \le 75 \\ \left[0.118 + \left(\frac{0.108 - 0.118}{100 - 75}\right)(z - 75)\right] & \text{if } 75 < z \le 100 \\ \left[0.108 + \left(\frac{0.095 - 0.108}{150 - 100}\right)(z - 100)\right] & \text{if } 100 < z \le 150 \\ \left[0.095 + \left(\frac{0.085 - 0.095}{200 - 150}\right)(z - 150)\right] & \text{if } 150 < z \le 200 \end{cases}$$

Appendix 4

$$I_2(z) := \begin{cases} 0.207 \text{ if } 0 \le z \le 3 \\ \left[0.207 + \left(\frac{0.196 - 0.207}{5 - 3}\right)(z - 3)\right] \text{ if } 3 < z \le 5 \\ \left[0.196 + \left(\frac{0.183 - 0.196}{10 - 5}\right)(z - 5)\right] \text{ if } 5 < z \le 10 \\ \left[0.183 + \left(\frac{0.176 - 0.183}{15 - 10}\right)(z - 10)\right] \text{ if } 10 < z \le 15 \\ \left[0.176 + \left(\frac{0.171 - 0.176}{20 - 15}\right)(z - 15)\right] \text{ if } 15 < z \le 20 \\ \left[0.171 + \left(\frac{0.162 - 0.171}{30 - 20}\right)(z - 20)\right] \text{ if } 20 < z \le 30 \\ \left[0.162 + \left(\frac{0.156 - 0.162}{40 - 30}\right)(z - 30)\right] \text{ if } 30 < z \le 40 \\ \left[0.156 + \left(\frac{0.151 - 0.156}{50 - 40}\right)(z - 40)\right] \text{ if } 40 < z \le 50 \\ \left[0.151 + \left(\frac{0.140 - 0.151}{75 - 50}\right)(z - 50)\right] \text{ if } 50 < z \le 75 \\ \left[0.140 + \left(\frac{0.131 - 0.140}{100 - 75}\right)(z - 75)\right] \text{ if } 75 < z \le 100 \\ \left[0.131 + \left(\frac{0.117 - 0.131}{150 - 100}\right)(z - 100)\right] \text{ if } 100 < z \le 150 \\ \left[0.117 + \left(\frac{0.107 - 0.117}{200 - 150}\right)(z - 150)\right] \text{ if } 150 < z \le 200 \end{cases}$$

Appendix 4

$$I_3(z) := \begin{cases} 0.271 & \text{if } 0 \le z \le 3 \\ \left[0.271 + \left(\frac{0.271 - 0.271}{5 - 3}\right)(z - 3)\right] & \text{if } 3 < z \le 5 \\ \left[0.271 + \left(\frac{0.239 - 0.271}{10 - 5}\right)(z - 5)\right] & \text{if } 5 < z \le 10 \\ \left[0.239 + \left(\frac{0.225 - 0.239}{15 - 10}\right)(z - 10)\right] & \text{if } 10 < z \le 15 \\ \left[0.225 + \left(\frac{0.215 - 0.225}{20 - 15}\right)(z - 15)\right] & \text{if } 15 < z \le 20 \\ \left[0.215 + \left(\frac{0.203 - 0.215}{30 - 20}\right)(z - 20)\right] & \text{if } 20 < z \le 30 \\ \left[0.203 + \left(\frac{0.195 - 0.203}{40 - 30}\right)(z - 30)\right] & \text{if } 30 < z \le 40 \\ \left[0.195 + \left(\frac{0.188 - 0.195}{50 - 40}\right)(z - 40)\right] & \text{if } 40 < z \le 50 \\ \left[0.188 + \left(\frac{0.176 - 0.188}{75 - 50}\right)(z - 50)\right] & \text{if } 50 < z \le 75 \\ \left[0.176 + \left(\frac{0.166 - 0.176}{100 - 75}\right)(z - 75)\right] & \text{if } 75 < z \le 100 \\ \left[0.166 + \left(\frac{0.150 - 0.166}{150 - 100}\right)(z - 100)\right] & \text{if } 100 < z \le 150 \\ \left[0.150 + \left(\frac{0.139 - 0.150}{200 - 150}\right)(z - 150)\right] & \text{if } 150 < z \le 200 \end{cases}$$

Appendix 4

$$I_4(z) := \begin{cases} 0.342 & \text{if } 0 \le z \le 3 \\ \left[0.342 + \left(\frac{0.342 - 0.342}{5 - 3}\right)(z - 3)\right] & \text{if } 3 < z \le 5 \\ \left[0.342 + \left(\frac{0.342 - 0.342}{10 - 5}\right)(z - 5)\right] & \text{if } 5 < z \le 10 \\ \left[0.342 + \left(\frac{0.342 - 0.342}{15 - 10}\right)(z - 10)\right] & \text{if } 10 < z \le 15 \\ \left[0.342 + \left(\frac{0.342 - 0.342}{20 - 15}\right)(z - 15)\right] & \text{if } 15 < z \le 20 \\ \left[0.342 + \left(\frac{0.305 - 0.342}{30 - 20}\right)(z - 20)\right] & \text{if } 20 < z \le 30 \\ \left[0.305 + \left(\frac{0.285 - 0.305}{40 - 30}\right)(z - 30)\right] & \text{if } 30 < z \le 40 \\ \left[0.285 + \left(\frac{0.270 - 0.285}{50 - 40}\right)(z - 40)\right] & \text{if } 40 < z \le 50 \\ \left[0.270 + \left(\frac{0.248 - 0.270}{75 - 50}\right)(z - 50)\right] & \text{if } 50 < z \le 75 \\ \left[0.248 + \left(\frac{0.233 - 0.248}{100 - 75}\right)(z - 75)\right] & \text{if } 75 < z \le 100 \\ \left[0.233 + \left(\frac{0.210 - 0.233}{150 - 100}\right)(z - 100)\right] & \text{if } 100 < z \le 150 \\ \left[0.210 + \left(\frac{0.196 - 0.210}{200 - 150}\right)(z - 150)\right] & \text{if } 150 < z \le 200 \end{cases}$$

$H := H = 137\,m$

$$I_h(z) := \begin{cases} I_1(z) & \text{if } c_{terrain} = 1 \\ I_2(z) & \text{if } c_{terrain} = 2 \\ I_3(z) & \text{if } c_{terrain} = 3 \\ I_4(z) & \text{if } c_{terrain} = 4 \end{cases}$$

$$v_{basic} := \frac{V}{M_z\left(\frac{H}{m}\right)}$$

$$v_{des}(z) := v_{basic} \cdot M_z\left(\frac{z}{m}\right)$$

$$m_0 := \rho_b \cdot B \cdot D = 2.402 \times 10^5 \frac{kg}{m}$$

$g_v := 3.7$

$$g_r := \sqrt{2 \cdot \ln\left(600 \cdot \frac{n_1}{Hz}\right)} = 3.094$$

$$L_h(z) := 85 \cdot \left(\frac{z}{10m}\right)^{0.25} m \qquad L_h(H) = 163.531\,m$$

$$S := \frac{1}{\left[1 + \frac{3.5 \cdot n_1 \cdot H \cdot \left(1 + g_v \cdot I_h\left(\frac{H}{m}\right)\right)}{v_{des}(H)}\right] \cdot \left[1 + \frac{4 \cdot n_1 \cdot B \cdot \left(1 + g_v \cdot I_h\left(\frac{H}{m}\right)\right)}{v_{des}(H)}\right]} = 0.07$$

$$N := n_1 \cdot L_h(H) \cdot \frac{\left(1 + g_v \cdot I_h\left(\frac{H}{m}\right)\right)}{v_{des}(H)} = 1.672$$

Appendix 4

$$E_t := \frac{\pi \cdot N}{\left(1 + 70.8N^2\right)^{\frac{5}{6}}} = 0.064$$

$$a_{max} := \frac{3}{m_0 \cdot H^2} \cdot \frac{\rho_{air} \cdot g_r \cdot I_h\left(\frac{H}{m}\right) \cdot \sqrt{\frac{S \cdot E_t}{\zeta_1}}}{1 + 2 \cdot g_v \cdot I_h\left(\frac{H}{m}\right)} \cdot \left(C_w \cdot \int_0^H v_{des}(z)^2 \cdot B \cdot z \, dz - C_l \cdot v_{des}(H)^2 \cdot B \cdot H^2 \right) = 0.05 \cdot \frac{m}{s^2}$$

Across-wind

$$g_r := \sqrt{2 \cdot \ln\left(600 \cdot \frac{n_2}{Hz}\right)} = 3.261$$

$$k := 1$$

$$K_m := 0.76 + 0.24k = 1$$

$$V_n := \frac{v_{des}(H)}{n_2 \cdot B \cdot \left(1 + g_v \cdot I_h\left(\frac{H}{m}\right)\right)} = 1.663$$

$$C_{fs.log} := 0.000406V_n^4 - 0.0165V_n^3 + 0.201V_n^2 - 0.603V_n - 2.76 = -3.28$$

$$C_{fs} := 10^{C_{fs.log}} = 5.252 \times 10^{-4}$$

$$a_{y.max} := \frac{1.5 \cdot B \cdot g_r}{m_0} \cdot \left[\frac{0.5 \cdot \rho_{air} \cdot v_{des}(H)^2}{\left(1 + g_v \cdot I_h\left(\frac{H}{m}\right)\right)^2} \cdot K_m \cdot \sqrt{\frac{\pi \cdot C_{fs}}{\zeta_2}} \right] = 0.068 \frac{m}{s^2}$$

Along-wind

$$a_{max} = 0.05 \frac{m}{s^2}$$

Across-wind

$$a_{y.max} = 0.068 \frac{m}{s^2}$$